Aus dem Institut für Pflanzenbau und Pflanzenzüchtung

der Christian-Albrechts-Universität zu Kiel

Production of oilseed rape
with increased seed shattering resistance

Dissertation

zur Erlangung des Doktorgrades

der Agrar- und Ernährungswissenschaftlichen Fakultät

der Christian-Albrechts-Universität zu Kiel

vorgelegt von

M.Sc. Janina Braatz

aus Kamp-Lintfort

Kiel, 2017

Table of contents

List of abbreviations

2,4-D	2,4-Dichlorophenoxyacetic acid
%	Per cent
°C	Degree Celsius
μJ	Microjoule
μm	Micrometer
X^2	Chi square
A	Adenine
ADPG1/2	*ARABIDOPSIS DEHISCENCE ZONE POLYGALACTURONASE 1/2*
AFLP	Amplified fragment length polymorphism
AG	*AGAMOUS*
ALC	*ALCATRAZ*
Amp	Ampicillin
ANCOVA	Analysis of covariance
A. thaliana, At	*Arabidopsis thaliana*
A. tumefaciens	*Agrobacterium tumefaciens*
BAP	6-Benzylaminopurine
bHLH	Basic helix-loop-helix
BLAST	Basic local alignment search tool
B. napus, Bn	*Brassica napus*
B. oleracea, Bo	*Brassica oleracea*
bp	Base pairs
BRAD	*Brassica* database
B. rapa, Br	*Brassica rapa*
C	Cytosine
Cas	CRISPR-associated
cDNA	Complementary DNA
CDS	Coding sequence
*Cel*I	*CELERY ENDONUCLEASE* 1
cm	Centimeter
CRISPR	Clustered regularly interspaced short palindromic repeats
crRNA	CRISPR-derived RNA
CTAB	Cetyltrimethyl ammonium bromide
cv	Cultivar
d	Day
DAP	Days after pollination
DH	Doubled haploid
DNA	Deoxyribonucleic acid
DNase	Deoxyribonuclease
dNTP	Deoxynucleotide triphosphate
DSB	Double-stranded break
E. coli	*Escherichia coli*
EDTA	Ethylene diaminetetraacetic acid
EMS	Ethyl methanesulfonate
ENA	European Nucleotide Archive
EPSPS	5-enolpyruvylshikimate-3-phosphate synthase
FIL	*FILAMENTOUS FLOWER*
F_n	n-th generation after cross
FRA 8	*FRAGILE FIBER 8*
FUL	*FRUITFULL*
g	Gram

G	Guanine
GA3OX1	*GIBBERELLIN 3-OXIDASE 1*
Gb	Giga base pairs
GM(O)	Genetically modified (organism)
h	Hour
HDR	Homology-directed repair
HRM	High-resolution melting curve analysis
Hz	Hertz
IBA	Indole-3-butyric acid
IND	*INDEHISCENT*
indel	Insertion/ deletion
IRX 3/4/5/10/12	*IRREGULAR XYLEM 3/4/5/10/12*
JAG	*JAGGED*
kb	Kilo base pairs
kg	Kilogram
l	Liter
LB	Lysogeny broth
LD	Long days
LL	Lignified layer
Mb	Mega base pairs
M_n	n-th generation after mutagenesis treatment
MES	2-(N-morpholino)ethanesulfonic acid
min	Minute
mg	Milligram
mJ	Millijoule
mm	Millimeter
mRNA	Messenger ribonucleic acid
MS	Murashige and Skoog
N	Newton
NAA	Naphthaleneacetic acid
NCBI	National Center for Biotechnology Information
NHEJ	Non-homologous end-joining
NGS	Next-generation sequencing
nm	Nanometer
NST1/2/3	*NAC SECONDARY WALL THICKENING PROMOTING FACTOR 1/2/3*
nt	Nucleotides
OD	Optical density
OMT 1	*O-METHYLTRANSFERASE 1*
PAM	Protospacer-adjacent motif
PID	*PINOID*
PIN 3	*PIN-FORMED 3*
PCR	Polymerase chain reaction
PPT	Phosphinothricin
PRX 13/30/55	*PEROXIDASE 13/30/55*
r.h.	Relative humidity
RIT	Random impact test
RJAI	Replum-valve joint area index
RNA	Ribonucleic acid
RNAi	RNA interference
RNase	Ribonuclease
RNP	Ribonucleoproteins

RPL	*REPLUMLESS*
rpm	Revolutions per minute
RT-qPCR	Real-time quantitative PCR
SD	Standard deviation
s	Second
SEM	Scanning electron microscopy
sgRNA	Single guide RNA
SHP1/2	*SHATTERPROOF 1/2*
SL	Separation layer
SNP	Single nucleotide polymorphism
Spec	Spectinomycin
SPT	*SPATULA*
STK	*SEEDSTICK*
T	Thymine
T. aestivum	*Triticum aestivum*
TALE(N)	Transcription activator-like effector (nuclease)
TAR	Transcriptional activation region
TAIR	The Arabidopsis Information Resource
T. dicoccoides	*Triticum dicoccoides*
T. dicoccum	*Triticum dicoccum*
T-DNA	Transfer DNA
T. durum	*Triticum durum*
TE	Tris EDTA
TILLING	Targeting induced local lesions in genomes
T_n	n-th generation after transformation
tracrRNA	Trans-activating crRNA
Tris	Tris (hydroxymethyl) amino methane
UTR	Untranslated region
VB	Vascular bundle
WGS	Whole genome shotgun
YAB 3	*YABBY 3*
ZFN	Zinc finger nuclease

1 General introduction

1.1 Oilseed rape

Oilseed rape (*Brassica napus*) is a major oil crop in temperate climates. The main producing countries are Canada and China, followed by India and Germany. In 2014, the worldwide rapeseed yield comprised 73.8 million tons harvested from an area of 36.1 million hectares (FAOSTAT, 2014). While in former times the exploitation of rapeseed oil was restricted to mechanical uses due to high amounts of anti-nutritional compounds like erucic acid and glucosinolates, this has changed thanks to breeding of so called 00-quality ('canola') varieties. Meanwhile, rapeseed oil is also used in the food and feed industry. In Europe, rapeseed oil is majorly processed to obtain biodiesel (60% in market year 2015/16; Krautgartner et al. 2017).

The genome of oilseed rape (2n = 38, AACC) comprises two subgenomes A and C, originating from a natural hybridization of *Brassica rapa* (2n = 20, AA) and *Brassica oleracea* (2n = 18, CC) which occurred presumably 7,500 to 12,500 years ago (Chalhoub et al. 2014). About 79% of the 1,130 Mb genome is covered by the reference sequence of winter rapeseed line Darmor-*bzh* (Chalhoub et al. 2014). This resource contains 314.2 Mb of the A subgenome and 525.8 Mb of the C subgenome, and a total of 101,040 annotated gene models. Further genomic resources involve the resequencing data of 52 diverse rapeseed accessions (Schmutzer et al. 2015).

B. napus is closely related to the model plant Arabidopsis (*Arabidopsis thaliana*). However, depending on evolution, the allopolyploid rapeseed genome is far more complex. In the course of the diversification of the *Brassicacea,* a genome triplication took place (Lysak et al. 2005). Because of the combination of the two subgenomes of *B. rapa* and *B. oleracea* in *B. napus*, approximately six paralogs occur for each gene present in Arabidopsis. This number can vary due to more recent sequence losses or duplications (Liu et al. 2014; Wang et al. 2011b; Chalhoub et al. 2014). The amount of redundant gene copies complicates breeding processes as many favorable traits, including low levels of polyunsaturated fatty acids and low sinapine content, rely on loss-of-function alleles (Wells et al. 2014; Emrani et al. 2015). Consequently, multiple homoeologous knock-down alleles have to be combined by crossing.

Nowadays in Germany, the majority of released rapeseed cultivars are hybrids, which are making up 76% of registered winter type varieties (Beschreibende Sortenliste 2016, www.bundessortenamt.de). In hybrid breeding, two genetically distant parental lines are crossed to exploit the heterosis effects of the F_1 generation. Because rapeseed is an autogamous species, it is necessary to ensure the cross-pollination for hybrid seed production by utilization of self-incompatibility or male sterility systems. Different hybrid systems like 'Male Sterility Lembke' and 'Ogura' have been developed.

Under greenhouse conditions, the common generation cycles of spring and winter rapeseed comprise approximately six to seven months. In order to reach 99% homozygosity after an initial cross, seven generations of selfing have to be performed. Aiming at an accelerated breeding process, doubled haploid (DH) techniques are employed to obtain full homozygosity within just a single generation. Microspore cultures are routinely used for DH production. Chromosome doubling is induced by colchicine treatment and can be validated by flow cytometry of regenerated plantlets (Weber et al. 2005).

Current rapeseed breeding objectives can be categorized in three main classes: quality-related traits, resistances, and yield. For the food and feed industry, the quality of rapeseed-based

products is largely dependent on anti-nutritive contents. Sensitive livestock suffer especially from glucosinolate uptake (reviewed in Tripathi and Mishra 2007). Furthermore, the fatty acid composition of oilseed rape seeds is subject to optimization. The ideal composition depends on the intended use. While low levels of saturated fatty acids bear health benefits, high erucic acid contents are favorable for various industrial uses (reviewed in Scarth and Tang 2006). Concerning disease resistance, major breeding efforts address fungal pathogens like *Leptosphaeria maculans* (anamorph *Phoma lingam*), which induces *Phoma* stem canker (blackleg disease). Resistance breeding against members of the genera *Verticillium* and *Sclerotinia*, which cause wilt and stem rot, is of similar importance. Finally, farmers are mostly interested in the output of their rapeseed fields. Therefore, apart from an increased seed yield, also improved yield stability is desired. Thus, breeders select among other traits for winter hardiness, drought tolerance, and silique shatter resistance.

1.2   Silique shattering as a problem in *Brassica* crops

Plant species of the genus *Brassica* share a common seed dispersal system. They produce elongated fruits, the so called siliques, which dry out at maturity. The dry siliques are fragile and dehisce easily at the application of low forces.

Two major harvesting systems are applied for oilseed rape: direct cutting of standing rapeseed plants and swathing. After swathing, cut immature plants are left on the field to ripen. This method speeds up the maturation process and is used in Canada to exploit the short summer as a growing season and to escape frosts. However, swathing causes yield losses of up to 25% because of the increased handling of the fragile siliques (Price et al. 1996). Concerning directly cut winter rapeseed, natural pre-harvest seed shedding reduces the yield by up to 7% (Price et al. 1996; Pari et al. 2012). Exemplary natural causes for silique shattering are birds, crushing siliques to feed on the seeds, and weather conditions like hail or strong wind. Additional silique shattering is induced by combine harvesters. The seed loss due to the harvesting process depends on the type of equipment, a conveyor-assisted header for instance can reduce the shedding by half (Hobson and Bruce 2002).

Actually, the shed seeds cause more trouble than just the apparent yield loss. The addition to the soil seed bank results in the growth of volunteer plants in following seasons. One year after rapeseed production, rapeseed volunteers were detected with average densities of up to 5 plants/m^2 in 90% of 131 surveyed Canadian fields (Simard et al. 2002). The same study reports a yearly reduction of volunteer densities that reached 0.2 plants/m^2 after five years, given that volunteer control measures have been taken. Lutman et al. (2005) suggested that a 95% reduction of oilseed rape seeds from the soil takes about nine years. In practice, volunteers appear even seventeen years after the intended cultivation (Jørgensen et al. 2007).

Contaminations by rapeseed volunteers can reduce the harvest quality of oilseed rape with different fatty acid compositions (Baux et al. 2011). Furthermore, seed admixtures of genetically modified (GM) rapeseed volunteers into seed lots of conventional varieties can exceed accepted GM thresholds (Messéan et al. 2007), resulting in the obligation to label all products as 'genetically modified'.

There are efforts to develop chemicals which can be sprayed on rapeseed fields to reduce silique shattering (Kuai et al. 2015; Nunes et al. 2015), but growing shatter resistant varieties would be more cost effective.

1.2.1 Silique structure and dehiscence zone formation

The structure of rapeseed siliques is similar to Arabidopsis. They have two seed chambers which are surrounded by two valves (Figure 1A). A beak is situated at the tip. On the plant, siliques are attached to the branch via the pedicel. In the center of the silique, the valves are fixed to the replum. However, this connection weakens during maturation and is thus the predetermined breaking point (dehiscence zone) at which the valves will finally detach (Meakin and Roberts 1990b).

The dehiscence zone consists of two distinct cell layers, out of which one is fortified during maturation (lignified layer) whereas the other is partially degraded (separation layer) (Meakin and Roberts 1990b). In Arabidopsis, cell identity within the dehiscence zone is defined by a network of transcription factors (dehiscence zone identity genes; Figure 1B), whose functions were revealed by mutant studies (Table 1). Knock-out lines of the redundant MADS-box transcription factors SHATTERPROOF 1 and 2 (SHP1/2) lacked both types of dehiscence zone tissues (Liljegren et al. 2000). Mutations in the atypical basic helix-loop-helix (bHLH) transcription factor INDEHISCENT (IND) also caused a loss of these cell layers (Liljegren et al. 2004), whereas mutant siliques of the bHLH gene *ALCATRAZ* (*ALC*) developed only the lignified layer but not the separation layer (Rajani and Sundaresan 2001). By comparing different mutant combinations of *alc*, *ind,* and *shp1/2*, it was concluded that *SHP1/2* act upstream of *ALC* and *IND* (Liljegren et al. 2004). The expansion of dehiscence zone tissue throughout the whole silique is then prevented by repression of *SHP1/2* through FRUITFULL (FUL) within the valve and REPLUMLESS (RPL) within the replum (Ferrándiz 2000; Roeder et al. 2003). The analysis of *ind shp1 shp2 ful* and *alc shp1 shp2 ful* quadruple mutants in comparison with *ind ful* and *alc ful* double mutants revealed that the *SHP* genes have additional functions which are independent of the *IND* and *ALC* pathways (Liljegren et al. 2004). A third bHLH gene, *SPATULA* (*SPT*), shares redundant functions with *ALC* and *IND* but acts mainly on early gynoecium development (Girin et al. 2011; Groszmann et al. 2011).

With yeast two-hybrid experiments, Arnaud et al. (2011) demonstrated the interaction of ALC with DELLA proteins. DELLA proteins can block transcription factor activities by attaching to their DNA-binding domains, but this effect is abolished by gibberellin-mediated degradation of the DELLAs (De Lucas et al. 2008; Feng et al. 2008). Because IND promotes gibberellin synthesis through direct activation of *GIBBERELLIN 3-OXIDASE 1* (*GA3OX1*) expression, IND can regulate ALC on a post-transcriptional level (Arnaud et al. 2011).

The downstream mechanisms of *IND* and *ALC*, which ultimately lead to dehiscence zone differentiation, are under ongoing investigation. An important factor for separation layer development is the orchestration of auxin levels, which is influenced by IND through the transcriptional regulation of auxin efflux carriers and protein kinases (Sorefan et al. 2009; van Gelderen et al. 2016). Ogawa et al. (2009) proposed that later during silique development, the separation layer is partially degraded by hydrolysis through ARABIDOPSIS DEHISCENCE ZONE POLYGALACTURONASEs 1 and 2 (ADPG1/2). This is supported by the absence of *ADPG1* expression in valve margins of *ind* siliques (Ogawa et al. 2009). Meanwhile, *NAC SECONDARY WALL THICKENING FACTOR*s *1* and *3* (*NST1/3*) are necessary for the proper establishment of the lignified layer (Mitsuda and Ohme-Takagi 2008). However, the direct induction of *NST1/3* expression through IND has not yet been demonstrated.
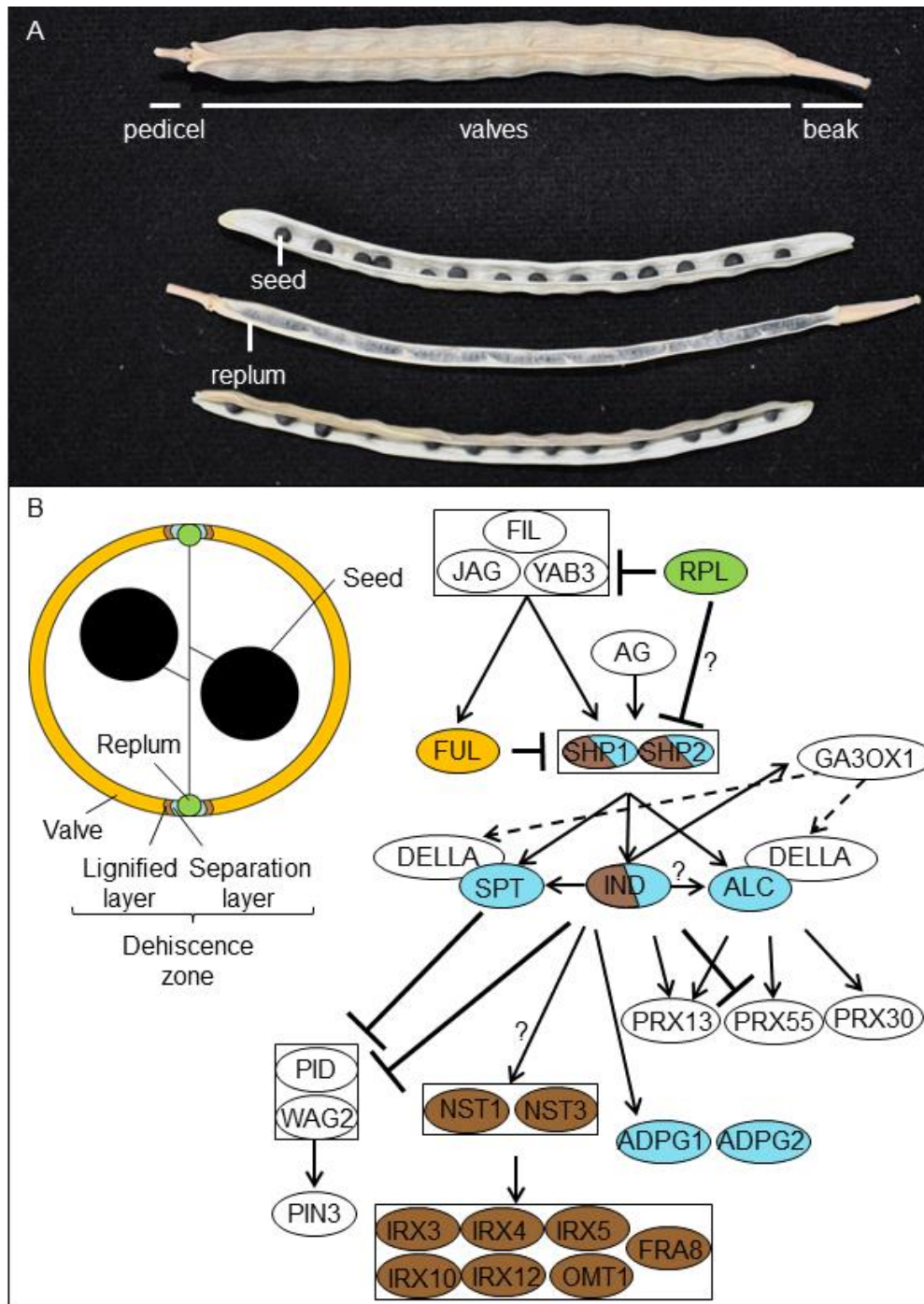
Figure 1. Silique structure and dehiscence zone differentiation. A, Intact and shattered rapeseed siliques at maturity. Shed seeds were collected and draped according to their positions within the seed chambers. B, Model of a silique cross section and the gene network required for dehiscence zone differentiation. Gene interactions were identified by mutant studies in Arabidopsis (Table 1). The colors refer to the tissues in which the genes play important roles. Dashed arrows indicate indirect activation of *SPT* and *ALC* through gibberellin-mediated degradation of DELLAs. To make the figure comprehensible, the number of arrows was reduced by pooling genes which are similarly induced/ repressed and which regulate the same downstream agents (black boxes). ARABIDOPSIS DEHISCENCE ZONE POLYGALACTURONASE 1/2 (ADPG1/2), AGAMOUS (AG), ALCATRAZ (ALC), FILAMENTOUS FLOWER (FIL), FRAGILE FIBER 8 (FRA8), FRUITFULL (FUL), GIBBERELLIN 3-OXIDASE 1 (GA3OX1), INDEHISCENT (IND), IRREGULAR XYLEM 3/4/5/10/12 (IRX3/4/5/10/12), JAGGED (JAG), NAC SECONDARY WALL THICKENING PROMOTING FACTOR 1/3 (NST1/3), O-METHYLTRANSFERASE 1 (OMT1), PINOID (PID), PIN-FORMED 3 (PIN3), PEROXIDASE 13/30/55 (PRX13/30/55), REPLUMLESS (RPL), SHATTERPROOF 1/2 (SHP1/2), SPATULA (SPT), YABBY 3 (YAB3)

Table 1. Overview of mutant studies with genes which are involved in dehiscence zone formation. Figure 1B was prepared based on these references.

Species	Target gene	Mutagenesis	Main results	Reference
A. thaliana	*AG*	Knock-down type of mutagenesis not specified (seeds obtained from another laboratory)	*AG* induces *AGL1* (*SHP1*) and *AGL5* (*SHP2*)	Savidge et al. 1995
A. thaliana	*SHP1/2*	EMS, T-DNA insertion, overexpression	Functional redundancy; establishment of lignified and separation layer	Liljegren et al. 2000
A. thaliana	*FUL, SHP1/2*	EMS, T-DNA insertion, overexpression	*FUL* represses *SHP1/2*	Ferrándiz et al. 2000
A. thaliana	*ALC*	Transposon insertion	Promotes differentiation of separation layer	Rajani and Sundaresan 2001
A. thaliana	*RPL*	EMS	*RPL* represses *SHP*	Roeder et al. 2003
A. thaliana	*ALC, FUL, IND, SHP1/2*	EMS	*IND* is required for establishment of lignified and separation layer	Liljegren et al. 2004
A. thaliana	*IND*	Transposon insertion	*IND* is required for dehiscence zone differentiation	Wu et al. 2006
A. thaliana	*NST1/3*	T-DNA insertion, overexpression	*NST1/3* induce genes related to secondary wall synthesis	Mitsuda et al. 2007
A. thaliana	*NST1/3*	T-DNA insertion	Partial redundancy; *IND* and *SHP1/2* still expressed in *nst1 nst3* mutant	Mitsuda and Ohme-Takagi 2008
A. thaliana	*ADPG1/2*	T-DNA insertion, complementation studies	Essential for silique dehiscence; *IND* induces *ADPG1* expression in dehiscence zone	Ogawa et al. 2009
A. thaliana	*IND*	*IND* promotor-controlled expression of bacterial auxin biosynthesis gene (*iaaM*), overexpression	*IND*-mediated auxin minimum is required for dehiscence zone differentiation	Sorefan et al. 2009
A. thaliana	*ALC, GA3OX1, IND*	EMS, transposon insertion	*IND* activates *GA3OX1;* ALC interacts with DELLA proteins	Arnaud et al. 2010

Species	Target gene	Mutagenesis	Main results	Reference
A. thaliana	*AG, ALC, FUL, IND, PRX13/30/55, RPL, SHP1/2*	EMS, T-DNA insertion, transposon insertion, overexpression	*PRX13/30/55* expression is regulated by *ALC, IND, SHP1/2*	Cosio and Dunand 2010
A. thaliana	*IND*	Knock-down type of mutagenesis not specified (seeds obtained from another laboratory)	*IND* induces *SPT*	Groszmann et al. 2010
A. thaliana	*IND, SPT*	EMS, transposon insertion, overexpression	*IND* induces *SPT*; partial redundancy through control of auxin distribution	Girin et al. 2011
A. thaliana	*ALC, SPT*	EMS, transposon insertion, overexpression, complementation studies	Partial redundancy	Groszmann et al. 2011
A. thaliana	*IND, PID, WAG1/2*	Complementation study with altered promotor, fluorescence labelling	*IND* is required for auxin-triggered cell divisions in early silique development	van Gelderen et al. 2016
B. napus	*BnALC*	EMS	Shatter resistant double mutants	Laga 2013 (Patent)
B. napus	*BnSHP1*	RNAi	RNAi-induced shatter resistance; no detailed analyses	Kord et al. 2015
B. napus	*BnIND*	EMS	Shatter resistant double mutants	Laga et al. 2015 (Patent)
B. oleracea, B. rapa	*BoIND, BrIND*	EMS, RNAi	Conserved function of *BoIND, BrIND,* and *IND*	Girin et al. 2010
Lepidium campestre	*LcALC, LcFUL, LcIND, LcSHP1/2*	RNAi, overexpression	Conserved silique developmental pathway compared with *A. thaliana*	Lenser and Theißen 2013

1.2.2 Phenotyping strategies

A plethora of phenotyping strategies for silique shatter resistance has been described in the literature. The methods can be grouped into three major classes: Mechanical tests, microscopic observations, and field trials (Table 2). Mechanical tests and microscopic observations can highlight differences in silique strength or silique structure, from which shatter resistance can be inferred. In most cases, microscopic observations yield qualitative results whereas mechanical tests reveal quantitative distributions. However, being a quantitative trait, shatter resistance is prone to environmental influences. Consequently, field trials are inevitable for the final estimation of genotypic effects. In some studies, shatter resistance trials conducted in the laboratory were compared with field performance. Random impact tests explained 56-80% of variation in yield losses, depending on the origin of the assessed siliques (Wang et al. 2007). Siliques sampled from the field trial showed a higher correlation with seed losses than siliques from greenhouse experiments.

Table 2. Non-exhaustive overview of strategies for the estimation of silique shatter resistance.

	Phenotyping strategy	**Measure of shatter resistance**	**Reference**
Mechanical tests	Cantilever test	Bending energy (mJ)	Kadkol et al. 1984
	Pendulum test	Rupture energy (μJ)	Liu et al. 1994
	Peeling test with glue bridge	Maximum opening force (N)	Davies and Bruce 1997
	Random impact test (RIT); controlled agitation of siliques together with steel balls	Half-life (s)	Bruce et al. 2002
	Microfracture test of isolated silique sections	Fracture energy (μJ)	Child et al. 2003
	Variable-speed pod splitter test	Breakage speed (rpm)	Squires et al. 2003
Microscopic observations	Scanning electron microscopy of valve margins	Rough vs smooth surface	Morgan et al. 1998
	Stained silique cross sections	Presence/ absence of lignified layer	Liljegren et al. 2004
	Observation of replum valve-joint area	Replum valve-joint area index (mm^2)	Hu et al. 2015
Field trials	Visual and tactile scoring of shatter resistance	Field score (0-5)	Morgan et al. 2000
	Collection of shattered seeds	Seed loss (kg ha^{-1}, %)	Cavalieri et al. 2014

1.2.3 Current activities to breed silique shattering resistant oilseed rape

Breeding companies put substantial effort in the development of shatter resistant rapeseed varieties. Bayer CropScience developed shatter resistance through the selection of EMS (ethyl methanesulfonate)-induced *Bnind* mutations which they crossed into the hybrid varieties 'InVigor L140P' and 'InVigor L233P'. The genetic shatter resistance of Monsanto's breeding programs, which are distributed under the DEKALB trademark, originates from radish (*Raphanus raphanistrum*) and was introduced as a side-product of the 'Ogura' hybridization system. Nothing specific has been communicated about the shatter resistance genetics of varieties sold by Limagrain (e.g. 'Artoga' or 'Architect') and Pioneer Hi-Bred (e.g. '45M38' or '45CM36').

Although shatter resistant rapeseed varieties are on the market, it is difficult for other breeders to cross this trait into their own plant material. As discussed earlier, phenotyping shatter resistance is laborious and time-consuming. Therefore, reliable genetic markers are essential to track resistance-conferring alleles in breeding programs. As a prerequisite for marker

development, the underlying gene must be known. To my knowledge, to date only the *Bnind* alleles used by Bayer CropScience were described in detail but they are protected by a patent (Laga et al. 2015). Consequently, novel variation in shatter resistance is required to be made available to breeders worldwide.

1.3   Role of mutations in plant domestication and breeding

The genomes of all organisms are subject to spontaneous mutations, originating for example from errors in DNA synthesis or from lesions caused by chemical reactions like depurination and deamination (reviewed in Maki 2002). Rates of spontaneous mutations differ between species (Drake et al. 1998). For Arabidopsis, 7×10^{-9} base substitutions per site per generation were estimated by whole genome sequencing of mutation accumulation lines obtained after 30 inbreeding cycles (Ossowski et al. 2010). Thus, spontaneous mutations contribute to genetic variation, which ultimately drives evolution.

By domesticating wild plants, humans unconsciously started to exploit genetic variation. The common understanding is that approximately 12,000 years ago, hunter-gatherers began deliberately collecting and growing wild plants (Meyer and Purugganan 2013). In the course of domestication, plants with traits superior for human consumption or for cultivation were selected so that their progenies diversified more and more from the wild origin. A prominent example is the domestication from wild emmer (*Triticum dicoccoides*) into cultivated emmer (*T. dicoccum*), which involved the selection of a non-brittle rachis that reduced yield losses. The causal mutations underlying the non-brittle rachis domestication trait, an essential trait for modern bread wheat and durum wheat (*T. aestivum, T. durum*), were recently identified (Avni et al. 2017).

While early farmers could only select favorable mutations indirectly based on the phenotype, scientists nowadays have access to genomic resources, which makes breeding more effective. Sequence information is for example necessary for the development of molecular markers (Garcia and Mather 2014), which can be used to identify polymorphisms that cause a certain trait (map-based cloning). To cite examples, recent mapping studies revealed natural genetic variation for enhanced soybean (*Glycine max*) yield (Lu et al. 2017) and resistance to a parasitic weed in sorghum (*Sorghum bicolor*; Gobena et al. 2017). Such traits can then be introduced into breeding programs by crossing.

Both domestication and modern breeding create genetic bottlenecks by preferential propagation of selected plants (reviewed in Shi and Lai 2015). The consequence is a reduction of genetic diversity, which seems to have been higher during the lengthy process of domestication than during recent breeding history (Hyten et al. 2006; Hufford et al. 2012).

Oilseed rape is a relatively young crop with a low genetic variation due to strong selection of 00-quality traits. In the resequencing data of Schmutzer et al. (2015), 61% of gene models showed little to no variation between 52 *B. napus* accessions. However, breeding progress relies on a broad variation so that favorable characteristics can be selected. Wide crosses with other *Brassicaceae* as well as the resynthesis of *B. napus* by deliberately crossing *B. rapa* and *B. oleracea* can introduce novel alleles. Often, incompatibility of components of wide crosses leads to nonviable embryos. This issue can be overcome by ovary and embryo culture approaches (Wen et al. 2008). This strategy has for example been followed to introduce auxinic herbicide tolerance from *Sinapis arvensis* or sclerotinia resistance from *B. oleracea* (Jugulam et al. 2015; Mei et al. 2015). Genes from even more distant organisms that cannot be crossed, can be brought in by genetic transformation. An influential example is the resistance to the herbicide glyphosate. Glyphosate inhibits the plants' 5-enolpyruvylshikimate-3-phosphate synthase (EPSPS) which usually catalyzes the

biosynthesis of aromatic amino acids (Steinrücken and Amrhein 1980). By providing a bacterial EPSPS that is not affected through glyphosate, herbicide resistance can be achieved in a transgenic manner (Comai et al. 1985; Kahrizi et al. 2007). Another strategy to increase genetic variation is the induction of mutations.

1.3.1 Mutation induction and detection

There are two main categories of mutation induction, namely random mutagenesis and targeted mutagenesis. While the first experiments involving random mutagenesis began in the 1920s (Muller 1927), targeting mutations in desired genomic sequences has just become possible with recent methodological developments.

1.3.1.1 Random mutagenesis

Random mutations can for example be induced through the transformation of T-DNA, by irradiation, and through chemical agents.

T-DNA mutagenesis involves the genetic transformation of a target organism with a T-DNA construct including a selectable marker, which integrates at a random position in the genome. Transgenic plants are selected and screened for T-DNA insertion sites. Homozygous lines containing genes disrupted by T-DNA sequences can then be used for functional analysis. A famous example of random T-DNA mutagenesis is the large Arabidopsis mutant collection, which is curated by the The Salk Institute for Biological Studies and can be accessed by scientists through several seed stock centers (Alonso et al. 2003).

Ionizing rays like gamma rays or fast neutrons affect DNA integrity in various complex ways, for example through the induction of reactive oxygen species which are able to cause double strand breaks (reviewed in Reisz et al. 2014). Naito et al. (2005) described Arabidopsis mutant alleles generated by gamma irradiation which comprised small to large deletions (1 bp to >6 Mbp) and sequence inversions. Fast neutron mutagenesis of Arabidopsis yielded 0.8 to 12 kb long deletions, sometimes erasing more than one complete gene (Li et al. 2001).

The list of chemical mutagens is long and keeps growing. Commonly, EMS is applied to plant seeds. EMS is an alkylating agent which mainly alters the constitution of guanine in a way that it can pair with thymine instead of cytosine, leading to C/G to T/A substitutions after DNA repair (Kim et al. 2006). Therefore, EMS mutagenesis can yield various types of single point mutations including splice site mutations, missense mutations, and premature stop codon mutations.

Several strategies were developed to identify mutations of interest from plant populations mutagenized by irradiation or chemical treatment. In case the underlying gene is not yet known, forward genetics studies involving map-based cloning can be employed (Dally et al. 2014). A common reverse genetics approach is termed Targeting Induced Local Lesions in Genomes (TILLING). Pooled DNA of mutant plants is amplified by PCR with fluorescence-labelled, gene-specific primers. Then, the PCR products are denatured and reannealed, thus forming heteroduplexes of polymorphic sequences which are restricted by a single-strand specific nuclease (*Cel*I). The digested fragments are visualized by denaturing polyacrylamide gel electrophoresis (Till et al. 2006). The TILLING strategy has since been improved with the advance of analysis techniques like high-resolution melting curve analysis (HRM) and next-generation sequencing (NGS; Lochlainn et al. 2011; Gilchrist et al. 2013).

Important to mention, a major drawback of random mutagenesis by irradiation or chemical treatments is the amount of undesired background mutations. In an EMS-treated rapeseed

mutant population, mutation frequencies ranged between 1/12 kb to 1/72 kb (Harloff et al. 2012; Guo et al. 2014), which sums up to 16-94 thousand mutations per single plant (rapeseed genome size: 1,130 Mb; Chalhoub et al. 2014). Consequently, the plants show numerous mutation-related traits which can reduce the general fitness and need to be crossed out before the plants can be integrated into breeding programs. Nonetheless, mutants have been extensively used in crop breeding: The International Atomic Energy Agency hosts an online database with currently 3,249 officially registered mutant varieties which originated from physical and chemical mutagenesis (https://mvd.iaea.org, accessed 23.08.2017; Maluszynski 2001).

1.3.1.2 Targeted mutagenesis

In general, targeted mutagenesis begins with the induction of double-stranded breaks (DSBs) at specific sites in the genome. Cells have natural DNA repair systems which, however, from time to time cannot fully restore the initial DNA sequence. While the non-homologous end-joining (NHEJ) pathway ligates overlapping ends properly back together, other DSBs need to be processed before they can be fixed, thereby introducing indel mutations (reviewed in Lieber 2008). Another mechanism, the homology-directed repair (HDR), involves homologous recombination with a repair template like the sister chromatid (reviewed in Puchta 2004). By providing an artificial repair template with homology arms, HDR can be exploited for targeted sequence insertion after DNA cleavage (Puchta et al. 1996). But how to cause a DSB at a desired position in the first place?

One way is to engineer meganucleases like microbial homing endonucleases, which are defined by their long DNA recognition sites and thus cut only at a few loci per genome. Although the targeted restriction of meganucleases is difficult to customize (reviewed in Stoddard 2011), such an approach was for example followed to insert herbicide resistance genes into cotton (*Gossypium hirsutum*; D'Halluin et al. 2013).

The invention of zinc finger nucleases (ZFNs), hybrid molecules of zinc finger DNA-binding domains fused to a non-sequence-specific cleavage domain (Smith et al. 2000), markedly facilitated the targeted restriction of desired sequences. Each zinc finger binds a DNA triplet (Pavletich and Pabo 1991), making the ZFN a modular system. The ZFN concept was since validated through mutagenesis of different plant species including tobacco (*Nicotiana tabacum*) and soybean (Townsend et al. 2009; Sander et al. 2011).

While zinc fingers recognize DNA triplets, Boch et al. (2009) revealed that the tandem repeats of transcription activator–like effectors (TALEs) identify single bases. After the addition of DNA cleavage domains, TALE nucleases (TALENs) were employed to mutate among others rice (*Oryza sativa*), maize (*Zea mays*), and wheat (Li et al. 2012; Wang et al. 2014; Kelliher et al. 2017).

The latest advance in targeted mutagenesis strategies was the discovery of RNA-programmable endonucleases which are part of the bacterial adaptive immune system (Jinek et al. 2012). Prokaryotes acquire a genetic memory of invading DNAs in the form of clustered regularly interspaced short palindromic repeats (CRISPR; Bolotin et al. 2005; Pourcel et al. 2005). CRISPR-derived RNAs (crRNAs) are able to bind to complementary DNA which is then degraded with the help of CRISPR-associated (Cas) proteins (Jore et al. 2011). Noticeably, the presence of a protospacer adjacent motif (PAM) is required for target sequence recognition (Mojica et al. 2009). Currently, five CRISPR/Cas systems are known, involving different sets of Cas proteins (Makarova et al. 2011). In the type II system, a single multi domain protein, namely Cas9, locates and restricts the target DNA after forming a complex with crRNA and trans-activating crRNA (tracrRNA; Jinek et al. 2012). Figure 2

illustrates how the CRISPR/Cas system is exploited for targeted mutagenesis: Cas9 together with a personalized single guide RNA (sgRNA, fused crRNA and tracrRNA; Jinek et al. 2012) is introduced into the target cell where it induces DSBs. In this way, desired mutant traits have been induced in multiple plant species, some through NHEJ-related frameshift mutations (Wang et al. 2014; Chandrasekaran et al. 2016; Zhou et al. 2016), others involving the provision of an artificial repair template for HDR-mediated sequence replacement (Li et al. 2016a; Sauer et al. 2016).

To be able to judge putative risks posed by targeted mutagenesis, several studies assessed off-target activities of Cas9. While some sgRNAs caused detectable, undesired mutations (Cradick et al. 2013; Shan et al. 2013), others did not (Nekrasov et al. 2013; Feng et al. 2014). A comprehensive test of >700 sgRNA variants delivered to human cells suggested that Cas9 specificity depends on the position and number of mismatches between sgRNA and DNA (Hsu et al. 2013). Specifically, Hsu et al. (2013) concluded that an 8 to 14 bp seed sequence determines the cleavage accuracy. This finding allows for a well-informed Cas9 target design with a reduced probability of off-target events. However, even if off-target mutations occurred *in planta*, they could be crossed out in following generations.
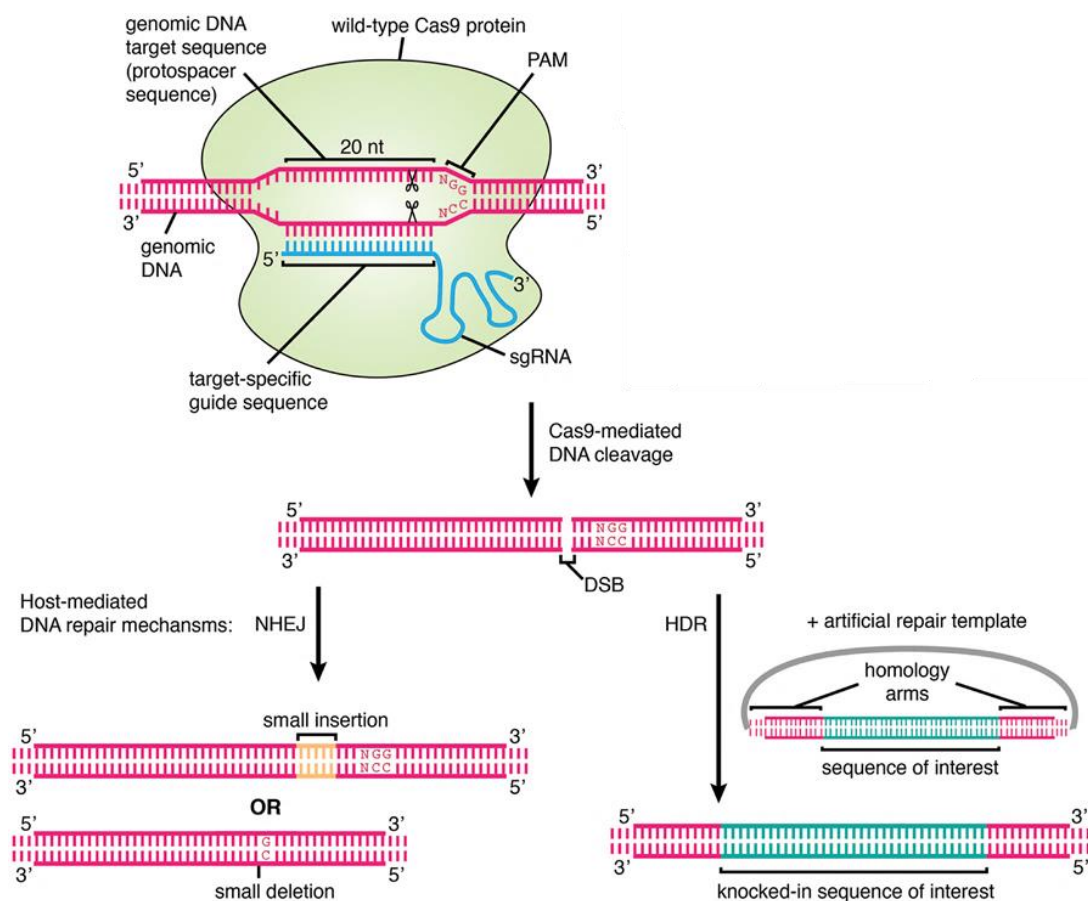
Figure 2. The mechanism of Cas9-mediated mutagenesis. A sgRNA molecule with a 20 nt user-defined target guide sequence leads the Cas9 protein to the genomic DNA target, which must lie next to a protospacer adjacent motif (PAM). Cas9 induces a double strand break (DSB) which is repaired by the cell's innate repair mechanisms. Non-homologous end-joining (NHEJ) can cause indel mutations whereas homology-directed repair (HDR) can introduce specific sequences, for example artificially provided as a plasmid, by homologous recombination. (modified from Agrotis and Ketteler 2015)

1.4 Hypotheses and objectives

This study was built on two hypotheses: (1) Rapeseed plants carrying loss-of-function mutations in all homoeologs of dehiscence zone identity genes, which are transcriptionally active in the silique, are shatter resistant. (2) CRISPR/Cas9-mediated mutagenesis can knock out several homoeologs at a time.

There were three major questions to answer:
1. Can Cas9 efficiently mutate multiple homoeologs in parallel?
2. How do mutations in selected dehiscence zone identity genes alter the shatter resistance in rapeseed?
3. Can shatter resistance be reliably phenotyped by bench-top experiments with silique samples collected from greenhouse trials?

Therefore, the main objectives of this study comprised: the detection of EMS-induced mutations in coding sequences of dehiscence zone identity genes, the targeted mutagenesis of dehiscence zone identity genes by a CRISPR/Cas9 approach, the phenotypic characterization of the mutants obtained, and the correlation of greenhouse experiments with field trials.

2   CRISPR-Cas9 targeted mutagenesis leads to simultaneous modification of different homoeologous gene copies in polyploid oilseed rape (*Brassica napus*)

2.1   Summary

A single CRISPR-Cas9 target efficiently induces heritable mutations in two rapeseed gene homoeologs.

2.2   Abstract

In polyploid species, altering a trait by random mutagenesis is highly inefficient due to gene redundancy. We have stably transformed tetraploid oilseed rape (*Brassica napus*) with a CRISPR-Cas9 construct targeting two *ALCATRAZ* (*ALC*) homoeologs. *ALC* is involved in valve-margin development and thus contributes to seed shattering from mature fruits. Knocking out *ALC* would increase shatter resistance to avoid seed loss during mechanical harvest. We obtained a transgenic T_1 plant with four *alc* mutant alleles by the use of a single target sequence. All mutations were stably inherited to the mprogeny. The T_2 generation was devoid of any wild type alleles, proving that the underlying T_1 was a non-chimeric double heterozygote. T-DNA and *ALC* loci were not linked as indicated by random segregation in the T_2 generation. Hence, we could select double mutants lacking the T-DNA already in the first offspring generation. However, whole genome sequencing data revealed at least five independent insertions of vector backbone sequences. We did not detect any off-target effects in two genome regions homologous to the target sequence. The simultaneous alteration of multiple homoeologs by CRISPR-Cas9 mutagenesis without any background mutations will offer new opportunities for using mutant genotypes in rapeseed breeding.

2.3   Introduction

The primary gene pool of oilseed rape (*Brassica napus*, 2n = 38, AACC) has a low genetic diversity (Bus et al. 2011). Apart from wide crosses and genetic modification, spontaneous and induced mutations have been used to increase genetic variation. Inducing mutations with a measurable phenotypic effect is complicated by its amphidiploid nature. The nuclear genome consists of two genomes A and C originating from a hybridization between *Brassica rapa* (2n = 20, AA) and *Brassica oleracea* (2n = 18, CC). Consequently, every ortholog of Arabidopsis (*Arabidopsis thaliana*) is represented by at least two rapeseed homoeologs with putatively redundant functions. To alter a monogenic trait, it is therefore necessary to combine mutated homoeologs from both subgenomes (Emrani et al. 2015; Wells et al. 2014).

The acquisition of novel desired mutations has been facilitated by the introduction of the CRISPR-Cas9 system. The Cas9 nuclease can easily be programmed to induce double strand breaks within a target sequence (Doudna and Charpentier 2014). Those breaks are quickly mended by the innate repair system via non-homologous end joining (NHEJ). However, this repair mechanism frequently creates small insertions and deletions, which if located within a coding sequence often result in frame shift mutations. The application of CRISPR-Cas9 targeted mutagenesis in plants has been demonstrated not only in Arabidopsis (Fauser et al. 2014; Feng et al. 2014) but also in crops like wheat (*Triticum aestivum*), tomato (*Solanum lycopersicum*) and rice (*Oryza sativa*) (Wang et al. 2014; Brooks et al. 2014; Li et al. 2016b).

To our knowledge a proof of concept in oilseed rape has not been published yet. Lawrenson et al. (2015) reported the successful application of a CRISPR-Cas9 approach in *B. oleracea*, suggesting that a transfer to oilseed rape would also be feasible. There is one more feature of the CRISPR-Cas9 system which is of particular interest for the application in oilseed rape. The Cas9 protein when directed to multiple target sites can induce mutations simultaneously in different (homoeologous) sequences as has already been demonstrated in the tetraploid potato (*Solanum tuberosum*, 2n = 4x = 48) to alter starch synthesis (Andersson et al. 2017).

We applied the CRISPR-Cas9 system for targeted mutagenesis to reduce yield loss in oilseed rape. A major issue of rapeseed production is its natural seed dispersal strategy that involves shattering of dry fruits, the so-called siliques. In extreme cases, pre-harvest losses of up to 25 % have been reported (Price et al. 1996). Numerous studies in the model plant Arabidopsis, recently reviewed by Ballester and Ferrándiz (2017), have unraveled a gene network controlling the development of specialized silique tissues essential for fruit dehiscence. The basic regulators are the transcription factors *SHATTERPROOF1* and *2*, *INDEHISCENT* and *ALCATRAZ* (*ALC*). *SHATTERPROOF1* and *2* redundantly induce expression of *INDEHISCENT* and *ALCATRAZ*. While *indehiscent* mutants are completely indehiscent due to the absence of both lignified cells and separation layer at the predetermined breaking point of the silique (Liljegren et al. 2004), *alc* mutants only lack the separation layer (Rajani and Sundaresan 2001). We hypothesize that rapeseed plants with knocked-out *alc* function produce siliques with an intermediate level of shatter resistance which could result in lower seed loss during threshing.

Here, we report the targeted mutagenesis of two *BnALC* homoeologs by a CRISPR-Cas9 approach. All four alleles were mutated in a single T_1 plant using only one target sequence. This demonstrates the potential of CRISPR-Cas9 mediated genome editing for the simultaneous modification of different homoeologous gene copies in a polyploid species.

2.4   Results

2.4.1   Sequence identification for multiple homoeolog targeting

We aimed to knock out two rapeseed *ALC* homoeologs, *BnaA.ALC.a* (BnaA07g12110D) and *BnaC.ALC.a* (BnaC07g16290D) by CRISPR-Cas9 mediated mutations. For this purpose, we searched for sequences with high similarity between both genes. We chose a 20 bp target region from the *BnaA.ALC.a* homoeolog located in exon 1B upstream of the bHLH transcription factor domain (Figure 3A). This sequence is highly conserved between both homoeologs and is located adjacent to a 'NGG' protospacer-adjacent motif (PAM), which is an essential targeting component for Cas9. The only difference between the target sites is a SNP in the *BnaC.ALC.a* homoeolog 10 bp upstream of the PAM sequence (95 % identity).
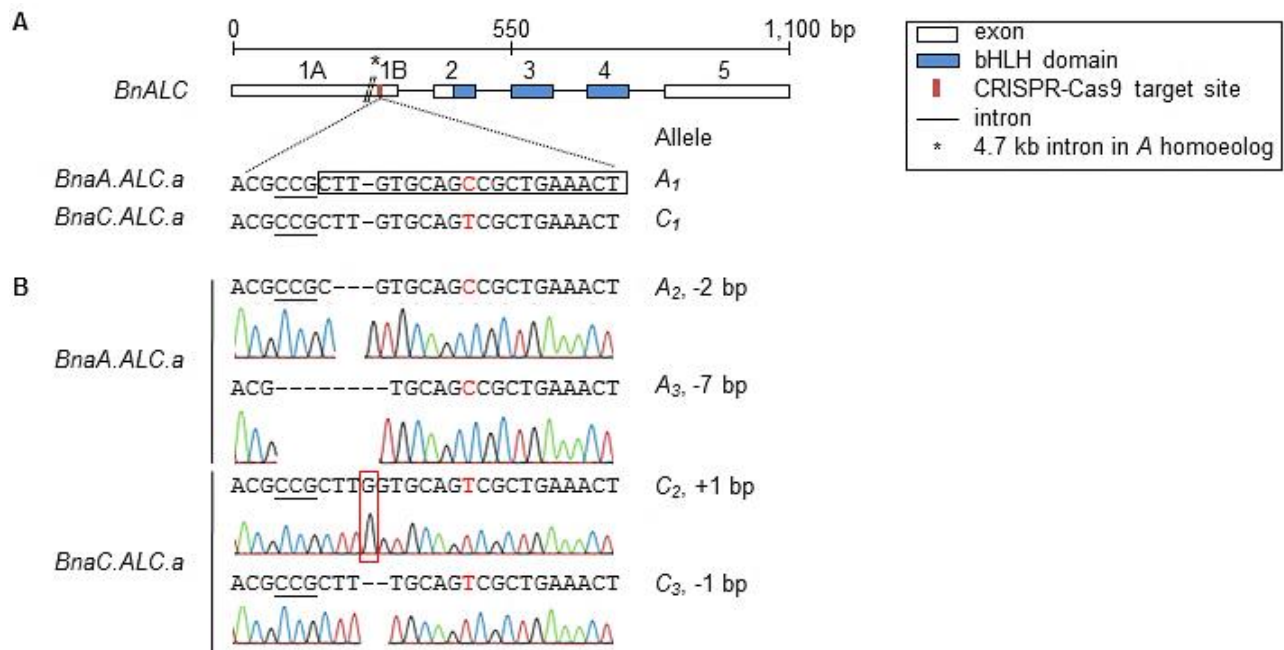
Figure 3. NHEJ-mediated knock-out of two *BnALC* homoeologs. A, CRISPR-Cas9 target upstream of the bHLH domain of *BnALC*. The protospacer-adjacent motif (PAM) is underlined. The boxed target sequence was based on *BnaA.ALC.a* and comprised a single-nucleotide polymorphism (SNP) to *BnaC.ALC.a* at position 10, highlighted in red. B, Four CRISPR-Cas9 induced mutant alleles detected by Sanger sequencing of a single double heterozygous T_1 rapeseed plant. The size of each deletion/ insertion and the name of the allele are indicated on the right. The inserted base of allele C_2 is highlighted by a red box.

Then, we performed a BLAST search with our target sequence against the rapeseed genome (Darmor-*bzh*, version 4.1). Apart from the targeted *BnALC* paralogs, only two sequences were found which are located next to a PAM site (Figure 4). The first sequence which is 90% identical to the selected one belongs to gene model BnaC04g13390D which is predicted to encode a protein with a bHLH domain. The sequence similarity between the bHLH domains of *BnaA.ALC.a* and BnaC04g13390D is 81% whereas the similarity between the overall amino acid sequences is much lower (53%). The second sequence (80% identity) is located on chromosome C02 but without any predicted gene model. Based on these findings we expected a *BnALC* gene-specific mutagenesis without off-target effects.

Figure 4. Alignment of the CRISPR-Cas9 target sequences from *BnaA.ALC.a* and *BnaC.ALC.a* in comparison to two potential off-target sites identified in the reference genome of Darmor-*bzh* by a BLAST search. The protospacer-adjacent motifs (PAM) are underlined. SNPs are highlighted in red.

2.4.2 Rapeseed transformation and T_2 seed production

We cloned the 20 bp target sequence into the pChimera plasmid (Fauser et al. 2014) upstream of the chimeric sgRNA and under the control of the Arabidopsis Ubiquitin 6-26 promotor. Then, the construct was cloned into the final pCas9-TPC plasmid (Fauser et al. 2014), containing a *bar* resistance cassette and a plant codon-optimized *Streptococcus pyogenes* Cas9 nuclease under the control of the constitutive *Petroselinum crispum* Ubiquitin 4-2 promotor.

We co-cultivated 625 hypocotyl explants of the spring rapeseed cv Haydn with *Agrobacterium tumefaciens* containing the recombinant pCas9-TPC plasmid. We obtained 370 independent calli of which 112 initiated shoot regeneration under herbicide selection. Four shoots from four independent events (named CP1-4) survived an extended herbicide treatment and were regenerated as rooted plantlets after 9 to 11 months in tissue culture. These four T_1 plants were transferred to the greenhouse, where they produced T_2 seeds after self-pollination. We used the T_1/T_2 nomenclature in accordance with inbred populations where the F_2 is the first segregating generation.

2.4.3 Identification of CRISPR-Cas9 induced *BnALC* mutations

We performed a PCR test using Cas1_f and Cas1_r primers (Table S1) to select T_1 plants which carry the transgene insertion. The primers amplify a T-DNA region containing the CRISPR-Cas9 target sequence and the sgRNA. Only one plant (CP1) turned out to be transgenic which results in a transformation rate of 0.9% as calculated by the number of induced shoots. The rate of false-positive shoots, surviving prolonged herbicide selection but being non-transgenic, was 2.7%.

Then, we sequenced both *BnALC* homoeologs of the transgenic CP1 plant. We expected that this plant carries at least one mutation in one out of four *BnALC* alleles. To our surprise, we found mutations in all target sequences, two in *BnaA.ALC.a* and two in *BnaC.ALC.a* (Figure 3B). For easiness of understanding, the respective alleles were termed A_2, A_3, C_2, and C_3. Thus, CP1 does not contain non-mutated ('wild type') alleles (A_1/C_1) any more, at least not in the leaf tissue we analyzed. It could either be a double heterozygote or a chimeric plant. As expected, the CRISPR-Cas9 induced mutations occurred in the vicinity of the PAM sequence. We identified deletions of 1, 2 and 7 bp and a 1 bp insertion, respectively. Those frame shift mutations will most likely result in non-functional proteins. Moreover, in silico analysis revealed that the mutations gave rise to premature stop codons upstream of the bHLH domain. In conclusion, we reason that CP1 has no functional *BnALC* gene any more.

2.4.4 Inheritance of *BnALC* mutations

We wanted to know how the mutations and the transgene are inherited. If CP1 was not a chimera we expected a digenic segregation pattern. Moreover, we expected that the *BnALC* loci and the transgene locus are not linked. The mutant plant CP1 yielded 858 T_2 seeds. First, we screened 36 T_2 plants by PCR using the Cas1_f and Cas1_r primers which bind to the multiple cloning site of the pCas-TPC vector (Table S1). We found 27 transgenic and nine non-transgenic plants which is perfectly matching a Mendelian segregation for a single gene (Table 3). Thus, CP1 carries a single Cas9 insertion.

Then, both *BnALC* homoeologs from all T_2 plants were sequenced. All plants carried the mutated alleles, proving that CP1 was a non-chimeric double heterozygote (A_2A_3/C_2C_3). Furthermore, the segregation pattern was in accordance with a digenic inheritance and random segregation between genes. The transgene insertion and the mutations were not linked, as we could find non-transgenic plants with all four mutant alleles. Altogether, we found eight out of nine genotypes expected for random segregation. Only A_2A_2/C_3C_3 was missing from the T_2 plants investigated which is not surprising because the expected frequency is only 6.25 %. A phenotypical inspection of the T_2 plants did not reveal any visible differences from cv Haydn. The plants displayed the same architecture and their fertility was not different from the wild type (Figure 5). Taken together, we have produced in one step a non-chimeric double mutant devoid of any wild type allele but carrying mutations in all *BnALC* homoeologs.

Table 3. Inheritance of CRISPR-Cas9 induced *BnALC* mutations. Thirty-six T_2 plants were tested for the presence of the transgene by PCR. Both *BnALC* homoeologs were sequenced to identify the mutated alleles. E, expected number of plants; O, observed number of plants

Plants	Transgene Genotypes			*alc* Genotypes									
	Transgenic	Nontransgenic	X^2 Test[a]	A_2A_2/C_2C_2	A_2A_2/C_2C_3	A_2A_2/C_3C_3	A_2A_3/C_2C_2	A_2A_3/C_2C_3	A_2A_3/C_3C_3	A_3A_3/C_2C_2	A_3A_3/C_2C_3	A_3A_3/C_3C_3	X^2 Test[b]
O	27	9	0	3	4	0	3	14	2	1	6	3	8.52
E[c]	27	9	2.25	2.25	4.25	2.25	4.25	9	4.25	2.25	4.25	2.25	

[a] 3:1 segregation, $X^2_{(0.999,2)} = 13.82$. [b] 1:2:1:2:4:2:1:2:1 segregation, $X^2_{(0.999;8)} = 26.12$. [c] Under the assumption that the T_1 parent CP1 was nonchimeric (A_2A_3/C_2C_3).
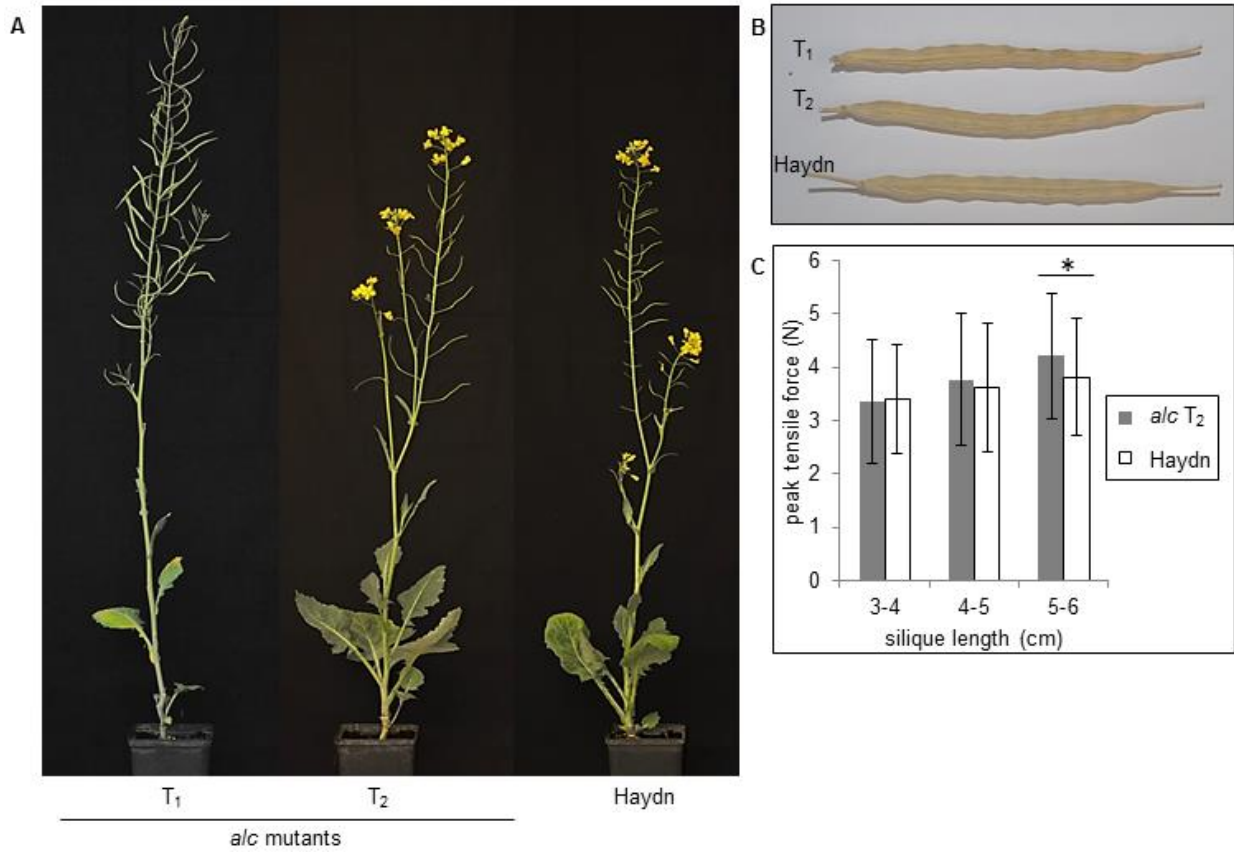
Figure 5. Growth types of CRISPR-Cas9 *alc* mutants resemble the wild type while siliques are more shatter resistant. A, T_1 and T_2 rapeseed plants carrying CRISPR-Cas9 mutated *BnALC* alleles next to cv Haydn which had been used for transformation. Plants were grown in 11 x 11 cm pots in the greenhouse. B, *alc* mutations show no visible effect on mature siliques of T_1 and T_2 mutants compared with cv Haydn. C, Results of shatter resistance measurements of *alc* T_2 in comparison with cv Haydn. Peak tensile forces are displayed as means of siliques grouped according to their length. Error bars represent standard deviation. A significant difference is indicated by the asterisk (Student's *t* test, $P < 0.05$).

2.4.5 Searching for putative off-target effects

We searched in our mutant plant CP1 for possible off-target activities of the Cas9 endonuclease. We assumed that if any of these activities had occurred, mutations are to be expected within the two sequences with high similarity to our *BnALC* genes (BnaC04g13390D and the non-coding sequence on C02). We designed PCR primers which bind to flanking sequences of the potential off-target sites (Table S1). We sequenced the resulting PCR products from CP1 and from five T_2 offspring. As we did not find any sequence variations compared to the Darmor-*bzh* reference genome, we reason that the plants probably do not carry off-target mutations in these regions.

2.4.6 Analysis of whole genome sequence regarding T-DNA insertions

We wanted to know whether CP1 houses any other T-DNA vector sequences apart from the expected T-DNA insertion. This information is important for field cultivation as a non-GMO plant. Whole genome sequence data of the T_1 plant CP1 was produced by Illumina sequencing. A total of 412 million raw data paired-end reads were produced. After quality trimming, the genome coverage was, on average, 20x.

The reads were mapped against the sequence of the transformation vector to validate the assumption of a single T-DNA insertion which was based on segregation analysis. The coverage of T-DNA reads was 20x like the average genome coverage, thus confirming a single-copy locus (Figure S2).

Unexpectedly, the whole genome data mapped not only against the T-DNA but also against a 700 bp vector backbone region. This region encodes a bacterial origin of replication (pUC19 ori) and was strongly enriched with >100x coverage. Furthermore, Illumina sequence reads anchored the pUC19 ori to five different rapeseed genomic sequences, suggesting at least five insertions of the vector fragment in the plant genome.

2.4.7 Silique shatter resistance

We assessed shatter resistance of T_2 *alc* mutants in comparison with cv Haydn by disrupting single siliques that we attached to a force meter. Maximum tensile forces were measured as the silique walls were torn away from the replum. We grouped siliques according to their lengths into three size classes of 3 to 4 cm, 4 to 5 cm, and 5 to 6 cm. Longer siliques tended to be more robust than short siliques, implicating a correlation of silique length and shatter resistance (Figure 5C). Regarding 3- to 4-cm-long and 4- to 5-cm-long siliques, no difference in silique robustness was observed between the two genotypes. However, 5- to 6-cm-long siliques of the *alc* mutants were more shatter resistant than same-sized siliques of the cultivar.

2.5 Discussion

We have demonstrated the potential of CRISPR-Cas9-targeted mutagenesis in the rapeseed genome. The main findings can be summarized as follows. (1) Frame-shift mutations have been induced within the target sequence of *BnaA.ALC.a*. (2) Moreover, mutations were also induced within the second *BnALC* homoeolog *BnaC.ALC.a* although it differs from the sgRNA target by one SNP. (3) The mutation efficiency was 100% and the T_1 plant was nonchimeric; all T_2 offspring were mutants. (4) The lack of mutations within two potential off-target sites with high homology to the sgRNA target sequence indicates that CRISPR-Cas9 targeted mutagenesis in rapeseed could be very precise. (5) We recovered T_2 plants with four mutated *BnALC* alleles that did not contain any T-DNA sequences. (6) Whole genome

sequencing data revealed the integration of vector backbone sequences into the rapeseed genome. (7) Five- to 6-cm-long siliques of *alc* mutants were more shatter resistant than siliques of cv Haydn.

2.5.1 Specificity of the Cas9 system

We had designed a sgRNA which is identical to the *BnaA.ALC.a* target region whereas it differs from *BnaC.ALC.a* by a SNP 10 nucleotides upstream of the PAM site. Finding induced mutations also in *BnaC.ALC.a* is in line with previous reports that Cas9 tolerates mismatches within the target site (Hsu et al. 2013; Endo et al. 2015; Lawrenson et al. 2015). Regarding polyploid species like rapeseed, this opens up new opportunities for a one-step modification of whole gene families. Simultaneous editing of three homoeoalleles in hexaploid bread wheat was previously reported by the use of a transcription activator-like effector nuclease (TALEN; Wang et al. 2014). Meanwhile, mutating three to four closely related genes with a single CRISPR-Cas9 target has been achieved for Arabidopsis and tetraploid potato (Yan et al. 2016; Andersson et al. 2017).

We did not observe any off-target effects in two sequences which are homologous to the intended *BnALC* target. The number and location of SNPs between the target sequence and the potential off-target site are likely to play a role as was already described for an extensive off-target study in human cells with more than 700 sgRNA variants tested (Hsu et al. 2013). In our study, the off-target sites contained either two SNPs at positions 10 and 12 upstream of the PAM or four SNPs at positions 4, 14, 19 and 20 (Figure 4). This minimizes the probability for off-target mutations to occur in any other sequence of the genome with an even lower similarity to the sgRNA.

2.5.2 Integration of vector backbone fragments

After *A. tumefaciens*-mediated transformation, we expected to find only T-DNA insertions of the region flanked by left and right border into the plant genome. However, we also detected sequences of the pUC19 origin of replication in our T_1 plant. The observation of integrated vector backbone fragments was recently reported for transgenic Arabidopsis, wheat, and rice (Schouten et al. 2017; Wang et al. 2016; Li et al. 2016c). Thus, backbone insertions seem to be common across plant species.

To some extent, those sequence insertions are a shortcoming of *A. tumefaciens*-mediated CRISPR-Cas9 transformations. We will establish a PCR based protocol to select homozygous mutants lacking any vector sequences. This will allow us to perform field trials even under strict European GMO regulations. In the future, this problem could be avoided by using DNA-free transformation techniques like in vitro pre-assembled Cas9-sgRNA ribonucleoproteins (RNPs). Successful induction of CRISPR-Cas9 mutations by RNPs has been demonstrated for Arabidopsis, tobacco (*Nicotiana tabacum*), rice, lettuce (*Lactuca sativa*), and maize (*Zea mays*; Woo et al. 2015; Svitashev et al. 2016), although a routine application in crops remains to be demonstrated.

2.5.3 The efficiency of the CRISPR-Cas9 mutation system in rapeseed in comparison with EMS mutagenesis

The 100% success rate regarding mutations in all *BnALC* alleles suggests high Cas9 activity in early stages of tissue culture, giving rise to nonchimeric plants. Lawrenson et al. (2015) reported lower mutation frequencies in first generation transgenic barley (*Hordeum vulgare*) and *B. oleracea* plants of 23% and 10%, respectively. The frequencies of potato lines with multiple mutated alleles ranged between 20% and 67% (Andersson et al. 2017). In rice, the expression level of Cas9 and sgRNA as well as the extent of the culture period of the

transgenic callus impact the frequency of CRISPR-Cas9 induced mutations. Mikami et al. (2015) reported that high expression levels and long culture periods increased the number of mutations. In our experiment, we did not measure the expression rate of the transgenic sequences in T_1 plants because we assume a strong expression under the control of the constitutive ubiquitin promotors. Moreover, their high transcriptional activity was confirmed by the mutations in the target sequences. In conclusion, we do not see a reason to modify the expression cassettes for future CRISPR-Cas9 experiments with rapeseed.

Conventionally, novel genetic variation has been induced into breeding programs by random mutagenesis through irradiation or treatment with chemicals like EMS. A well-established method is the identification of mutations from randomly-mutagenized plant populations by TILLING (Till et al. 2006). However, the huge background mutation load is a severe drawback of randomly induced mutations. For rapeseed, after an EMS mutation experiment the number of background mutations was estimated to be in a range of 130,000 mutations per plant (Harloff et al. 2012). They can have a negative impact on various characters. We have observed stunted growth, abnormal inflorescence, and reduced seed yield in the M_2 generation (unpublished data).

Another problem arises mainly in polyploids if several homoeologs contribute independently to a phenotype. Chemical and irradiation mutagenesis only yield plants with single mutations in one or another homoeolog. The probability for double mutations to occur is extremely low. However, in many cases single mutations do not have the desired effect. As a consequence, different mutations must be combined in one genotype by time-consuming crossing and backcrossing procedures which can take many years. This has recently been demonstrated for genes which are involved in the biosynthesis of sinapine. Knockout of only one homoeolog had no measurable effect whereas a double mutant obtained after crossing two single mutants showed significantly reduced sinapine contents in the seed (Emrani et al. 2015).

In conclusion, the CRISPR-Cas9 system is clearly superior to classical mutagenesis. We propose that in the future, all members of a given gene family can be knocked out by a single CRISPR-Cas9 experiment and without off-target effects. Thus, targeted mutation induction will accelerate the introduction of mutants into breeding programs.

2.5.4 Silique measurements imply increased shatter resistance due to *alc* mutations

We assessed shatter resistance of *alc* mutants and cv Haydn by measuring the peak tensile force necessary to tear silique walls apart from the replum. While the genotypes had no effect on shatter resistance of short siliques, we observed an increased shatter resistance of *alc* siliques longer than 5 cm. This finding is promising, because field grown rapeseed usually produces siliques greater than 5 cm. Therefore, we expect to find stronger effects in the field as a verification of our greenhouse observations.

Compared to other rapeseed cultivars, cv Haydn has an elevated shatter resistance (data not shown). We had chosen this genotype for our experiments because of its high transformation efficiency (Boszoradova et al. 2011). However, cv Haydn is considered an old variety because it was released in the year 2000. The mutations can easily be introduced into current elite material by marker-assisted selection to breed new varieties with a high shatter resistance.

2.6   Conclusion

We demonstrate the power of the CRISPR-Cas9 system for targeted mutation induction in rapeseed. This technique opens new possibilities to precisely alter the function of genes avoiding the obstacles of random mutagenesis. Simultaneous modification of several homoeologs is of key interest to create new genetic variation in a polyploid species. Although the legal situation in Europe is not yet clear, we expect that CRISPR-Cas9 induced single (or oligo) nucleotide mutations will increase the genetic basis for rapeseed breeding in the future. Moreover, we demonstrated the power of whole genome sequencing to detect transformation vector backbone fragments in the recipient genome which must be eliminated from segregating offspring by marker-assisted selection. The next efforts of our research group regarding targeted mutagenesis will concern genes controlling the biosynthesis of secondary metabolites such as glucosinolates or phytic acid, which negatively impact the seed quality.

2.7   Materials and methods

2.7.1   Plant material

We used the spring rapeseed (*Brassica napus* 'Haydn') for hypocotyl transformation. Seeds were obtained from the seed company Norddeutsche Pflanzenzucht Hans-Georg Lembke.

For hypocotyl transformation, seeds were sterilized and plants were grown for 7 d on germination medium in complete darkness. Etiolated hypocotyls were cut into 1-cm pieces.

T_1 and T_2 plants were grown in 11- x 11-cm pots in the greenhouse (16 h of light/ 8 h of dark, 20 °C-23 °C). We mounted selfing bags at the beginning of flowering to control pollination.

2.7.2   *BnALC* sequences and putative off-target sites

Genomic sequences of the two *BnALC* homoeologs *BnaA.ALC.a* and *BnaC.ALC.a* were obtained from Hua et al. (2009). We performed a BLAST search of the sequences against the rapeseed reference genome (Darmor-*bzh* version 4.1) and identified them to correspond to gene models BnaA07g12110D and BnaC07g16290D (http://www.genoscope.cns.fr/brassicanapus/), located on chromosomes A07 and C07. The coding sequences span 657 and 651 bp and are organized in five exons. *BnaA.ALC.a* contains an additional intron of about 4.7 kb, splitting exon 1 into exon 1 A and B. A conserved basic helix-loop-helix (bHLH) domain ranges from exon 2 to 4.

Putative off-target sites were identified by performing a BLAST search of the target sequence against the reference genome. We designed primers for the amplification of off-target regions (Table S1). PCR amplicons from T_1 and T_2 plants were Sanger sequenced.

2.7.3   Vector construction and plant transformation

For targeted mutagenesis, we used the binary vector system pChimera and pCas9-TPC (Fauser et al. 2014). The transformation plasmid pCas9-TPC contains a *bar* cassette for herbicide selection in plants. A 20 bp target sequence neighboring a 5′-NGG PAM was selected in an exonic region upstream of the bHLH domain in *BnALC* (Figure 3A) and was cloned into the respective plasmid (Figure S1). The *Agrobacterium tumefaciens* strain GV3101 pMP90RK was used for plant transformation.

For rapeseed hypocotyl transformation, we followed the protocol described by Zarhloul et al. (2006) with modifications regarding the selection. We applied 500 mg L^{-1} carbenicillin to deplete *A. tumefaciens* and 6 mg L^{-1} phosphinothricin to select transgenic plants.

2.7.4   Mutant identification

Genomic DNA was isolated from leaf samples by a standard CTAB method. The presence of the transformation cassette was tested by PCR using primers Cas1_f and Cas1_r (Table S1; Figure S1).

CRISPR-Cas9 targeted mutations were identified by Sanger sequencing of PCR amplicons using primer combinations ALC33/ALC16 and ALC13/ALC12 (Table S1). In addition, PCR fragments of the T_1 plant were cloned into the pGEM-T Easy vector system (Promega, Mannheim, Germany) and transformed into *Escherichia coli*. Single colonies were picked for PCR and the amplicons were sequenced in the same way.

2.7.5   Illumina sequencing and sequence analysis

Genomic DNA isolated from leaf material of the T_1 plant CP1 was used for Illumina sequencing. A whole-genome shotgun library was constructed using standard procedures (TruSeq DNA; Illumina) and provided with Illumina adapter indices (AD002, AD004, and AD007). The library was quantified using real-time PCR (Mascher et al. 2013). Cluster formation using the cBot device and paired-end sequencing (HiSeq2500, 2 x 101 cycles, index read, rapid run modus) were performed according to the manufacturer's instructions (Illumina).

Sequence reads of CP1 and a negative control cultivar, Grossluesewitzer (Schmutzer et al. 2015), were aligned to a reference consisting of the rapeseed reference genome (Chalhoub et al. 2014) and the vector sequence with BWA mem version 0.7.15 (Li 2013). The resultant SAM file was converted to BAM format with SAMtools (Li et al. 2009) and sorted by reference position using Novosort (http://www.novocraft.com/products/novosort/). Read depth was calculated with the command samtools depth using only uniquely aligned reads with a mapping quality of 20 or greater and plotted with standard R functions (R Core Team 2015).

2.7.6   Shatter resistance measurements

Siliques were harvested manually at maturity and stored in paper bags. The samples were equilibrated for moisture content in a climate control cabinet (VB0714; Vötsch Industrietechnik) at 25 °C and 40% relative humidity for at least 3 d prior to measurement. Equilibration conditions were derived from Bruce et al. (2002).

To determine the force necessary to tear the valves of a silique apart from the replum, siliques were fixed with two alligator clamps attached to a Newton meter (type FH10) on a manual test stand (model TVL; Sauter). Maximum peak tensile forces were measured. Silique length was recorded for every data point. The beak of the silique was excluded from length measurement. A total of 150 siliques pooled from five to seven individual plants were measured per genotype. Siliques were grouped according to their lengths to calculate mean peak tensile forces of three size classes (3–4 cm, 4–5 cm, and 5–6 cm). Student's *t* tests were run to assess the significance of observed differences.

2.8   Accession numbers

The WGS sequence of T_1 plant CP1 can be found in the EMBL European Nucleotide Archive (ENA) under accession number PRJEB20660.

2.9   Supplemental data

The following supplemental materials are available.

Figure S1. Vector map of the recombinant pCas9-TPC plasmid used for this study.

Figure S2. Mapping results of genome sequence of the transgenic T_1 plant CP1 (upper chart) and the negative control cv Grossluesewitzer (lower chart) against the transformation vector sequence.

Table S1. Primers used in this study.

Table S2. Results of silique shatter trials.

2.10 Acknowledgements

2.11 Literature cited

Andersson M, Turesson H, Nicolia A, Falt AS, Samuelsson M, Hofvander P (2017) Efficient targeted multiallelic mutagenesis in tetraploid potato (*Solanum tuberosum*) by transient CRISPR-Cas9 expression in protoplasts. Plant Cell Rep 36 (1):117-128. doi:10.1007/s00299-016-2062-3

Ballester P, Ferrándiz C (2017) Shattering fruits: variations on a dehiscent theme. Current Opinion in Plant Biology 35:68-75. doi:10.1016/j.pbi.2016.11.008

Boszoradova E, Libantova J, Matusikova I, Poloniova Z, Jopcik M, Berenyi M, Moravcikova J (2011) *Agrobacterium*-mediated genetic transformation of economically important oilseed rape cultivars. Plant Cell Tiss Org 107 (2):317-323. doi:10.1007/s11240-011-9982-y

Brooks C, Nekrasov V, Lippman ZB, Van Eck J (2014) Efficient gene editing in tomato in the first generation using the clustered regularly interspaced short palindromic repeats/CRISPR-associated9 system. Plant Physiol 166 (3):1292-1297. doi:10.1104/pp.114.247577

Bruce DM, Farrent JW, Morgan CL, Child RD (2002) Determining the oilseed rape pod strength needed to reduce seed loss due to pod shatter. Biosystems Engineering 81 (2):179-184. doi:10.1006/bioe.2001.0002

Bus A, Körber N, Snowdon RJ, Stich B (2011) Patterns of molecular variation in a species-wide germplasm set of *Brassica napus*. Theor Appl Genet 123 (8):1413-1423. doi:10.1007/s00122-011-1676-7

Chalhoub B, Denoeud F, Liu SY, Parkin IAP, Tang HB, Wang XY, Chiquet J, Belcram H, Tong CB, Samans B (2014) Early allopolyploid evolution in the post-Neolithic

Brassica napus oilseed genome. Science 345 (6199):950-953. doi:10.1126/science.1253435

Doudna JA, Charpentier E (2014) The new frontier of genome engineering with CRISPR-Cas9. Science 346 (6213). doi:10.1126/science.1258096

Emrani N, Harloff H-J, Gudi O, Kopisch-Obuch F, Jung C (2015) Reduction in sinapine content in rapeseed (*Brassica napus* L.) by induced mutations in sinapine biosynthesis genes. Mol Breeding 35 (1):37. doi:10.1007/s11032-015-0236-2

Endo M, Mikami M, Toki S (2015) Multigene knockout utilizing off-target mutations of the CRISPR/Cas9 system in rice. Plant Cell Physiol 56 (1):41-47. doi:10.1093/Pcp/Pcu154

Fauser F, Schiml S, Puchta H (2014) Both CRISPR/Cas-based nucleases and nickases can be used efficiently for genome engineering in *Arabidopsis thaliana*. Plant J 79 (2):348-359. doi:10.1111/Tpj.12554

Feng ZY, Mao YF, Xu NF, Zhang BT, Wei PL, Yang DL, Wang Z, Zhang ZJ, Zheng R, Yang L, Zeng L, Liu XD, Zhu JK (2014) Multigeneration analysis reveals the inheritance, specificity, and patterns of CRISPR/Cas-induced gene modifications in *Arabidopsis*. P Natl Acad Sci USA 111 (12):4632-4637. doi:10.1073/pnas.1400822111

Harloff HJ, Lemcke S, Mittasch J, Frolov A, Wu JG, Dreyer F, Leckband G, Jung C (2012) A mutation screening platform for rapeseed (*Brassica napus* L.) and the detection of sinapine biosynthesis mutants. Theor Appl Genet 124 (5):957-969. doi:10.1007/s00122-011-1760-z

Hsu PD, Scott DA, Weinstein JA, Ran FA, Konermann S, Agarwala V, Li Y, Fine EJ, Wu X, Shalem O, Cradick TJ, Marraffini LA, Bao G, Zhang F (2013) DNA targeting specificity of RNA-guided Cas9 nucleases. Nat Biotech 31 (9):827-832. doi:10.1038/nbt.2647

Hua S, Shamsi IH, Guo Y, Pak H, Chen M, Shi C, Meng H, Jiang L (2009) Sequence, expression divergence, and complementation of homologous *ALCATRAZ* loci in *Brassica napus*. Planta 230 (3):493-503. doi:10.1007/s00425-009-0961-z

Lawrenson T, Shorinola O, Stacey N, Li C, Østergaard L, Patron N, Uauy C, Harwood W (2015) Induction of targeted, heritable mutations in barley and *Brassica oleracea* using RNA-guided Cas9 nuclease. Genome Biol 16:258. doi:10.1186/s13059-015-0826-7

Li H, Handsaker B, Wysoker A, Fennell T, Ruan J, Homer N, Marth G, Abecasis G, Durbin R, Proc GPD (2009) The Sequence Alignment/Map format and SAMtools. Bioinformatics 25 (16):2078-2079. doi:10.1093/bioinformatics/btp352

Li H (2013) Aligning sequence reads, clone sequences and assembly contigs with BWA-MEM. arXiv preprint arXiv:1303.3997

Li T, Yaokui L, Dan Z, Bigang M, Qiming L, Yuanyi H, Ye S, Yan P, Binran Z, Shitou X (2016a) Characteristic and inheritance analysis of targeted mutagenesis mediated by genome editing in rice. Yi Chuan 38 (8):746-755. doi:10.16288/j.yczz.16-052

Li W, Wu S, Liu Y, Jin G, Zhao H, Fan L, Shu Q (2016b) Genome-wide profiling of genetic variation in *Agrobacterium*-transformed rice plants. J Zhejiang Univ-Sc B 17 (12):992-996. doi:10.1631/jzus.B1600301

Liljegren SJ, Roeder AHK, Kempin SA, Gremski K, Ostergaard L, Guimil S, Reyes DK, Yanofsky MF (2004) Control of fruit patterning in *Arabidopsis* by *INDEHISCENT*. Cell 116 (6):843-853. doi:10.1016/S0092-8674(04)00217-X

Liu J, Huang SM, Sun MY, Liu SY, Liu YM, Wang WX, Zhang XR, Wang HZ, Hua W (2012) An improved allele-specific PCR primer design method for SNP marker analysis and its application. Plant Methods 8. doi:10.1186/1746-4811-8-34

Mascher M, Richmond TA, Gerhardt DJ, Himmelbach A, Clissold L, Sampath D, Ayling S, Steuernagel B, Pfeifer M, D'Ascenzo M, Akhunov ED, Hedley PE, Gonzales AM, Morrell PL, Kilian B, Blattner FR, Scholz U, Mayer KFX, Flavell AJ, Muehlbauer GJ, Waugh R, Jeddeloh JA, Stein N (2013) Barley whole exome capture: a tool for genomic research in the genus *Hordeum* and beyond. Plant J 76 (3):494-505. doi:10.1111/tpj.12294

Mikami M, Toki S, Endo M (2015) Parameters affecting frequency of CRISPR/Cas9 mediated targeted mutagenesis in rice. Plant Cell Rep 34 (10):1807-1815. doi:10.1007/s00299-015-1826-5

Price JS, Hobson RN, Neale MA, Bruce DM (1996) Seed losses in commercial harvesting of oilseed rape. Journal of Agricultural Engineering Research 65 (3):183-191. doi:10.1006/jaer.1996.0091

Rajani S, Sundaresan V (2001) The *Arabidopsis* myc/bHLH gene *ALCATRAZ* enables cell separation in fruit dehiscence. Curr Biol 11 (24):1914-1922. doi:10.1016/S0960-9822(01)00593-0

R Core Team (2015) R: A Language and Environment for Statistical Computing. R Foundation for Statistical Computing

Schmutzer T, Samans B, Dyrszka E, Ulpinnis C, Weise S, Stengel D, Colmsee C, Lespinasse D, Micic Z, Abel S, Duchscherer P, Breuer F, Abbadi A, Leckband G, Snowdon R, Scholz U (2015) Species-wide genome sequence and nucleotide polymorphisms from the model allopolyploid plant *Brassica napus*. Sci Data 2. doi:10.1038/Sdata.2015.72

Schouten HJ, vande Geest H, Papadimitriou S, Bemer M, Schaart JG, Smulders MJM, Perez GS, Schijlen E (2017) Re-sequencing transgenic plants revealed rearrangements at T-DNA inserts, and integration of a short T-DNA fragment, but no increase of small mutations elsewhere. Plant Cell Rep 36 (3):493-504. doi:10.1007/s00299-017-2098-z

Svitashev S, Schwartz C, Lenderts B, Young JK, Mark Cigan A (2016) Genome editing in maize directed by CRISPR–Cas9 ribonucleoprotein complexes. Nat Commun 7:13274. doi:10.1038/ncomms13274

Till BJ, Zerr T, Comai L, Henikoff S (2006) A protocol for TILLING and Ecotilling in plants and animals. Nat Protoc 1 (5):2465-2477. doi:10.1038/nprot.2006.329

Wang G-P, Yu X-D, Sun Y-W, Jones HD, Xia L-Q (2016) Generation of marker- and/or backbone-free transgenic wheat plants via *Agrobacterium*-mediated transformation. Frontiers in Plant Science 7 (1324). doi:10.3389/fpls.2016.01324

Wang YP, Cheng X, Shan QW, Zhang Y, Liu JX, Gao CX, Qiu JL (2014) Simultaneous editing of three homoeoalleles in hexaploid bread wheat confers heritable resistance to powdery mildew. Nat Biotechnol 32 (9):947-951. doi:10.1038/Nbt.2969

Wells R, Trick M, Soumpourou E, Clissold L, Morgan C, Werner P, Gibbard C, Clarke M, Jennaway R, Bancroft I (2014) The control of seed oil polyunsaturate content in the polyploid crop species *Brassica napus*. Mol Breeding 33 (2):349-362. doi:10.1007/s11032-013-9954-5

Woo JW, Kim J, Kwon SI, Corvalan C, Cho SW, Kim H, Kim S-G, Kim S-T, Choe S, Kim J-S (2015) DNA-free genome editing in plants with preassembled CRISPR-Cas9 ribonucleoproteins. Nat Biotech 33 (11):1162-1164. doi:10.1038/nbt.3389

Yan W, Chen D, Kaufmann K (2016) Efficient multiplex mutagenesis by RNA-guided *Cas9* and its use in the characterization of regulatory elements in the *AGAMOUS* gene. Plant Methods 12 (23). doi:10.1186/s13007-016-0125-7

Zarhloul KM, Stoll C, Lühs W, Syring-Ehemann A, Hausmann L, Töpfer R, Friedt W (2006) Breeding high-stearic oilseed rape (*Brassica napus*) with high- and low-erucic background using optimised promoter-gene constructs. Mol Breeding 18 (3):241-251. doi:10.1007/s11032-006-9032-3

3 The effect of *INDEHISCENT* point mutations on silique shatter resistance in oilseed rape (*Brassica napus*)

Under review

3.1 Summary

Silique shattering is a major factor reducing the yield stability of oilseed rape (*Brassica napus*). Attempts to improve silique robustness often include the use of mutations in target genes identified from Arabidopsis (*Arabidopsis thaliana*). A variety of phenotyping methods assessing the level of shatter resistance were previously described. However, a comparative and comprehensive evaluation of the methods has not yet been undertaken. We verified the increase of shatter resistance in *indehiscent* double knock-down mutants obtained by TILLING with a systematic approach comparing three independent phenotyping methods. A positive correlation of silique length and robustness was observed and accounted for in the analyses. Microscopic studies ruled out the influence of different lignification patterns. Instead, we propose a model to explain increased shattering resistance by altered cell shapes and sizes within the contact surfaces of replum and valves.

3.2 Introduction

Rapeseed (*Brassica napus*, AACC, 2n = 38) is mainly grown in temperate regions for its oil-containing seeds. The use of rapeseed oil is widespread and covers food and feed as well as industrial production chains. Because seeds are the most important yield component, the plant's natural propagation mechanism troubles farmers: *B. napus* siliques dry out at maturity and burst open at application of low forces, shedding the seeds. This process of silique shattering, also called dehiscence or fruit shedding, can cause pre-harvest losses of up to 25% in adverse weather conditions (Price et al. 1996). Up to 10% pre-harvest losses were reported from commercial rapeseed production in Canada (Gulden et al. 2003). Therefore, increasing shatter resistance is an important breeding objective. However, a careful fine-tuning is necessary to obtain siliques that can still be opened in commercial processing and avoid the application of high forces which might harm the seeds and reduce oil quality.

Seed shattering is promoted by the development of specialized cell layers called dehiscence zone, which act as a predetermined breaking point between the two valves and the central replum (Meakin and Roberts 1990b). The dehiscence zone consists of a lignified layer, turning rigid at maturity, and a separation layer, secreting enzymes that cause breakdown of the middle lamella (Sander et al. 2001; Ogawa et al. 2009). This labile structure easily breaks after physical impact.

A network of transcription factors termed 'dehiscence zone identity genes' was identified in Arabidopsis. The basic helix-loop-helix (bHLH) transcription factor INDEHISCENT (IND) controls both differentiation of lignified and separation layer (Liljegren et al. 2004). ALCATRAZ (ALC) and SPATULA (SPT), also bHLH proteins, are essential for separation layer development (Rajani and Sundaresan 2001; Girin et al. 2011). A feedback-loop between IND and ALC/SPT was suggested (Lenser and Theißen 2013). Further upstream, the redundant MADS box transcription factors SHATTERPROOF 1 and 2 (SHP1/2) induce *IND*, *ALC,* and *SPT* expression (Ferrándiz 2000; Liljegren et al. 2000). Studies describing indehiscent *shp1/2*, *alc, ind,* and *spt* mutants of Arabidopsis support the concept of knocking-out dehiscence zone identity genes to increase shatter resistance (Ferrándiz 2000; Liljegren et al. 2000; Rajani and Sundaresan 2001; Liljegren et al. 2004; Groszmann et al. 2011). *ALC, IND,* and *SHP2* gene homologs were identified in rapeseed (Hua et al. 2009; Tan et al. 2009; Girin et al. 2010) and the functional conservation of *BrIND* and *BoIND* was described in

Brassica rapa and *Brassica oleracea* (Girin et al. 2010). A granted patent and a patent application filed by Bayer CropScience claim the increased shatter resistance of rapeseed *Bnind* and *Bnalc* double mutants (Laga 2013; Laga et al. 2015). The breeding company Limagrain provides genetically fixed shatter resistance within several rapeseed hybrid cultivars. However, the underlying gene remains to be kept a company secret.

TILLING (Targeting Induced Local Lesions in Genomes) is a reverse genetics approach that combines mutagenesis and mutant identification. Mutations are induced randomly across the genome e.g. by application of chemicals like ethyl methane sulfonate (EMS). DNA of M_2 plants is then pooled and target regions are amplified by PCR. Mutant screening is performed by heteroduplex restriction visualized on denaturing polyacrylamide gels (Till et al. 2006). According to European law, the identified mutants are not considered to be genetically modified organisms and can therefore be introduced into breeding programs by backcrossing to elite material. Thus, silique shattering resistance can be fixed in novel rapeseed varieties.

Various phenotyping methods for silique shatter resistance in rapeseed have previously been described. One of the older methods is a cantilever test, in which pressure force is applied to single siliques in order to assess rupture energy (Kadkol et al. 1984). The current standard approach, however, comprises the random impact test (RIT) first described by Bruce et al. (2002). Intact siliques are accelerated in a container together with steel balls. The measure of shatter resistance is the time necessary to disrupt 50% of invested siliques ($T_{1/2}$). Most of the subsequent studies suggested a positive correlation of silique length and $T_{1/2}$ (Summers et al. 2003; Udall et al. 2006), whereas Wang et al. (2007) proposed a negative correlation which they supported by yield loss assessed from field trials. Furthermore, high $T_{1/2}$ values were correlated with large replum-valve joint areas (Hu et al. 2015).

Our study aimed at assessing the effect of *Bnind* mutations on silique shatter resistance and silique structure in rapeseed. Furthermore, we wanted to elucidate whether cultivars with high shatter resistance differ in *BnALC* and *BnIND* gene structures.

3.3   Results

3.3.1   *BnIND* expression increases during silique development

Rapeseed comprises two *BnIND* homoeologs, *BnaA.IND.a* (BnaA03g27180D) and *BnaC.IND.a* (BnaC03g32180D) which contain a single exon with a conserved bHLH domain. For an initial characterization, the expression of both genes was assessed during four stages of silique development at 0, 15, 25, and 42 days after pollination (DAP). While 0 DAP describes the day of pollination, 42 days later siliques were close to maturation, what could easily be observed by a change of color from green to yellow. Dehiscence zone tissue was enriched during sampling so that a dilution of *BnIND* levels due to a high proportion of non-expressing tissues was prevented.

The housekeeping gene *BnACTIN2* was utilized for normalization of RT-qPCR values. Both *BnIND* homoeologs were equally low expressed at 0 and 15 DAP (Figure 6). Upon 25 DAP, the expression of both genes was induced. The increased expression levels were retained until 42 DAP. At 42 DAP, *BnaA.IND.a* levels were approximately 2.5-fold higher than *BnaC.IND.a* levels but, probably due to a reduced number of biological replicates for this developmental stage, the difference was not significant.
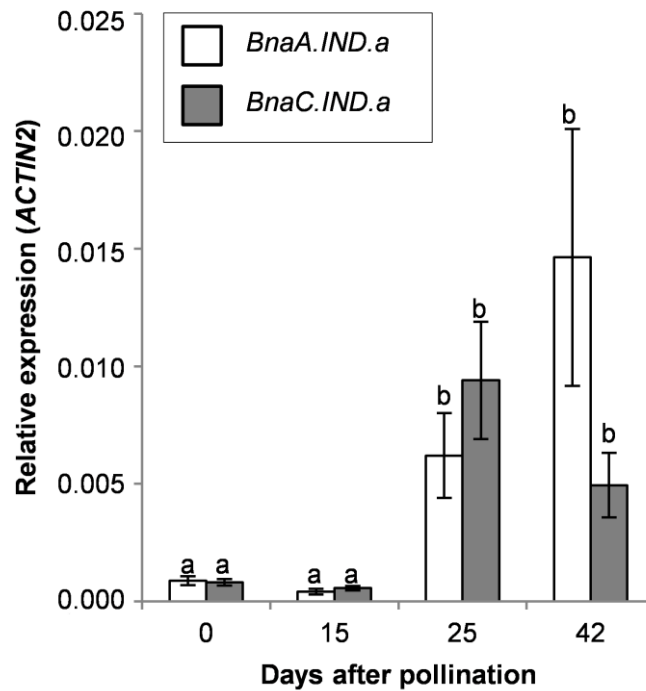
Figure 6. Relative gene expression of *BnIND* homoeologs in pistil and silique tissue of the rapeseed variety Express at 0, 15, 25, and 42 DAP. Expression was normalized against *BnACTIN2*. Values are expressed as means of biological and technical replicates plus standard error of the mean. A shared letter implies no significant difference (two-sided *t*-test, $\alpha > 0.05$).

3.3.2 EMS mutations in *BnIND* homoeologs were identified

To obtain *Bnind* mutants, 3,840 M_2 individuals of an EMS mutant population of winter rapeseed cultivar Express (Harloff et al. 2012) were screened by TILLING. Homoeolog-specific PCR amplicons spanned 789 bp and 792 bp of *BnaA.IND.a* and *BnaC.IND.a*, respectively. Thus, 98 and 90% of the coding sequences were covered, including the bHLH domain. A total of 29 missense mutations, two 3' UTR mutations and one nonsense mutation were identified (Table S3; Figure S3). Three mutations in *BnaA.IND.a* (*ind-1* to *ind-3*) and four mutations in *BnaC.IND.a* (*ind-4* to *ind-7*) were selected for further analysis (Figure 7a). The selection comprised four missense mutations outside of the bHLH domain, two missense mutations within the bHLH domain, and the premature stop codon mutation. Double mutant plants with two impaired *BnIND* homoeologs were produced by crossing.
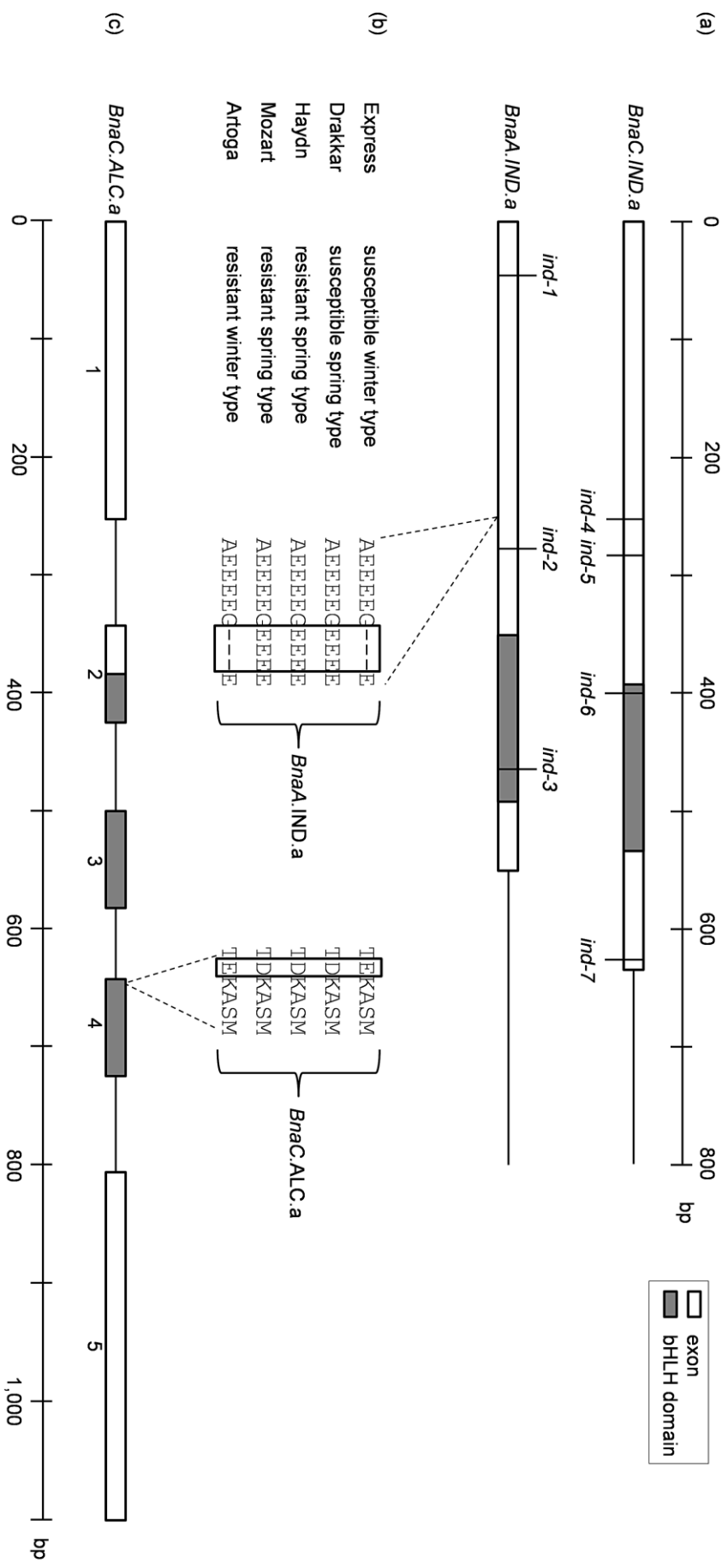
Figure 7. Gene models. (a) *BnIND* gene models and positions of selected point mutations detected by TILLING. (b) Protein alignment of *BnIND* and *BnALC* sequences of five rapeseed cultivars. Fractured lines show the location of sequence excerpts and black boxes highlight polymorphisms. (c) *BnaC.ALC.a* gene model.

3.3.3 Silique length and shatter resistance are positively correlated

To assess silique shatter resistance, three different phenotyping methods were implemented. They comprised a random impact test (RIT), a tensile force measurement, and a cantilever trial. In order to identify ideal test settings, we first tested siliques of cultivar Express which varied in lengths.

In the RIT, we assessed the time necessary to disrupt 50% of invested siliques ($T_{1/2}$) by agitating them in a cylindrical container in the presence of steel balls. Three size classes were considered, comprising 3- to 4-cm-, 4- to 5-cm-, and 5- to 6-cm-long siliques. $T_{1/2}$ increased significantly with silique lengths (Figure S4a). However, we observed that the steel balls could not take up full speed when 5- to 6-cm-long siliques were tested.

Regarding the tensile force trial, 3- to 8-cm-long siliques were fixed by attaching alligator clamps to both valves. Then, tensile forces were measured while tearing the valves apart. When plotting the silique length against the peak tensile force, a weak positive linear correlation was observed with a Pearson correlation coefficient of r = 0.33 (Figure S4b). Regression values reached from 1.098 N at a silique length of 3 cm to 1.643 N at a silique length of 8 cm.

To exclude the effect of silique length, a cantilever test was employed. Single siliques were fixed on a plane in a way that the pedicel end overlapped by 1.5 cm. Then, pressure force was applied to this fixed silique segment, which was of the same length for each sample. We did not expect to find a correlation, when plotting silique length against peak pressure force. Surprisingly, the positive linear correlation was even more pronounced (r = 0.64, Figure S4c). The regression was steeper, with 0.758 N at 3 cm and 2.445 N at 8 cm silique length.

From these initial findings we concluded that for each phenotyping method, it is necessary to account for silique length in order to produce results comparable between genotypes. In practice, we performed all following RITs with 3- to 4-cm-long siliques. Regarding force measurements, we calculated linear regressions of silique length and force for each genotype and compared regression values at a fixed silique length of 4 cm.

We focused on force measurements instead of RITs because they yield more data points by considering single siliques. Therefore, a more pronounced differentiation between genotypes was expected.

3.3.4 *Bnind* double mutants display higher shatter resistance

Next, we measured peak tensile forces of siliques collected from M_4 *Bnind* single mutants and segregating F_3 double mutant families. Maximum tensile forces (N_{max}) are displayed as differences by subtracting the force values of Express from the respective genotype. Positive differences indicate a higher shatter resistance compared with Express, while negative differences imply a reduced shatter resistance.

Out of the seven selected *Bnind* single mutants, five could be assessed for shatter resistance. The remaining two had a reduced fertility due to EMS background mutations and did not set a sufficient amount of siliques for the tests. Mutants *ind-1*, *ind-2*, *ind-5*, and *ind-7* did not differ in shatter resistance compared with Express (Figure 8a). This was expected because only one *BnIND* homoeolog was impaired so that the functional second homoeologs could rescue the phenotype. However, invested forces for the disruption of *ind-4* siliques were 0.544 N higher compared with Express.
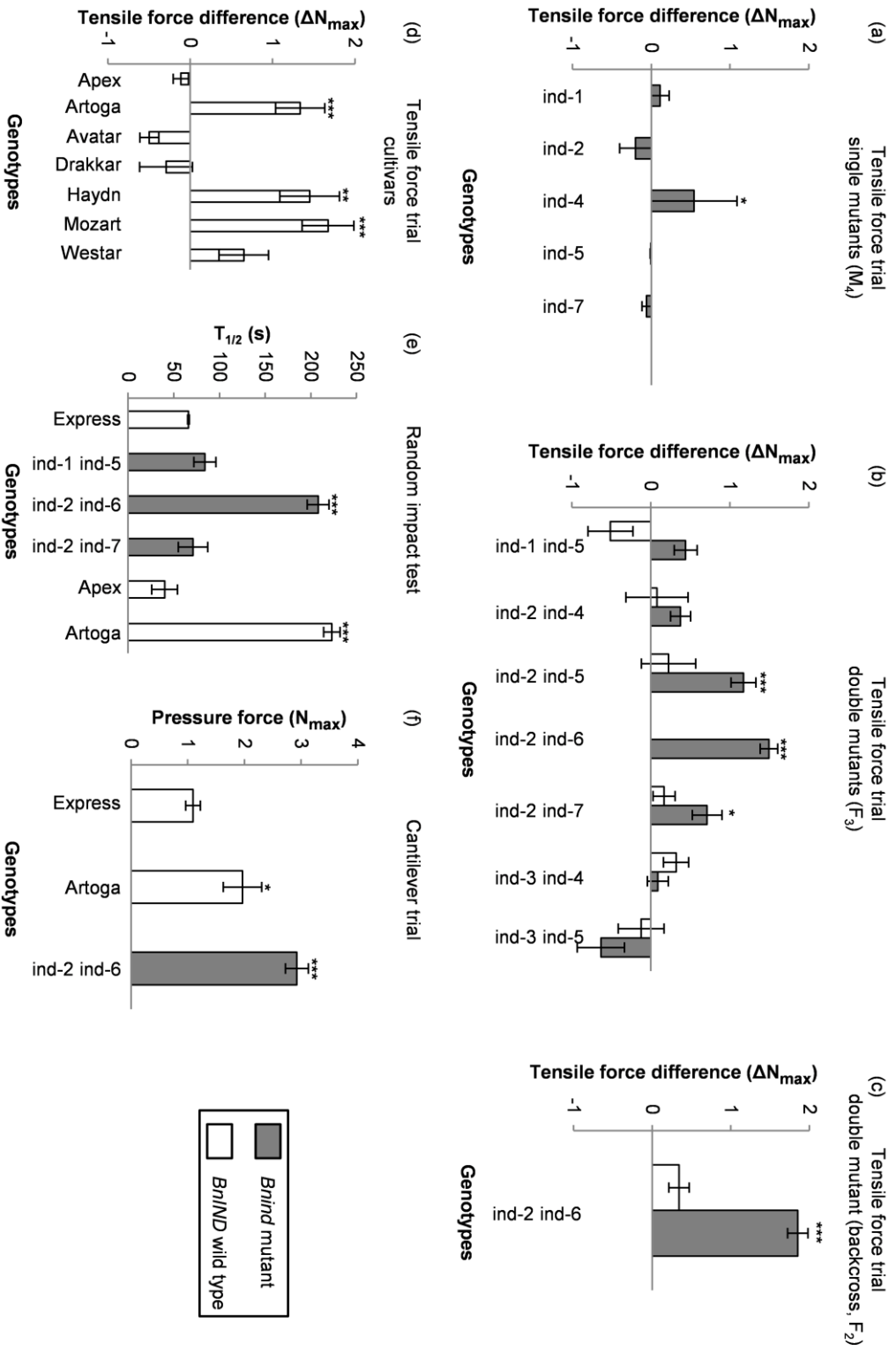
Figure 8. Shatter resistance of *Bnind* mutants and rapeseed cultivars. (a-d) Tensile force trials. Forces are displayed as difference between mutant genotype and Express control, calculated from regression values at a silique length of 4 cm. Bars represent standard error. (e) Random impact test. Values are means of quadruple measurements of 3- to 4-cm-long siliques and standard deviation. (f) Cantilever trial. Forces are displayed as regression values at a silique length of 4 cm and standard error. Significant differences from Express are indicated by asterisks (* $P < 0.05$; ** $P < 0.01$; *** $P < 0.001$).

F_3 double mutants with two mutated *BnIND* homoeologs were compared with segregating *BnIND* wild types sharing the same EMS mutation background (Figure 8b). While the shatter resistance of EMS plants with wild type *BnIND* alleles and Express was similar, three out of seven *Bnind* double mutants showed a significant increase. They shared the premature stop codon mutation *ind-2* in *BnaA.IND.a* and differed in mutations within *BnaC.IND.a*. The most pronounced effect with an increase of peak forces by 1.495 N compared with Express was observed for double mutant *ind-2 ind-6*, which combines the nonsense mutation with a missense mutation located within the functional domain. No F_3 *BnIND* wild type EMS plants were available for this mutation combination. To account for possible background effects, the double mutant was backcrossed with the donor line Express. In the segregating F_2, sufficient silique material was produced to compare double mutant and wild type. The effect of the double mutation *ind-2 ind-6* could be verified, while EMS plants with *BnIND* wild type alleles did not differ significantly from Express (Figure 8c).

Apart from Express, seven additional rapeseed cultivars were evaluated by the tensile force measurement (Figure 8d). Siliques of Apex, Avatar, Drakkar, and Westar were as susceptible as those of Express. In contrast, tensile forces of Artoga, Haydn, and Mozart were comparable to the best performing *Bnind* double mutant. The siliques of Artoga were so robust that tearing the valves apart was rarely possible. Instead of detaching dehiscence zones, often the valves themselves collapsed. As a result, only a reduced number of measurements could be considered for the evaluation but they still yielded a significant effect.

As a cross-validation of the tensile force measurements, three *Bnind* double mutants and three cultivars were subjected to RIT (Figure 8e). After 66 ± 1 seconds, half of the siliques of Express were disrupted. As expected, $T_{1/2}$ values of double mutant *ind-1 ind-5* and cultivar Apex did not differ from Express. At the same time, double mutant *ind-2 ind-6* and cultivar Artoga had increased $T_{1/2}$ values of 208 ± 12 and 223 ± 9 seconds, respectively. Only double mutant *ind-2 ind-7* had no positive effect on shatter resistance in RIT, although it was classified as shatter resistant according to the tensile force trial.

In a third round of phenotyping, Artoga, Express, and the best performing double mutant *ind-2 ind-6* were assessed by the cantilever test (Figure 8f). About 1.095 ± 0.128 N pressure force caused 4-cm-long siliques of Express to burst. For Artoga and the *Bnind* double mutant, increased forces of 1.967 ± 0.339 N and 2.926 ± 0.201 N were measured. Summarizing, all phenotyping methods provided consistent results.

3.3.5 Shatter resistant *Bnind* double mutant shows altered silique structure

Because it was known that *BnIND* is involved in the development of dehiscence zone tissues in Arabidopsis, cryosections of 15- and 42-DAP-old siliques from Express, the F_2 double mutant *ind-2 ind-6,* and the segregating *BnIND* wild type were investigated under the light microscope. Surprisingly, neither the lignification pattern nor the separation layer was changed (Figure S6).

However, at a closer inspection of the contact surfaces of replum and valves, we realized a thickened replum-valve joint area in the mutants. To correlate shatter resistance and replum-valve joint area index (RJAI), we performed tensile force measurements with Express and the F_3 double mutant *ind-2 ind-6*. In order to be able to dissect the influence of silique length, we evaluated 2- to 3-cm- and 5- to 6-cm-long siliques. Then, the RJAI was assessed under the microscope (Figure S7).

As expected, the RJAI increased in positive correlation with the silique length (r = 0.74, Table 4). Short siliques of the double mutant had an RJAI of 0.48 ± 0.15 mm^2, whereas long siliques

had an RJAI of 1.51 ± 0.48 mm^2. This effect was less pronounced in Express with RJAIs of 0.45 ± 0.12 mm^2 and 1.02 ± 0.38 mm^2. Thus, significantly enlarged RJAIs fitted well to the increase of shatter resistance between long Express siliques (1.584 ± 0.499 N) and long mutant siliques (3.313 ± 0.783 N). Nonetheless, we still lacked the rationale for the strength of short mutant siliques (2.197 ± 0.807 N) because they were more robust than Express siliques (short and long) albeit having comparably low RJAIs.

Table 4. Silique parameters assessed in the RJAI experiment. Shatter resistance was assessed by tensile force measurement. Values are expressed as mean and standard deviation. n = 50. Statistic evaluation was based on pairwise *t*-tests. Values that share the same letters (a, b) do not differ significantly ($P \geq 0.05$).

Genotype	Size class	Mean silique length ± SD (cm)	Mean RJAI ± SD (mm^2)	Mean tensile force ± SD (N$_{max}$)
F$_3$ double mutant *ind-2 ind-6*	2 – 3 cm	2.7 ± 0.3 [a]	0.48 ± 0.15 [a]	2.197 ± 0.807
	5 – 6 cm	5.4 ± 0.3 [b]	1.51 ± 0.48	3.313 ± 0.783
Express	2 – 3 cm	2.7 ± 0.3 [a]	0.45 ± 0.12 [a]	0.923 ± 0.437
	5 – 6 cm	5.5 ± 0.3 [b]	1.02 ± 0.38	1.584 ± 0.499

In order to further approach the underlying structures for shatter resistance, we performed scanning electron microscopy (SEM) of the contact surface of replum and valve of short and long siliques of Express and the F$_3$ double mutant *ind-2 ind-6*. The average length of cells was assessed from four regions per silique. The regions under observation were the pedicel end and the middle of the silique for both replum and valve (Figure 9). While the contact surfaces of Express siliques were made up of almost rectangular, oblong cells, mutant siliques showed cells of varying shapes with a high proportion of smaller, rounded cells. The average length of cells ranged from 22 to 39 µm in Express and from 13 to 21 µm in the mutant (Table 5). In contrast to the RJAI, differences in cell dimensions were already apparent for short siliques. Within genotypes, cell lengths at the replum base did not differ significantly, whereas the cell lengths in the remaining three regions were negatively correlated with silique size. Consequently, the data imply a link between small cell sizes in dehiscence zone surfaces and shatter resistance. We suggest that the shatter resistant *Bnind* phenotype is based on the combined effect of enlarged RJAIs together with smaller cells in the dehiscence zone.

Table 5. Silique parameters assessed in the SEM experiment. Peak pressure forces were obtained from cantilever tests. Values are means and standard deviation of n observations. Statistic evaluation was based on pairwise *t*-tests. Values within the same row that share the same letters (a, b) do not differ significantly (p ≥ 0.05).

		Sample							
		Express				F$_3$ double mutant *ind-2 ind-6*			
		Silique 1		Silique 2		Silique 1		Silique 2	
		Mean	n	Mean	n	Mean	n	Mean	n
Silique measures	Silique length (cm)	3.5	1	7.2	1	3.5	1	5.1	1
	Pressure force (N$_{max}$)	0.278	1	3.450	1	1.543	1	6.285	1
Length of cells	Replum pedicel end (µm)	28 ± 6 [a]	13	24 ± 8 [a]	14	17 ± 6 [b]	26	17 ± 6 [b]	37
	Replum middle (µm)	28 ± 6	24	23 ± 6	24	20 ± 7	67	15 ± 6	70
	Valve pedicel end (µm)	39 ± 17	20	22 ± 9 [a]	43	21 ± 5 [a]	28	13 ± 5	67
	Valve middle (µm)	34 ± 10	39	22 ± 9 [a]	63	21 ± 5 [a]	32	17 ± 6	32
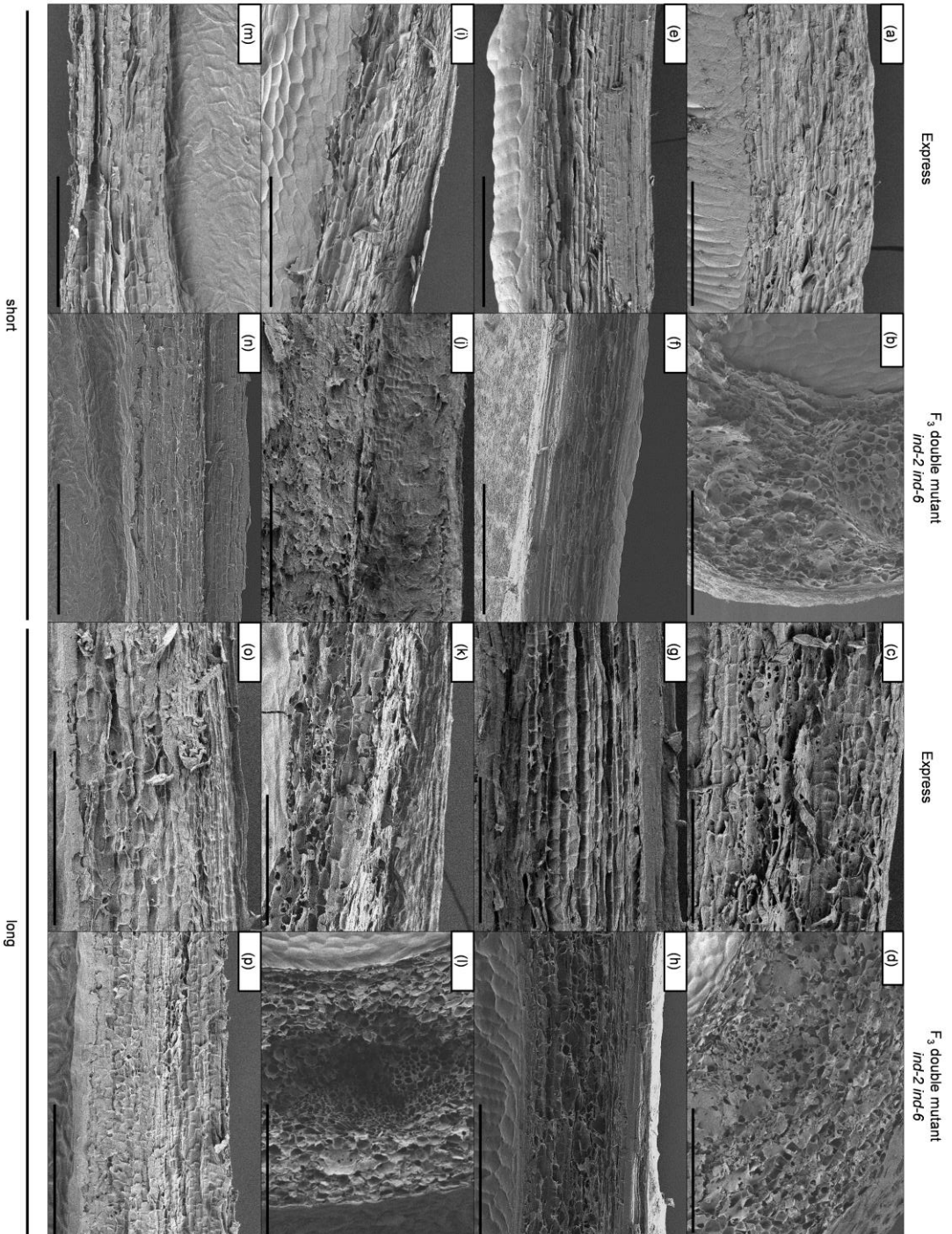
Figure 9. Dehiscence zone surfaces of the variety Express and the F_3 double mutant *ind-2 ind-6* as observed by SEM. Valve surfaces (a-h) and replum surfaces (i-p) of short and long siliques were investigated at two positions. Pictures were taken at the pedicel end (a-d, i-l) as well as in the middle of the siliques (e-h, m-p). 250x to 350x magnification, 200 µm scale bars.

3.3.6 Partial sequencing of dehiscence zone identity genes revealed polymorphisms among rapeseed cultivars

As the mechanism of genetic regulation underlying the increased shatter resistance of the rapeseed cultivars is not yet fully understood, we sequenced essential parts of the dehiscence zone identity genes *BnaA.ALC.a* (BnaA07g12110D), *BnaC.ALC.a* (BnaC07g16290D), *BnaA.IND.a*, and *BnaC.IND.a* to check for putative causal mutations. PCR amplicons covering at least 73.5% of the coding sequence of each gene, including the bHLH domain (Figure S5; Table S9), were subjected to Sanger sequencing. In addition to the shatter resistant genotypes Artoga, Haydn, and Mozart, the susceptible cultivars Drakkar and Express were included. The observed coding sequences of *BnaA.ALC.a* and *BnaC.IND.a* were identical within all five cultivars. Within *BnaA.IND.a,* a 9-nucleotide-long polymorphism resulting in the presence/absence variation of three amino acids, was identified upstream of the bHLH domain (Figure 7b). The spring types Drakkar, Haydn, and Mozart shared three additional glutamic acids at amino acid positions 74-76. However, the polymorphism correlated only with the growth type and not with shatter resistance. The same cultivars contained a SNP within the bHLH domain of *BnaC.ALC.a*, which leads to the exchange of glutamic acid with aspartic acid (E55D, Figure 7c).

3.4   Discussion

3.4.1 *BnIND* expression profiles differed from literature

BnIND expression increased after 25 DAP. The data indicated a differential expression of the two homoeologs at 42 DAP, which could not be finally validated due to a limited number of biological replicates. The lack of a sufficient number of replicates was owed to the difficulty of recovering RNA from mature siliques.

In contrast to the expression pattern that we describe, Kay et al. (2013) reported the highest expression of *IND* in floral buds of Arabidopsis and reduced levels in developing siliques. However, these findings are misleading because they did not enrich dehiscence zone tissue prior to RNA isolation, although *IND* expression is limited to a few cell layers (Liljegren et al. 2004; Girin et al. 2010). Therefore, *IND* expression was diluted with increasing silique size. The same problem arises from previously reported RT-qPCR measurements of *BnIND* and *BrIND* in rapeseed and *B. rapa* (Zhang et al. 2016). Again, dilution of dehiscence zone-specific genes with increasing silique length was not considered. Furthermore, only a single primer combination was used so that a differentiation between the homoeologs was not possible. By overcoming these issues, we provided novel insights into *BnIND* gene regulation in *B. napus*.

3.4.2 Shatter resistance measurements

Positive effects of silique length on RIT results have been reported before (Summers et al. 2003; Udall et al. 2006; Hu et al. 2015). Regarding our RIT set-up, part of this effect might have been caused by the experimental design, as steel balls in the container with longer siliques did not catch up as much speed as with shorter ones. We performed direct force measurements to further elucidate the correlation of shatter resistance and silique length. While it was not a surprise that the tensile force measurements confirmed a correlation of silique length and disruptive force, the cantilever test should have been independent of length, as all siliques had been fixed at the same length. However, there was a clear effect, which we explain by an increased contact surface at the silique end (namely RJAI values). This is in

accordance with a study by Hu et al. (2015), which demonstrated the association of large RJAIs with shatter resistance.

The three employed phenotyping methods consistently identified a *Bnind* double mutant with superior shatter resistance. Because no F$_3$ *BnIND* wild type EMS plants were available for this specific mutation combination, a backcross with Express was performed. In the segregating F$_2$, *Bnind* double mutants were more shatter resistant than *BnIND* wild types and Express. This proved that the effect was not caused by the EMS mutation background.

A comparison of shatter resistance measurements with preceding studies is complicated by the lack of a shared standard protocol. Even though there are many research groups who phenotype by RIT, there are differences regarding the sizes of test containers, the number and weight of the steel balls, and the speed of shaking. Often, silique lengths of tested samples are not indicated. Nevertheless, our results are in accordance with previous findings. We confirmed the advertised shatter resistance of cultivar Artoga in three independent phenotyping approaches. Furthermore, we classified Apex as susceptible which resembles a study by Bruce et al. (2002).

For applied plant breeding, bench-top phenotyping is of little use unless it can be related to field observations. In a preceding study, T$_{1/2}$ values from greenhouse grown rapeseed plants explained 56% of variation in field losses, while T$_{1/2}$ values of siliques sampled from the field explained 80% (Wang et al. 2007). Likewise, correlations of cantilever trial results and field observations were reported (Kadkol et al. 1984). Because RIT, cantilever trial, and tensile force trial classified our *Bnind* double mutant as shatter resistant, we assume to find an improved field performance as well. Nonetheless, the final proof is pending.

3.4.3 Mechanical influence of dehiscence zone cell structure on silique shatter resistance

Since the lignification pattern and the separation layer of siliques from Express and the *ind-2 ind-6* double mutant were similar, we assume the differences in shatter resistance to be a result of the altered cell structure in the dehiscence zone. Compared to siliques from Express, the cell size in the double mutant is significantly smaller and thus showed an enhanced cell density (number of cells per unit area). Enhanced shatter resistance (adhesive strength) between two solid bodies by distributing the contact on many smaller subcontacts rather than on one large contact (Figure 10), is a well-known principle in biological adhesive systems (Arzt et al. 2003; Varenberg et al. 2010), known as contact splitting. The benefits of contact splitting lie in an increased robustness of individual smaller subcontacts (Gao et al. 2003) and a more homogeneous distribution of the stress acting on individual subcontacts (Hui et al. 2004) caused by external applied forces (e.g. during the impact of steel balls in the RIT or the applied forces during the tensile and cantilever tests). Moreover, adhesive failure always occurs by the propagation of a crack (here the local detachment of individual cell contacts) in the adhesive interface. In an adhesive interface consisting of many individual subcontacts, the crack has to be reinitiated at each subcontact, which hampers the propagation and thus the adhesive failure. This principle is known as crack trapping (Hui et al. 2004). Interestingly, similar to the here observed increased shatter resistance due to the contact of more smaller cells, a concept for a bio-inspired handling device based on many small pressurized adhesives membranes has recently been proposed (Dening et al. 2014).

(a)   (b)
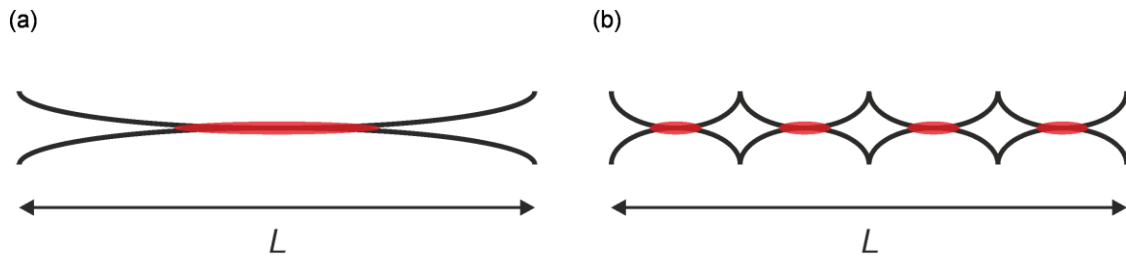
Figure 10. Schematic illustration of the principle of contact splitting. Black lines represent the cross-section of contacting cell walls, whereas the region of the adhesive interface is highlighted in red. According to the principle of contact splitting, the adhesive strength of one large contact (a) will be lower if compared with many smaller subcontacts (b) on the same length *L*.

3.4.4 Sequence polymorphisms in dehiscence zone identity genes and application in plant breeding

To understand the genetic basis of shatter resistance in rapeseed cultivars, *BnALC* and *BnIND* homoeologs were partially sequenced. The sequenced regions contained large parts of the coding sequence including the bHLH domain but omitted promotors.

Two identified polymorphisms correlated only with the growth type and not with shatter resistance. Thus, the underlying nucleotides are either not essential for the proper functioning of the respective genes or the second homoeolog compensated for the loss of function. This could be tested by targeted mutagenesis of the conserved homoeolog in shatter-prone cultivars.

Phenotypes of *ind* and *Brind* mutants in Arabidopsis and *B. rapa* depend on the underlying allele. Strong alleles like frameshift mutations or premature stop codons cause tube-like siliques without constrictions at valve margins (Liljegren et al. 2004; Girin et al. 2010). We did not observe such drastic alterations in rapeseed (Figure S8). This was expected because we could only identify a premature stop codon mutation in one of the *BnIND* homoeologs by TILLING and had to combine it with weaker missense mutations from the second gene copy. Clearly, this is a weakness of random mutagenesis. However, the attained shatter resistance might already be sufficient for commercialization. If siliques turned too robust, problems could arise during the threshing process (Bruce et al. 2001).

The *BnIND* mutations we have identified can be introduced to commercial breeding programs. However, reduction of the mutation load is inevitable. Traditionally, this can be achieved by repeated backcrossing with an elite line which is a time-consuming procedure. We propose a marker assisted background selection (Jung 2010) where BC_1 plants are genotyped with numerous markers to select plants with a high share of the recipient genome. This can be done with *B. napus* SNP arrays (Mason et al. 2017) or by AFLPs (Amplified fragment length polymorphism; Schondelmaier et al. 1996) which are easy to apply and cheap multiplexing markers. Alternatively, non-mutagenized rapeseed lines are available such as the cultivar Artoga or the two cultivars Haydn and Mozart whose shatter resistance has been proven here for the first time. However, the QTLs controlling shatter resistance in these genotypes are unknown and it remains to be seen if they collocate with *BnALC* and *BnIND* loci. To avoid complicated phenotyping, marker assisted selection for shatter resistance is clearly preferred. This renders the new *BnIND* mutations superior because they can be selected for by a cheap marker assay. Moreover, they are non-transgenic and therefore accessible to European breeders.

3.5 Experimental procedures

3.5.1 Mutation screening

3,840 M_2 plants of the EMS Express winter rapeseed mutant population described by Harloff et al. (2012) were screened by TILLING. Homoeolog-specific primers were developed for *BnaA.IND.a* (BnaA03g27180D) and *BnaC.IND.a* (BnaC03g32180D) (Table S6). The genes were amplified from two dimensional 8-fold pools by PCR with 700 nm and 800 nm IRD fluorescence labeled primers (Biomers, Ulm, Germany). *Cel*I digestion of heteroduplices, sample purification and polyacrylamide gel electrophoresis on a LI-COR 4300 DNA analyzer (LI-COR Biosciences, www.licor.com) were performed according to Till et al. (2006). To identify mutations, restriction fragments were analyzed by the GelBuddy Software (Zerr and Henikoff 2005).

3.5.2 Plant material and greenhouse experiments

Selected *bnaA.ind.a* M_3 mutant plants were crossed with *bnaC.ind.a* mutants to obtain double mutants. Homozygous wild type, single and double mutant lines segregated within F_2 families. Fixed F_3 lines were grown in multiple independent experiments in the greenhouse to produce siliques for shatter resistance trials (22 °C, 16 h light/ 8 h dark). Comparability was assured by including cultivar Express as a calibrator genotype in every experiment. After 2-4 weeks of pre-culture, plantlets were vernalized for 8 weeks in a cold chamber (4 °C, 16 h light/ 8 h dark). After transferring the plants back to the initial greenhouse conditions, they were planted into 11x11 cm pots. Prior to flowering, plants were fertilized with 0.5 g Compo Blaukorn Classic universal fertilizer (Compo, Münster, Germany). Selfing bags were mounted at flowering.

A selected F_3 *Bnind* double mutant was crossed with Express. Homozygous *BnIND* wild types and *Bnind* double mutants of F_2 were grown under the described greenhouse conditions and further analyzed.

To compare the mutant performance with modern breeding material, eight rapeseed cultivars (Table S4) were grown under the same conditions.

3.5.3 RT-qPCR

Pistil and silique tissue was collected from Express at four developmental stages (0, 15, 25, and 42 DAP) at 10-12 h Zeitgeber. Exact stages were assured by hand pollination and tagging of single flowers. At 0 DAP, 20-30 pistils were collected. At 15, 25, and 42 DAP, single siliques were sampled and cut with a scalpel at 1 mm distance from the dehiscence zone. Only the enriched dehiscence zone tissue was kept.

RNA was isolated with the peqGold Plant RNA Kit (PEQLAB Biotechnologie GmbH, Erlangen, Germany) from five biological replicates of 0, 15, and 25 DAP samples and three biological replicates of 42 DAP samples. Samples were homogenized with two metallic beads (4 mm) using a MM2 Retsch mill (Retsch, Hann, Germany) at 94% 3 min. Milling containers and siliques were cooled in liquid nitrogen to prevent RNA degradation. Residual genomic DNA was removed with the peqGold DNase I Digest Kit (PEQLAB Biotechnologie, Erlangen, Germany). First strand cDNA was synthesized with Oligo(dT)$_{18}$ primers, using a First Strand cDNA Synthesis Kit (ThermoFisher Scientific, Waltham, United States).

RT-qPCR was run with Platinum SYBR Green qPCR SuperMix-UDG (Invitrogen, Carlsbad, United States) in a Bio-Rad CFX96 Real-Time System with a built-in Bio-Rad C1000 Thermal Cycler (Bio-Rad Laboratories, Munich, Germany). Primer pairs are specified inTable

S5. The cycling conditions were: 95 °C 3 min, 40 cycles (95 °C 10 s, 60 °C 30 s, 72 °C 30 s), 95 °C 10 min. Standard curve calibration was based on dilution series of cloned PCR fragments. The amplification curves were analyzed using the Bio-Rad CFX Manager 3.1 and the average Ct values of three technical replicates were used to calculate relative expression in comparison with the reference gene based on Pfaffl (2001).

3.5.4 Equilibration of silique samples for shatter trials

Siliques were harvested manually at maturity and stored in paper bags. The samples were equilibrated for moisture content in a climate control cabinet VB0714 (Vötsch Industrietechnik, Balingen-Frommern, Germany) at 25 °C and 40% r.h. for >3 days prior to measurement. Equilibration conditions were derived from Bruce et al. (2002).

3.5.5 Random impact test

The random impact test was based on Bruce et al. (2002). 20 intact siliques of 3-4 cm length were put in a cylindrical container (Ø9 cm) together with six steel balls (Ø1 cm, 7.05 g). The container was agitated on a SM-30 shaker (Edmund Bühler, Hechingen, Germany) at 5 Hz with 30 mm stroke for accumulative times of 10, 20, 40, 80, and 160 s. If less than half of the siliques were disrupted after 160 s, measurements were prolonged to 320 and 640 s. After each round of agitation, opened siliques were counted. Siliques were regarded as 'open' when at least one valve was detached.

The percentage of open siliques (p) was transformed with the logit transformation (1) and plotted against the log10 of the time. The time needed for the opening of 50% of the siliques ($T_{1/2}$) was calculated by linear regression. Standard deviation was determined from quadruplicate measurement. To obtain enough material for replicated experiments, siliques of five single plants per genotype were pooled and equally distributed for each measurement.

$$\mathrm{logit}\, p \;=\; \log_e \left(\frac{p}{100} - p \right) \tag{1}$$

3.5.6 Tensile force trial

To determine the force necessary to tear the valves of a silique apart from the replum, siliques were fixed with two alligator clamps attached to a Newton meter type FH5 on a manual test-stand (SAUTER, Balingen, Germany). Maximum disrupting forces were measured. Silique length was recorded excluding the beak. Thirty siliques per plant were measured for five single plants of every genotype that produced enough material. Silique sizes were equally distributed across 3-6 cm.

3.5.7 Cantilever test

The experimental set-up was inspired by Kadkol et al. (1984). Siliques were fixed with modeling clay on a Lab Boy lifting plate with the replum being in horizontal orientation. The pedicel end of the silique overlapped the edge of the plate by 1.5 cm. A force measurement machine of type zwickiLine Z0.5 (Zwick, Ulm, Germany) was equipped with a load cell (type Xforce HP) and a razor blade to accurately apply force at the pedicel, 2 mm from the silique walls. The blade was pressed down against the pedicel for 2 cm at a speed of 1 mm/s. The maximum compression force (N_{max}) was recorded. Additionally, the length and the breaking behavior of each silique were noted down. Peak forces detected from siliques that did not

break or siliques that only broke at the edge of the Lab Boy lifting plate were excluded from the analysis.

3.5.8 Statistical analysis

Results of tensile force measurement and cantilever trial were evaluated by analysis of covariance (Cochran 1957) with the software R (R Core Team 2015). An appropriate statistical mixed model was defined (Laird and Ware 1982; Verbeke and Lesaffre 1997) to fit a regression to the data. Based on a graphical residual analysis the data were assumed to be normally distributed and heteroscedastic due to the different genotypes. The statistical model included the genotype, the covariate silique length as well as their interaction term as fixed factors. The single plants were regarded as random factors (2). One-sided multiple comparisons for the genotypes against the Express wild type at a covariate value of 4 cm silique length were conducted. Absolute regression values at a covariate value of 4 cm are shown in Table S7 and Table S8.

$$Y \sim \text{genotype} + \text{silique length} + \text{genotype:silique length} + \text{plant} + \text{residual variance,} \tag{2}$$

where Y is the vector of observations, consisting of silique lengths (cm) and associated force values (N).

3.5.9 Replum-valve joint area index

The replum-valve joint area index (RJAI) was assessed after Hu et al. (2015). Twenty mature siliques in five biological replicates were observed under a Zeiss Stemi SV11 light microscope (Carl Zeiss, Oberkochen, Germany). The pictures were analyzed with AxioVision software (release 4.8, Carl Zeiss).

$$RJAI = L_1 * L_2, \tag{3}$$

where L_1 is the length of the vertical border and L_2 the horizontal border in the replum at the pedicel end (Figure S7).

3.5.10 Sequence analysis of rapeseed cultivars

Two *ALC* (BnaA07g12110D, BnaC07g16290D) and two *IND* (BnaA03g27180D, BnaC03g32180D) homoeologs were partially sequenced in rapeseed cultivars to check for causative mutations. The amplicons were designed to cover the bHLH domain on the basis of sequence information from Express. Primer sequences for amplification prior to Sanger sequencing are given in Table S6.

3.5.11 Light microscopy

Flowers were labeled at anthesis and sampled at 15 and 42 DAP. At 15 DAP, siliques were green and fully grown, while they turned yellow at 42 DAP. Two 0.7-1.0 cm segments of the central and basal parts of the siliques were fixed in 4% paraformaldehyde in standard phosphate buffered saline (PBS) buffer (Mulisch and Welsch 2015). Overnight, samples were subjected to a 0.5% sucrose solution in PBS at 4 °C. After embedding in tissue freezing medium, 40 μm cryosections were taken with a cryostat type CM3050 S (Leica Biosystems, Nussloch, Germany) and dried onto the object holders by the use of silica gel overnight at -20 °C. Sections were stained for 3 min at room temperature with FCA dye containing fuchsin, chryosidin and astra blue (Etzold 2002). Sections were visualized with a Nikon Eclipse Ni-E microscope (Nikon, Düsseldorf, Germany).

3.5.12 Scanning electron microscopy

Dehiscence zone fractures were examined using scanning electron microscopy (SEM). Small samples (0.5 x 0.5 cm) of fractured plant material were air-dried, mounted on metal holders by means of conductive carbon double-sided adhesive tape, sputter-coated with gold–palladium (3–6 nm), and studied in a SEM Hitachi S-4800 (Hitachi High-Technologies Corporation, Tokyo, Japan) at 3 kV accelerating voltage. Morphometrical variables of cells located within an area of 200 x 100 μm were measured from digital images using NIS Elements BR Imaging Software (version 4.40, Nikon).

3.6   Acknowledgements

3.7   Supporting information

The following supplemental materials are available.

Figure S3. Positions of TILLING amplicons and detected mutations within *BnIND*.

Figure S4. Positive correlation of silique length and shatter resistance of cultivar Express in three independent phenotyping methods.

Figure S5. Localization of PCR amplicons for partial sequencing of *BnALC* and *BnIND*.

Figure S6. The observed *Bnind* mutations do not lead to a loss of the lignified layer of the dehiscence zone.

Figure S7. RJAI of Express and F_3 double mutant *ind-2 ind-6* at a silique length of 5 to 6 cm.

Figure S8. Siliques of Express and F_3 double mutant *ind-2 ind-6*. Bar represents 1 cm.

Table S3. Nucleotide positions and amino acid exchanges of EMS mutations detected in *BnaA.IND.a* and *BnaC.IND.a.*

Table S4. Rapeseed cultivars assessed for shatter resistance.

Table S5. RT-qPCR primers.

Table S6. Homoeolog-specific primers used for TILLING and genotyping.

Table S7. Original data of shatter resistance trials of M_4 *Bnind* single mutant families and Express.

Table S8. Original data of shatter resistance trials of *Bnind* double mutant families and eight cultivars.

Table S9. *BnALC* and *BnIND* amplicons of Artoga, Drakkar, Express, Haydn, and Mozart were sequenced.

3.8 References

Arzt E, Gorb S, Spolenak R (2003) From micro to nano contacts in biological attachment devices. Proc Natl Acad Sci 100 (19):10603-10606. doi:10.1073/pnas.1534701100

Bruce DM, Farrent JW, Morgan CL, Child RD (2002) Determining the oilseed rape pod strength needed to reduce seed loss due to pod shatter. Biosyst Eng 81 (2):179-184. doi:10.1006/bioe.2001.0002

Bruce DM, Hobson RN, Morgan CL, Child RD (2001) Threshability of shatter-resistant seed pods in oilseed rape. J Agr Eng Res 80 (4):343-350. doi:10.1006/jaer.2001.0748

Cochran WG (1957) Analysis of covariance - its nature and uses. Biometrics 13 (3):261-281. doi:10.2307/2527916

Dening K, Heepe L, Afferrante L, Carbone G, Gorb SN (2014) Adhesion control by inflation: implications from biology to artificial attachment device. Applied Physics A 116 (2):567-573. doi:10.1007/s00339-014-8504-2

Etzold H (2002) Simultanfärbung von Pflanzenschnitten mit Fuchsin, Chrysoidin und Astrablau. Mikrokosmos 91 (5):316

Ferrándiz C (2000) Negative regulation of the *SHATTERPROOF* genes by *FRUITFULL* during Arabidopsis fruit development. Science 289 (5478):436-438. doi:10.1126/science.289.5478.436

Gao H, Ji B, Jäger IL, Arzt E, Fratzl P (2003) Materials become insensitive to flaws at nanoscale: lessons from nature. Proc Natl Acad Sci 100 (10):5597-5600. doi:10.1073/pnas.0631609100

Girin T, Paicu T, Stephenson P, Fuentes S, Korner E, O'Brien M, Sorefan K, Wood TA, Balanza V, Ferrándiz C, Smyth DR, Ostergaard L (2011) INDEHISCENT and SPATULA interact to specify carpel and valve margin tissue and thus promote seed dispersal in Arabidopsis. Plant Cell 23 (10):3641-3653. doi:10.1105/tpc.111.090944

Girin T, Stephenson P, Goldsack CMP, Kempin SA, Perez A, Pires N, Sparrow PA, Wood TA, Yanofsky MF, Østergaard L (2010) Brassicaceae *INDEHISCENT* genes specify valve margin cell fate and repress replum formation. Plant J 63 (2):329-338. doi:10.1111/j.1365-313X.2010.04244.x

Groszmann M, Paicu T, Alvarez JP, Swain SM, Smyth DR (2011) *SPATULA* and *ALCATRAZ*, are partially redundant, functionally diverging bHLH genes required for Arabidopsis gynoecium and fruit development. Plant J 68 (5):816-829. doi:10.1111/j.1365-313X.2011.04732.x

Gulden RH, Shirtliffe SJ, Thomas AG (2003) Harvest losses of canola (*Brassica napus*) cause large seedbank inputs. Weed Sci 51 (1):83-86

Harloff HJ, Lemcke S, Mittasch J, Frolov A, Wu JG, Dreyer F, Leckband G, Jung C (2012) A mutation screening platform for rapeseed (*Brassica napus* L.) and the detection of sinapine biosynthesis mutants. Theor Appl Genet 124 (5):957-969. doi:10.1007/s00122-011-1760-z

Hu Z, Yang H, Zhang L, Wang X, Liu G, Wang H, Hua W (2015) A large replum-valve joint area is associated with increased resistance to pod shattering in rapeseed. J Plant Res:1-7. doi:10.1007/s10265-015-0732-9

Hua S, Shamsi IH, Guo Y, Pak H, Chen M, Shi C, Meng H, Jiang L (2009) Sequence, expression divergence, and complementation of homologous *ALCATRAZ* loci in *Brassica napus*. Planta 230 (3):493-503. doi:10.1007/s00425-009-0961-z

Hui C-Y, Glassmaker N, Tang T, Jagota A (2004) Design of biomimetic fibrillar interfaces: 2. Mechanics of enhanced adhesion. J R Soc Interface 1 (1):35-48. doi:10.1098/rsif.2004.0005

Jung C (2010) Breeding with genetically modified plants. In: Kempken F, Jung C (eds) Genetic modification of plants: Agriculture, horticulture and forestry. Biotechnology in agriculture and forestry, vol 64. Springer Berlin Heidelberg, Berlin, Heidelberg, pp 103-116. doi:10.1007/978-3-642-02391-0_6

Kadkol GP, Macmillan RH, Burrow RP, Halloran GM (1984) Evaluation of *Brassica* genotypes for resistance to shatter. I. Development of a laboratory test. Euphytica 33 (1):63-73. doi:10.1007/bf00022751

Kay P, Groszmann M, Ross JJ, Parish RW, Swain SM (2013) Modifications of a conserved regulatory network involving INDEHISCENT controls multiple aspects of reproductive tissue development in Arabidopsis. New Phytol 197 (1):73-87. doi:10.1111/j.1469-8137.2012.04373.x

Laga B (2013) Brassica plant comprising a mutant *ALCATRAZ* allele. US Patent US20130291235A1, 31.10.2013

Laga B, Lambert B, Boer Bd (2015) Brassica plant comprising a mutant *INDEHISCENT* allele. Europe Patent EP2220239B1, 20.05.2015

Laird NM, Ware JH (1982) Random-effects models for longitudinal data. Biometrics 38 (4):963-974. doi:10.2307/2529876

Lenser T, Theißen G (2013) Conservation of fruit dehiscence pathways between *Lepidium campestre* and *Arabidopsis thaliana* sheds light on the regulation of *INDEHISCENT*. Plant J 76 (4):545-556. doi:10.1111/tpj.12321

Liljegren SJ, Ditta GS, Eshed HY, Savidge B, Bowman JL, Yanofsky MF (2000) *SHATTERPROOF* MADS-box genes control seed dispersal in *Arabidopsis*. Nature 404 (6779):766-770. doi:10.1038/35008089

Liljegren SJ, Roeder AHK, Kempin SA, Gremski K, Ostergaard L, Guimil S, Reyes DK, Yanofsky MF (2004) Control of fruit patterning in *Arabidopsis* by *INDEHISCENT*. Cell 116 (6):843-853. doi:10.1016/S0092-8674(04)00217-X

Mason AS, Higgins EE, Snowdon RJ, Batley J, Stein A, Werner C, Parkin IAP (2017) A user guide to the *Brassica* 60K Illumina Infinium™ SNP genotyping array. Theor Appl Genet 130 (4):621-633. doi:10.1007/s00122-016-2849-1

Meakin PJ, Roberts JA (1990) Dehiscence of fruit in oilseed rape (*Brassica napus* L) .1. Anatomy of pod dehiscence. J Exp Bot 41 (229):995-1002. doi:10.1093/Jxb/41.8.995

Mulisch M, Welsch U (eds) (2015) Romeis - Mikroskopische Technik. 19 edn. Springer-Verlag Berlin Heidelberg. doi:10.1007/978-3-642-55190-1

Ogawa M, Kay P, Wilson S, Swain SM (2009) ARABIDOPSIS DEHISCENCE ZONE POLYGALACTURONASE1 (ADPG1), ADPG2, and QUARTET2 are polygalacturonases required for cell separation during reproductive development in Arabidopsis. Plant Cell 21 (1):216-233. doi:10.1105/tpc.108.063768

Pfaffl MW (2001) A new mathematical model for relative quantification in real-time RT-PCR. Nucleic Acids Res 29 (9):e45. doi:10.1093/nar/29.9.e45

Price JS, Hobson RN, Neale MA, Bruce DM (1996) Seed losses in commercial harvesting of oilseed rape. J Agr Eng Res 65 (3):183-191. doi:10.1006/jaer.1996.0091

Rajani S, Sundaresan V (2001) The *Arabidopsis* myc/bHLH gene *ALCATRAZ* enables cell separation in fruit dehiscence. Curr Biol 11 (24):1914-1922. doi:10.1016/S0960-9822(01)00593-0

R Core Team (2015) R: A language and environment for statistical computing., 3.2.0 edn. R Foundation for Statistical Computing, Vienna

Sander L, Child R, Ulvskov P, Albrechtsen M, Borkhardt B (2001) Analysis of a dehiscence zone endo-polygalacturonase in oilseed rape (*Brassica napus*) and *Arabidopsis thaliana*: evidence for roles in cell separation in dehiscence and abscission zones, and in stylar tissues during pollen tube growth. Plant Mol Biol 46 (4):469-479. doi:10.1023/A:1010619002833

Schondelmaier J, Steinrücken G, Jung C (1996) Integration of AFLP markers into a linkage map of sugar beet (*Beta vulgaris* L.). Plant Breed 115 (4):231-237. doi:10.1111/j.1439-0523.1996.tb00909.x

Summers JE, Bruce DM, Vancanneyt G, Redig P, Werner CP, Morgan C, Child RD (2003) Pod shatter resistance in the resynthesized *Brassica napus* line DK142. J Agr Sci 140 (1):43-52. doi:10.1017/s002185960200285x

Tan XL, Xia ZW, Zhang LL, Zhang ZY, Guo ZJ, Qi CK (2009) Cloning and sequence analysis of oilseed rape (*Brassica napus*) *SHP2* gene. Bot Stud 50 (4):403-412

Till BJ, Zerr T, Comai L, Henikoff S (2006) A protocol for TILLING and Ecotilling in plants and animals. Nat Protoc 1 (5):2465-2477. doi:10.1038/nprot.2006.329

Udall JA, Quijada PA, Lambert B, Osborn TC (2006) Quantitative trait analysis of seed yield and other complex traits in hybrid spring rapeseed (*Brassica napus* L.): 2. Identification of alleles from unadapted germplasm. Theor Appl Genet 113 (4):597-609. doi:10.1007/s00122-006-0324-0

Varenberg M, Pugno NM, Gorb SN (2010) Spatulate structures in biological fibrillar adhesion. Soft Matter 6 (14):3269-3272. doi:10.1039/C003207G

Verbeke G, Lesaffre E (1997) The effect of misspecifying the random-effects distribution in linear mixed models for longitudinal data. Comput Stat Data An 23 (4):541-556. doi:10.1016/S0167-9473(96)00047-3

Wang R, Ripley VL, Rakow G (2007) Pod shatter resistance evaluation in cultivars and breeding lines of *Brassica napus*, *B. juncea* and *Sinapis alba*. Plant Breed 126 (6):588-595. doi:10.1111/j.1439-0523.2007.01382.x

Zerr T, Henikoff S (2005) Automated band mapping in electrophoretic gel images using background information. Nucleic Acids Res 33 (9):2806-2812. doi:10.1093/nar/gki580

Zhang Y, Shen YY, Wu XM, Wang JB (2016) The basis of pod dehiscence: anatomical traits of the dehiscence zone and expression of eight pod shatter-related genes in four species of *Brassicaceae*. Biol Plantarum:1-12. doi:10.1007/s10535-016-0599-1

4   EMS-induced point mutations in *ALCATRAZ* homoeologs increase silique shatter resistance of oilseed rape (*Brassica napus*)

Under review

4.1   Abstract

Previously, we demonstrated the increased silique shatter resistance of oilseed rape (*Brassica napus*) through Cas9-induced targeted mutations in *ALCATRAZ* (*BnALC*) (Braatz et al. 2017). In Arabidopsis (*Arabidopsis thaliana*), the transcription factor ALC is involved in the control of silique tissue identity, ensuring the establishment of a separation layer that contributes to the fragility of the dry fruit. Thus, a more robust silique through *Bnalc* loss-of-function mutations was hypothesized. However, in our Cas9-mutated plants, the effect was masked by the high shatter resistance of the transformed cultivar itself. In this study, we used a rapeseed genotype with low shattering resistance. We identified 23 *Bnalc* mutants by TILLING of an EMS-mutagenized 'Express' population. By measuring tensile forces necessary to disrupt mature siliques, we determined a double mutant with significantly increased shatter resistance. This mutant can readily be introduced into breeding programs.

4.2   Introduction

Silique shattering can cause severe yield losses in rapeseed (*Brassica napus*) through seed shedding from mature fruits prior and during harvesting. Up to 25% harvest losses were reported from swathed oilseed rape fields (Price et al. 1996). Direct cutting of standing plants can still cost 7% of seeds (Price et al. 1996; Pari et al. 2012) which fall to the ground and add to the soil seed bank (Gulden et al. 2003). Consequently, volunteer plants appear during the following seasons. If not properly controlled, volunteers can persist up to 17 years after intended cultivation (Jørgensen et al. 2007). Volunteer rapeseed can have various disadvantageous effects like contaminating seed lots of quality rapeseed (Baux et al. 2011) or helping pathogens to bridge the rotation gap between *Brassica* crops (Hwang et al. 2012). Thus, silique shattering needs to be reduced to optimize rapeseed cultivation by stabilizing yield and diminishing the necessity to control volunteer rapeseed.

The genetic background of silique shattering was extensively studied in Arabidopsis (*Arabidopsis thaliana*; reviewed in Dinneny and Yanofsky 2005), which is a model plant for crops of the *Brassicaceae* family. The basic helix-loop-helix (bHLH) transcription factors INDEHISCENT (IND) and ALCATRAZ (ALC) are major regulators of specialized tissue development in the predetermined breaking zone of the silique, which is termed dehiscence zone. The dehiscence zone is made up of two thin cell layers, a separation layer and a lignified layer. During maturation, the separation layer weakens as a result of enzymatic activities (Meakin and Roberts 1990a; Ogawa et al. 2009). Consequently, the neighbouring layers of rigid, lignified tissue and partially digested cells confer brittleness to the dry fruit. In Arabidopsis, strong *ind* mutant alleles cause a lack of both lignified and separation layer, resulting in tube-like siliques without valve margin constriction (Liljegren et al. 2004). Similar phenotypes were reported for *Brassica rapa* and *Brassica oleracea* (Girin et al. 2010). Arabidopsis *alc* mutants show a less severe phenotype without a separation layer but maintaining the lignified cells (Rajani and Sundaresan 2001). Hua et al. (2009) cloned two *BnALC* homoeologs in rapeseed and confirmed their conserved function by complementation of Arabidopsis *alc* mutants.

In a previous study, we performed a Cas9-mediated targeted mutagenesis of *BnALC* via the stable transformation of rapeseed hypocotyl explants (Braatz et al. 2017). However, the cultivar 'Haydn', which was used due to its reported transformation efficiency, was highly shatter resistant and masked the mutational effect. Therefore, we now investigated the effect of *Bnalc* mutations in the winter rapeseed variety 'Express' which has more fragile siliques. We selected *Bnalc* mutants by Targeting Induced Local Lesions in Genomes (TILLING) in an EMS mutagenized 'Express' population and combined mutated homoeologs by crossing. Due to the polyploid rapeseed genome (AACC), we expected shatter resistance only in double mutants. This expectation was confirmed through phenotyping of mature siliques by force measurements in the greenhouse.

4.3 Materials and methods

4.3.1 Mutation screening

2,688 and 3,840 M_2 plants of an 'Express' EMS mutant population (Harloff et al. 2012) were screened for mutations in *BnaA.ALC.a* (BnaA07g12110D) and *BnaC.ALC.a* (BnaC07g16290D) by TILLING. Homoeolog-specific, 700 nm and 800 nm IRD fluorescence labeled primers (Biomers, Ulm, Germany; Table S11) were utilized for amplification from two dimensional 8-fold pools. *Cel*I digestion of heteroduplices, sample purification, and polyacrylamide gel electrophoresis on a LI-COR 4300 DNA analyzer (LI-COR Biosciences, www.licor.com) were performed according to Till et al. (2006). Restriction fragments were analyzed by the GelBuddy Software (Zerr and Henikoff 2005) to identify mutations.

Mutation frequencies *F* were calculated on the basis of mutations per M_1 plant after Harloff et al. (2012):

$$F\left[1/kb\right] = 1 \left/ \left(\frac{(amplicon\ size\ [bp]-100)*(number\ of\ M1\ plants)}{(number\ of\ mutations)*1{,}000}\right)\right. \tag{4}$$

4.3.2 Plant material and greenhouse experiments

Double mutants were produced by crossing selected *bnaA.alc.a* and *bnaC.alc.a* mutants. For one combination, original M_3 single mutants were selected as parents. The other two crosses were conducted with M_3 plants once crossed to 'Express'.

To collect siliques for phenotyping, segregating F_2 families were grown alongside 'Express' in the greenhouse (22 °C, 16 h light/ 8 h dark). Two weeks of pre-culture were followed by eight weeks of vernalization in a cold chamber (4 °C, 16 h light/ 8 h dark). Then, plants were transferred into 11x11 cm pots and brought back to the initial greenhouse conditions. Fertilization with 0.5 g Compo Blaukorn Classic universal fertilizer (Compo, Münster, Germany) was conducted before flowering. At the point of flowering, selfing bags were mounted.

4.3.3 Shatter resistance measurements

Mature siliques were sampled manually and stored in a climate cabinet VB0714 (Vötsch Industrietechnik, Balingen-Frommern, Germany) at 25 °C and 40% r.h. for >3 days for moisture equilibration. Shatter resistance was assessed as maximum disrupting force, measured by tearing the valves of siliques apart with a Newton meter type FH10 mounted on a manual test-stand (SAUTER, Balingen, Germany; Figure S9). Silique length without the beak was recorded. For every genotype that produced enough material, thirty siliques of five

plants were measured. The statistical interpretation was based on an analysis of covariance (Cochran 1957) implemented with the software R (R Core Team 2015). The statistical model for the estimation of the regression is specified in (5). Y designates the vector of observations (force values, silique lengths). The genotype, the covariate silique length and their interaction term are included as fixed factors. Single plants are regarded as random factors. One-sided multiple comparisons of the genotypes against the 'Express' wild type were conducted.

$$Y \sim \text{genotype} + \text{silique length} + \text{genotype:silique length} + \text{plant} + \text{residual variance} \tag{5}$$

4.4 Results

4.4.1 Identification of EMS-induced *Bnalc* mutations by TILLING

We designed homoeolog-specific TILLING amplicons which covered 71% and 93% of *BnaA.ALC.a* and *BnaC.ALC.a,* respectively. Screening 2,688 M_2 plants for mutations in *BnaA.ALC.a* and 3,840 for mutations in *BnaC.ALC.a* resulted in the identification of 79 candidates (Table 6). As the size of the TILLING fragments yielded information about the position of each mutation, we sequenced only those candidates which were either close to a possible premature stop codon mutation site, a splice site, or which lay within the conserved bHLH domain. Regarding *BnaA.ALC.a*, one nonsense, two splice site, and three missense mutations were verified. For *BnaC.ALC.a* , we found one splice site and sixteen missense mutations (Figure 11a, Table S10). We calculated mutation frequencies of one mutation every 15 to 24 kb. Regarding the 1.1 Gb genome size of rapeseed, 47,000-75,000 background mutations caused by EMS can be expected in a single plant of the underlying mutant population.

Table 6. Overview of *Bnalc* mutations detected by TILLING.

	BnaA.ALC.a	*BnaC.ALC.a*
Screened M_2 plants	2,688	3,840
Candidates	21	58
Selection of promising candidates for sequencing	10	31
Verified by Sanger sequencing	9	29
Nonsense	1	0
Missense	3	16
Splice site	2	1
Silent	3	12
Mutation frequency [1/kb]	1/24	1/15
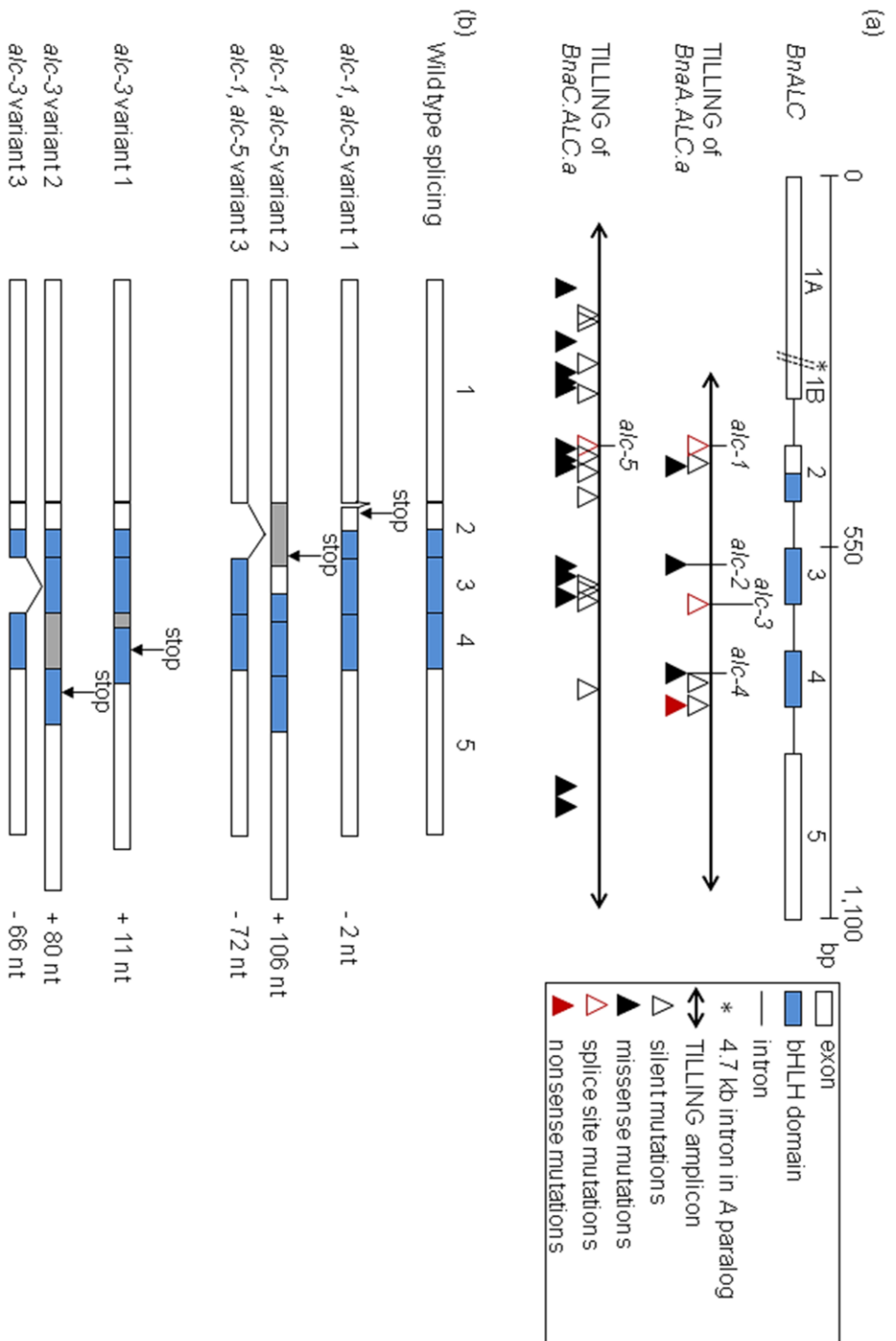
Figure 11. (a) *BnALC* gene structure and positions of EMS-induced mutations identified by TILLING. Displayed mutations were verified by Sanger sequencing of M₃ plants. Mutations *alc-1* to *alc-5* were further analyzed. (b) Proposed mis-splicing effects due to mutations *alc-1*, *alc-3*, and *alc-5*. In each case, splice variant 1 describes the usage of a nearby, alternative splice site, variant 2 involves complete intron retention, and variant 3 exon skipping. Premature stop codons are indicated by arrows, lost exonic sequences by solid lines, and retained intronic sequences by a grey box. The influence of the aberrant splice variants on the length of the spliced mRNA product is given in nucleotides (nt).

Three *bnaA.alc.a* mutants and one *bnaC.alc.a* mutant were selected for further studies
(Table 7). The selection consisted of three splice site mutations and two missense mutations
located within the bHLH domain. Mutations *alc-1* and *alc-4* were detected within a distance
of 334 bp in *BnaA.ALC.a* in the same M_2 plant. Therefore, the mutant was designated as a
'single mutant' (*alc-1/alc-4*). The premature stop codon mutation was considered as well but
due to poor performance of the M_3, development of plant material for phenotyping was
delayed. Further evaluations are on the way.

Plants with mutations in both *BnALC* homoeologs were produced following two approaches:
(1) By crossing M_3 single mutants (*alc-2* x *alc-5*) and (2) by crossing the F_1 of single mutants
once backcrossed to 'Express' (*alc-1/alc-4* x *alc-5* and *alc-3* x *alc-5*). Next, we phenotyped
the three segregating F_2 populations.

Table 7. *Bnalc* mutant selection. Positions of mutations were counted from the start codon 'ATG'.

M_3 seed code	Mutation	Amino acid change	Mutant code
150037	*bnaA.alc.a*_G5053A	splice site mutation	*alc-1*
	*bnaA.alc.a*_G5387A	Glu142Lys	*alc-4*
150038	*bnaA.alc.a*_G5229A	Glu116Lys	*alc-2*
150034	*bnaA.alc.a*_G5274A	splice site mutation	*alc-3*
150035	*bnaC.alc.a*_G352A	splice site mutation	*alc-5*

4.4.2 Shatter resistance of *Bnalc* mutants

We assessed shatter resistance by measuring maximum tensile forces at the disruption of
mature siliques. A positive correlation of tensile force and silique length was observed
(Pearson correlation coefficient r = 0.36, calculated for 'Express'; Figure S10). In average,
'Express' siliques of 4 cm, 5.5 cm, and 7 cm length disrupted at application of 0.853 N,
1.257 N, and 1.662 N, respectively (Figure 12; Table S12). Of the three *Bnalc* double mutant
families tested, two showed significant increases in shatter resistance compared with
'Express'. Regarding the double mutant combination *alc-2 alc-5*, the difference to 'Express'
was most pronounced for shorter siliques (1.559 N difference at 4 cm silique length). In
contrast, the effect of double mutant combination *alc-1/alc-4 alc-5* was higher considering
long siliques (1.065 N difference at 7 cm silique length). Only the combination *alc-3 alc-5* did
not significantly affect shatter resistance.

To study the effect of the mutant alleles in detail, we also compared the homozygous single
mutants (*aaCC*, *AAcc*) with double mutants (*aacc*) and wild types (*AACC*) of segregating
families (Figure 12). As expected, single mutants of the *alc-1/alc-4 alc-5* family showed no
significant difference in shatter resistance compared with 'Express'. In contrast, shatter
resistance of both single mutants of the *alc-2 alc-5* family was significantly increased.
However, in this family even the wild type had more robust siliques than the control, which
hints at a yet unknown dominant background mutation. As the combination of mutations *alc-2*
and *alc-5* was achieved by directly crossing M_3 plants, this F_2 family contains a doubled
background mutation load. Until background effects have been eliminated through
backcrossing, the shatter resistance of the according double mutant cannot be clearly assigned
to the *Bnalc* knock-down alleles.
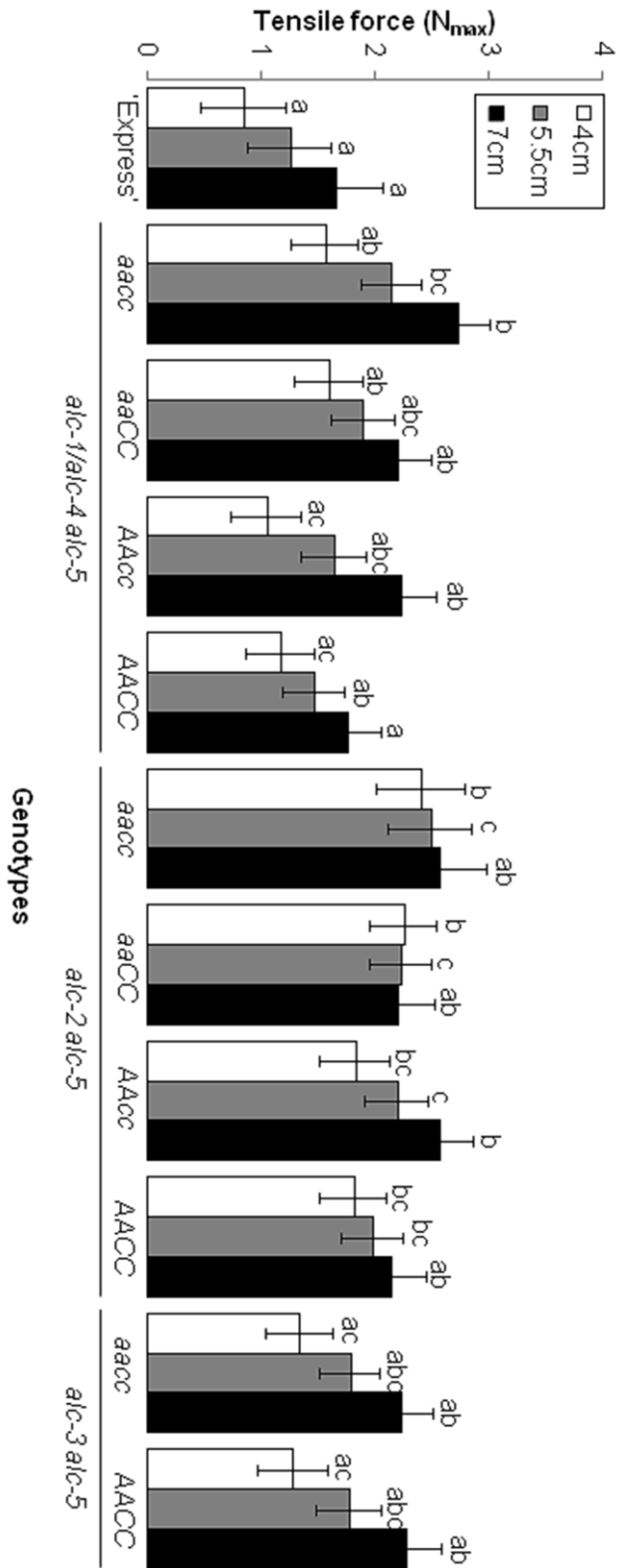
Figure 12. Shatter resistance of segregating *Bnalc* mutant families. All values were calculated from linear regressions. Statistical analyses were conducted as one-sided multiple comparisons of tensile forces at three silique lengths. Within each silique length, shared letters (a, b, c) indicate no significant difference ($P \geq 0.05$). Bars represent standard errors.

4.5   Discussion

4.5.1   Effect of *Bnalc* mutant alleles

The significantly increased shatter resistance of double mutant *alc-1/alc-4 alc-5* highlights the disruptive potential of splice site mutations. Both *alc-1* and *alc-5* are AG>AA transitions of the 3' AG splice acceptor site of intron 1, with *alc-1* being located in *BnaA.ALC.a* and *alc-5* in *BnaC.ALC.a*. The same type of 3' splice site mutation resulted in the activation of an alternative neighboring splice acceptor site in EMS-mutagenized wheat (Simmonds et al. 2016). In Arabidopsis, such a 3' splice site mutation triggered a more complex splicing pattern with four aberrant variants, comprising the complete retention of the intron and the use of three novel splice sites (Marchant and Bennett 1998). Meanwhile, a naturally occurring 5' splice site polymorphism in *BrFLC1* lead to a similar multi-faceted splicing pattern which in parallel to the use of novel splice sites also caused the loss of the affected exon (Yuan et al. 2009). Accordingly, we propose three possible mis-splicing effects caused by *alc-1* and *alc-5* (Figure 11b). Regarding both *BnALC* homoeologs, the usage of the next splice acceptor site downstream of *alc-1* and *alc-5* would lead to a two nucleotide (nt) AG deletion in the spliced mRNA, which results in a frameshift and a premature stop codon, already at the fourth amino acid position of exon 2. The retention of the complete intron, however, would add 106 nt which already include a premature stop codon. As both stop codon sites are located upstream of the bHLH domain, full knock-out alleles can be expected. Skipping of exon 2 would reduce the length of the spliced mRNA by 72 nt and result in the loss of the basic part of the bHLH transcription factor domain which is required for DNA binding (Voronova and Baltimore 1990). Consequently, this splice variant must also be non-functional. Considering all three scenarios, we assume that *alc-4*, the additional *bnaA.alc.a* mutation downstream of *alc-1*, is not causal for the shatter resistance of the *alc-1/alc-4 alc-5* double mutant.

Surprisingly, the third splice site mutation, *alc-3*, did not significantly influence silique robustness in combination with *alc*-5. *alc-3* is situated at the 5' GT splice donor site of intron 3. As a result of this mutation, we again expected the activation of a close-by alternative splice donor site, full intron retention or exon skipping (Figure 11b). The alternative splice donor site closest to *alc-3* is located 11 nt downstream and causes a frameshift and a premature stop codon. The same premature stop codon would result from the retention of intron 3 (80 bp). In this case, the basic region and the first helix of the bHLH domain would remain intact. However, bHLH proteins require both helices to successfully dimerize and bind target DNA (Davis et al. 1990; Voronova and Baltimore 1990). By skipping exon 3, a part of the basic region together with the complete first helix of the bHLH domain would be erased. Still, *alc-3 alc-5* double mutants were not shatter resistant. This can only be explained by a residual function of the *alc*-3 mutant allele. Interestingly, Isshiki et al. (1998) reported that a GT>TT 5' splice site mutant mRNA of the rice *waxy* locus was still spliced like the wild type variant, however with a greatly reduced efficiency. We accordingly propose a low abundance of functional wild type splice product of the *alc-3* allele and a higher abundance of the expected aberrant splice variants. Sequencing of cDNA will provide the final proof for this hypothesis.

The effect of the missense mutation *alc-2* cannot be estimated because unknown background mutations increased the shatter resistance throughout the segregating *alc-2 alc-5* F_2 family. This case shows that direct crossing of M_3 plants can interfere with the identification of phenotypic effects related to a specific mutation. Backcross generations are currently on the way.

4.5.2 Comparison of shatter resistance with previously described *Bnalc* and *Bnind* mutants

With this study, we confirmed the shatter resistant *Bnalc* phenotype which we previously reported for Cas9-induced mutations in the variety 'Haydn' (Braatz et al. 2017). For direct comparison of different experiments and different varieties, we subtracted the tensile force of the respective control variety from the mutant genotype. The resulting differences are displayed in Table 8.

As expected, we detected a bigger influence of *Bnalc* mutations on shatter resistance of the variety 'Express' compared with 'Haydn'. We measured a maximum difference of 0.888 N for *Bnalc* mutants in the 'Express' background, but only 0.414 N in the 'Haydn' background, although we assume a complete disruption of *Bn*ALC function in the latter due to frameshift mutations which lead to premature stop codons upstream of the bHLH domain (Braatz et al. 2017). The underlying mechanism of robustness of 'Haydn' siliques was not yet examined so that we can only speculate about a hampered response to *Bnalc* mutations based on an already impaired downstream target. However, since shatter resistance is a quantitative trait (Raman et al. 2014; Liu et al. 2016), epistatic interactions could also explain varying effects of *Bnalc* mutations on different genotypes.

Next, we compared our *Bnalc* mutants with *Bnind* mutants (Braatz et al., submitted). Both were identified by TILLING of the same 'Express' EMS population. *Bnind* double mutants produced stronger siliques than *Bnalc* double mutants (Table 8), which is in accordance with *IND* playing a dominant role in dehiscence zone development in Arabidopsis (Liljegren et al. 2004). A means to elucidate whether *BnALC* and *BnIND* homoeologs independently regulate dehiscence zone formation would be the production of quadruple mutants. However, crossing of our EMS double mutants would be inappropriate regarding the accumulation of background mutations. Cas9-targeted mutagenesis of *BnIND* in the *Bnalc* 'Haydn' plants is clearly superior.

Currently, the described shatter resistant phenotypes are restricted to greenhouse-grown rapeseed plants. Correlations of silique strength phenotyping strategies and field performance have been reported in the past (Kadkol et al. 1984; Wang et al. 2007). Field evaluation of our EMS material is on the way.

Table 8. Comparison of the effect of *Bnalc* and *Bnind* mutations on shatter resistance. Shatter resistance is expressed as the difference of tensile forces by subtracting the control cultivar from the double mutant genotype. The forces were calculated from linear regressions at a silique length of 5.5 cm. For EMS double mutants, the segregating F_2 (mutant x 'Express') was considered. The cultivar 'Express' appears twice in this table, because it was assessed in two different experiments.

Mutated genes	Mutations	Cultivar	Tensile force			Reference
			Mutant (N_{max})	Cultivar (N_{max})	Difference (ΔN_{max})	
BnaA.ALC.a, BnaC.ALC.a	EMS-induced mutations *alc-1/alc-4 alc-5*	'Express'	2.145	1.257	0.888	This study
BnaA.ALC.a, BnaC.ALC.a	Cas9-induced indels	'Haydn'	4.422	4.008	0.414	Braatz et al. 2017
BnaA.IND.a, BnaC.IND.a	EMS-induced mutations *ind-2 ind-6*	'Express'	3.757	1.065	2.692	Braatz et al., submitted

4.5.3 Use of *Bnalc* and *Bnind* mutations for breeding

Shatter resistance is a trait that needs to be carefully fine-tuned. While robust siliques reduce seed loss, an excess of silique strength would diminish the threshability by a combine harvester. Higher threshing intensities damage the released seeds. The maximum silique strength suitable for threshing was previously investigated (Bruce et al. 2001).

By identifying EMS-induced *Bnalc* and *Bnind* mutants with different levels of shatter resistance, we provide valuable material for breeders. Depending on the silique strength of their breeding material, they can introduce either *Bnalc* or the stronger *Bnind* alleles. However, the recessive nature of the mutant alleles has to be especially considered for hybrid breeding. All parental components need to carry the mutations in a homozygous state to assure shatter resistance in all of the progeny.

4.6 Acknowledgements

4.7 Supplements

The following supplemental materials are available.

Figure S9. Experimental set-up of the tensile force measurement.

Figure S10. Raw data of tensile force measurement of variety 'Express'.

Table S10. Nucleotide positions and amino acid exchanges of EMS mutations detected in *BnaA.ALC.a* and *BnaC.ALC.a*.

Table S11. Primers used for *BnALC* TILLING.

Table S12. Original data of shatter resistance trials of F_2 *Bnalc* double mutant families and 'Express'.

4.8 References

Baux A, Colbach N, Pellet D (2011) Crop management for optimal low-linolenic rapeseed oil production - Field experiments and modelling. Europ J Agronomy 35 (3):144-153. doi:10.1016/j.eja.2011.05.006

Braatz J, Harloff H-J, Mascher M, Stein N, Himmelbach A, Jung C (2017) CRISPR-Cas9 targeted mutagenesis leads to simultaneous modification of different homoeologous gene copies in polyploid oilseed rape (*Brassica napus*). Plant Physiol 174 (2): 935-942 doi:10.1104/pp.17.00426

Bruce DM, Hobson RN, Morgan CL, Child RD (2001) Threshability of shatter-resistant seed pods in oilseed rape. J Agr Eng Res 80 (4):343-350. doi:10.1006/jaer.2001.0748

Cochran WG (1957) Analysis of covariance - its nature and uses. Biometrics 13 (3):261-281. doi:10.2307/2527916

Davis RL, Cheng P-F, Lassar AB, Weintraub H (1990) The MyoD DNA binding domain contains a recognition code for muscle-specific gene activation. Cell 60 (5):733-746. doi:10.1016/0092-8674(90)90088-V

Dinneny JR, Yanofsky MF (2005) Drawing lines and borders: how the dehiscent fruit of *Arabidopsis* is patterned. Bioessays 27 (1):42-49. doi:10.1002/bies.20165

Girin T, Stephenson P, Goldsack CMP, Kempin SA, Perez A, Pires N, Sparrow PA, Wood TA, Yanofsky MF, Østergaard L (2010) Brassicaceae *INDEHISCENT* genes specify valve margin cell fate and repress replum formation. Plant J 63 (2):329-338. doi:10.1111/j.1365-313X.2010.04244.x

Gulden RH, Shirtliffe SJ, Thomas AG (2003) Harvest losses of canola (*Brassica napus*) cause large seedbank inputs. Weed Sci 51 (1):83-86

Harloff HJ, Lemcke S, Mittasch J, Frolov A, Wu JG, Dreyer F, Leckband G, Jung C (2012) A mutation screening platform for rapeseed (*Brassica napus* L.) and the detection of sinapine biosynthesis mutants. Theor Appl Genet 124 (5):957-969. doi:10.1007/s00122-011-1760-z

Hua S, Shamsi IH, Guo Y, Pak H, Chen M, Shi C, Meng H, Jiang L (2009) Sequence, expression divergence, and complementation of homologous *ALCATRAZ* loci in *Brassica napus*. Planta 230 (3):493-503. doi:10.1007/s00425-009-0961-z

Hwang SF, Ahmed HU, Zhou Q, Strelkov SE, Gossen BD, Peng G, Turnbull GD (2012) Assessment of the impact of resistant and susceptible canola on *Plasmodiophora brassicae* inoculum potential. Plant Pathol 61 (5):945-952. doi:10.1111/j.1365-3059.2011.02582.x

Isshiki M, Morino K, Nakajima M, Okagaki RJ, Wessler SR, Izawa T, Shimamoto K (1998) A naturally occurring functional allele of the rice *waxy* locus has a GT to TT mutation at the 5′ splice site of the first intron. Plant J 15 (1):133-138. doi:10.1046/j.1365-313X.1998.00189.x

Jørgensen T, Hauser TP, Jørgensen RB (2007) Adventitious presence of other varieties in oilseed rape (*Brassica napus*) from seed banks and certified seed. Seed Sci Res 17 (2):115-125. doi:10.1017/S0960258507708103

Kadkol GP, Macmillan RH, Burrow RP, Halloran GM (1984) Evaluation of *Brassica* genotypes for resistance to shatter. I. Development of a laboratory test. Euphytica 33 (1):63-73. doi:10.1007/bf00022751

Liljegren SJ, Roeder AHK, Kempin SA, Gremski K, Ostergaard L, Guimil S, Reyes DK, Yanofsky MF (2004) Control of fruit patterning in *Arabidopsis* by *INDEHISCENT*. Cell 116 (6):843-853. doi:10.1016/S0092-8674(04)00217-X

Liu J, Huang SM, Sun MY, Liu SY, Liu YM, Wang WX, Zhang XR, Wang HZ, Hua W (2012) An improved allele-specific PCR primer design method for SNP marker analysis and its application. Plant Methods 8. doi:10.1186/1746-4811-8-34

Liu J, Wang J, Wang H, Wang W, Mei D, Zhou R, Cheng H, Yang J, Raman H, Hu Q (2016) Multigenic control of pod shattering resistance in Chinese rapeseed germplasm

revealed by genome-wide association and linkage analyses. Front Plant Sci 7. doi:10.3389/fpls.2016.01058

Marchant A, Bennett MJ (1998) The *Arabidopsis AUX1* gene: a model system to study mRNA processing in plants. Plant Mol Biol 36 (3):463-471

Meakin PJ, Roberts JA (1990) Dehiscence of Fruit in Oilseed Rape (Brassica-Napus L) .2. The Role of Cell-Wall Degrading Enzymes and Ethylene. J Exp Bot 41 (229):1003-1011. doi:10.1093/jxb/41.8.1003

Ogawa M, Kay P, Wilson S, Swain SM (2009) ARABIDOPSIS DEHISCENCE ZONE POLYGALACTURONASE1 (ADPG1), ADPG2, and QUARTET2 are polygalacturonases required for cell separation during reproductive development in Arabidopsis. Plant Cell 21 (1):216-233. doi:10.1105/tpc.108.063768

Pari L, Assirelli A, Suardi A, Civitarese V, Del Giudice A, Costa C, Santangelo E (2012) The harvest of oilseed rape (*Brassica napus* L.): The effective yield losses at on-farm scale in the Italian area. Biomass Bioenerg 46:453-458. doi:10.1016/j.biombioe.2012.07.014

Price JS, Hobson RN, Neale MA, Bruce DM (1996) Seed losses in commercial harvesting of oilseed rape. J Agr Eng Res 65 (3):183-191. doi:10.1006/jaer.1996.0091

Rajani S, Sundaresan V (2001) The *Arabidopsis* myc/bHLH gene *ALCATRAZ* enables cell separation in fruit dehiscence. Curr Biol 11 (24):1914-1922. doi:10.1016/S0960-9822(01)00593-0

Raman H, Raman R, Kilian A, Detering F, Carling J, Coombes N, Diffey S, Kadkol G, Edwards D, McCully M, Ruperao P, Parkin IAP, Batley J, Luckett DJ, Wratten N (2014) Genome-wide delineation of natural variation for pod shatter resistance in *Brassica napus*. Plos One 9 (7):e101673. doi:10.1371/journal.pone.0101673

R Core Team (2015) R: A language and environment for statistical computing., 3.2.0 edn. R Foundation for Statistical Computing, Vienna

Simmonds J, Scott P, Brinton J, Mestre TC, Bush M, del Blanco A, Dubcovsky J, Uauy C (2016) A splice acceptor site mutation in *TaGW2-A1* increases thousand grain weight in tetraploid and hexaploid wheat through wider and longer grains. Theor Appl Genet 129 (6):1099-1112. doi:10.1007/s00122-016-2686-2

Till BJ, Zerr T, Comai L, Henikoff S (2006) A protocol for TILLING and Ecotilling in plants and animals. Nat Protoc 1 (5):2465-2477. doi:10.1038/nprot.2006.329

Voronova A, Baltimore D (1990) Mutations that disrupt DNA binding and dimer formation in the E47 helix-loop-helix protein map to distinct domains. Proc Natl Acad Sci 87 (12):4722-4726. doi:10.1073/pnas.87.12.4722

Wang R, Ripley VL, Rakow G (2007) Pod shatter resistance evaluation in cultivars and breeding lines of *Brassica napus*, *B. juncea* and *Sinapis alba*. Plant Breed 126 (6):588-595. doi:10.1111/j.1439-0523.2007.01382.x

Yuan Y-X, Wu J, Sun R-F, Zhang X-W, Xu D-H, Bonnema G, Wang X-W (2009) A naturally occurring splicing site mutation in the *Brassica rapa FLC1* gene is associated with variation in flowering time. J Exp Bot 60 (4):1299-1308. doi:10.1093/jxb/erp010

Zerr T, Henikoff S (2005) Automated band mapping in electrophoretic gel images using background information. Nucleic Acids Res 33 (9):2806-2812. doi:10.1093/nar/gki580

5   Cas9-induced mutagenesis of *BnNST1* homoeologs

5.1   Introduction

Oilseed rape (*Brassica napus*) is a crop that naturally sheds its seeds by producing dehiscent siliques. This strategy of seed dispersal has severe consequences for commercial rapeseed production like yield loss (Price et al. 1996; Gulden et al. 2003; Peltonen-Sainio et al. 2014) and growth of volunteers which can reduce harvest quality (Baux et al. 2011).

In rapeseed, silique shattering relies on the proper development of the so called 'dehiscence zone', which is the predetermined breaking zone between valves and replum. The dehiscence zone consists of a lignified cell layer next to a separation layer that is weakened by cell wall-degrading enzymes (Meakin and Roberts 1990b).

Mitsuda and Ohme-Takagi (2008) reported that the partially redundant *NAC SECONDARY WALL THICKENING PROMOTING FACTOR*s *1* and *3* (*NST1/3*) are needed for secondary wall thickening of valve margins in Arabidopsis (*Arabidopsis thaliana*) siliques: Both *nst1*and *nst1 nst3* knock-out lines produced indehiscent siliques. In the gene regulatory network that controls the dehiscence zone development, *NST1/3* are located downstream of the transcription factor INDEHISCENT (IND; Figure 1B). However, the direct induction of *NST1/3* expression through *IND* was not yet demonstrated. Earlier studies showed that *NST1* and *NST3* also regulate secondary wall formation in other woody tissues, resulting in a dramatic phenotype of *nst1 nst3* double mutants that is unable to stand erect (Mitsuda et al. 2007; Zhong et al. 2007). However, Arabidopsis *nst1* single mutants did not suffer from weakened stems (Mitsuda et al. 2005) and *BnNST1* genes are therefore possible targets for the improvement of shatter resistance in rapeseed, from which no adverse effects have to be expected. The intention of utilizing rapeseed *Bnnst* mutants to reduce lignification is encouraged by the functional conservation of *NST* homologs in poplar (*Populus trichocarpa*), rice (*Oryza sativa*), maize (*Zea mays*), and barrel clover (*Medicago truncatula*; Zhong et al. 2010; Zhong et al. 2011; Wang et al. 2011a). Four *NST3* homologs from poplar (*PtrWND1A* and *B, PtrWND2A* and *B*), two *NST3* homologs from rice (*OsSWN1* and *2*), and two *NST3* homologs from maize (*ZmSWN1* and *2*) complemented Arabidopsis *nst1 nst3* mutant phenotypes (Zhong et al. 2010; Zhong et al. 2011; Author's note: In both articles *NST3* is referred to by its alias '*SND1*'.). Moreover, the barrel clover *Mtnst1* mutant lacked lignification in interfascicular cells (Wang et al. 2011a).

NST1 belongs to the NAC domain transcription factor family. NAC is an acronym of the gene names <u>*NO APICAL MERISTEM*</u>, <u>*ATAF1/2*</u>, and <u>*CUP-SHAPED COTYLEDON2*</u>, which were the first genes within which the domain was identified (Souer et al. 1996; Aida et al. 1997). While the N-terminal NAC domain is highly conserved and necessary for DNA binding (Duval et al. 2002), the C-terminal transcriptional activation region (TAR) is more diverse between NAC family genes (Ooka et al. 2003). Ooka et al. (2003) identified thirteen conserved TAR motifs (named motif i to xiii) by sequence comparison of NAC family genes from Arabidopsis and rice. However, the distinct functions of the described motifs were not yet studied. X-ray crystallography showed that NAC transcription factors fold into a twisted β-sheet surrounded by helical elements (Ernst et al. 2004). They are able to bind DNA as homo- or heterodimers (Ernst et al. 2004; Olsen et al. 2005).

First of all, this study aimed at the identification of rapeseed *BnNST* genes through sequence comparison with homologs from Arabidopsis, *Brassica oleracea*, and *Brassica rapa*. To my knowledge, *BnNST*, *BoNST,* and *BrNST* genes have not yet been functionally characterized. Nonetheless, *BrNST* genes were already annotated in the *Brassica* database

(http://brassicadb.org, accessed 13.11.2014). *BoNST* genes, however, were not available and had to be identified by sequence analysis, too. In the following, I wanted to induce targeted mutations in *BnNST1* homoeologs by employing a Cas9-mediated mutagenesis approach, which has been demonstrated in various plant species including oilseed rape (Braatz et al. 2017). Another objective was therefore the selection of a Cas9 target sequence which is conserved between all *BnNST1* genes. As a result of this study, I report the annotation of thirteen *BnNST* and six *BoNST* homologs. After Cas9-mediated mutagenesis, I identified a set of thirteen *Bnnst1* mutant alleles within a single chimeric T$_1$ plant which in parallel still contains wild type sequences. Provided that mutations occurred in the germline and are transmitted to the next generation, this plant will be the basis for future experiments to elucidate the role of *BnNST1* genes on secondary wall formation and shatter resistance.

5.2   Materials and methods

5.2.1   Identification and characterization of *NST* sequences

AtNST sequences and related information like exon numbers were retrieved from 'The Arabidopsis Information Resource' (TAIR, www.arabidopsis.org, accessed 13.11.2014). *BrNST* sequences were retrieved from the '*Brassica* database' (BRAD, http://brassicadb.org, accessed 13.11.2014) and used as a query for a BLAST search in order to find homologs within the *B. oleracea* reference genome (version 1.1). Additional information about *BoNST* and *BrNST* genes were then also obtained from BRAD. To identify *BnNST* sequences, I performed a BLAST search with the coding sequence of *AtNST1* against the Darmor-*bzh* rapeseed reference genome (version 4.1). I built a phylogenetic tree of the coding sequences of the 50 best *BnNST* hits (lowest E-values, highest sequence identity) with the ClustalW program (Neighbor Joining algorithm, Jukes-Cantor distances, 100 bootstrap replicates) which was integrated in the CLC Main Workbench (QIAGEN Aarhus A/S, www.qiagenbioinformatics.com). *AtNST*, *BoNST,* and *BrNST* sequences served as controls. Furthermore, *BoNST* and *BrNST* homologs helped to identify the subgenome affiliation of the *BnNST* genes which I then named according to the standardized *Brassica* gene nomenclature (Ostergaard and King 2008). Locus names and exon numbers of putative *BnNST* genes were retrieved from the '*Brassica napus* Genome Browser' (http://www.genoscope.cns.fr/brassicanapus/, accessed 13.11.2014).

The coding sequences of the putative *BnNST1* genes were translated to protein sequences *in silico* to identify functional domains by comparison with the Pfam database (version 27) (Finn et al. 2014). Additionally, TAR motifs as described by Ooka et al. (2013) were identified.

5.2.2   Vector construction

The binary vector system pChimera and pCas9-TPC was used for targeted mutagenesis (Fauser et al. 2014). The transformation plasmid pCas9-TPC contains a *bar* cassette for herbicide selection in plants. A 20 bp target sequence which is conserved for the identified *BnNST1* homoeologs and is neighboring a 5′-NGG PAM was selected upstream of the NAC domain (Figure 15). I ordered DNA oligonucleotides of the target sequence plus an overhang for cloning in original and reversed complement orientation (Eurofins Genomics, Ebersberg, Germany) and let them anneal. The construct was then cloned it into the respective plasmid (Figure S11). The *Agrobacterium tumefaciens* strain GV3101 pMP90RK was used for plant transformation.

5.2.3 Plant material

I used the resynthesized rapeseed line 'RS306' (Lühs and Friedt 1994) for hypocotyl transformation because this genotype has been successfully transformed before (Zarhloul et al. 2006). Seeds were sterilized and plants were grown for 7 d on germination medium A1 (Table S13). Containers with seedlings were kept in a climate room (16 h of light/ 8 h of dark, 24 °C) and were shaded from the sides, allowing only indirect light from the top.

Regenerated T_1 plants were transplanted in 9- x 9-cm pots in the greenhouse (16 h of light/ 8 h of dark, 20-23 °C) after dusting their roots with root propagation powder (100 g talcum, 0.4% IBA). After two weeks of acclimation, plantlets were vernalized for eight weeks in a cold chamber (4 °C, 16 h light/ 8 h dark). Then, they were further cultivated under the previous conditions. After bolting, selfing bags were mounted to control pollination.

5.2.4 Hypocotyl transformation

One day before hypocotyl transformation, 15 ml of lysogeny broth (LB; 10 g/l Bacto Tryptone, 5 g/l yeast extract, 10 g/l NaCl) were supplemented with selective antibiotics (25 µg/ml rifampicin, 50 µg/ml gentamycin, 100 µg/ml spectinomycin) and inoculated with *A. tumefaciens* carrying the pCas9-TPC construct (16 h, 28 °C, 200 rpm). The bacterial solution was centrifuged (3000 rpm, 10 min) after reaching an optical density of $OD_{600} = 1.2$. The supernatant was discarded and the pellet was resuspended by shaking for two hours at 28 °C in 40 ml co-cultivation medium O2 (Table S13).

Etiolated hypocotyls were cut in 1 cm-segments and placed in the infected co-cultivation medium (45-60 min, room temperature). Then, the segments were briefly dried on sterile filter paper and transferred to solid co-cultivation medium O3. After two days in the climate room (16 h of light/ 8 h of dark, 24 °C), the segments were transferred to regeneration medium O4 which was exchanged monthly. Regenerating plantlets were cut from the hypocotyl segments and grown on selection medium O5. Plantlets which survived the herbicide selection were transferred to rooting medium O6.

5.2.5 Mutant identification

Genomic DNA was isolated from leaf samples by a standard CTAB method. The presence of the transformation cassette was tested by PCR using primers Cas1_f and Cas1_r (Table S14; Figure S11). To identify Cas9-induced mutations, PCR amplicons covering the target regions (NST1_13_NST1_14, NST1_15_NST1_24, NST1_11_NST1_25, and NST1_30_NST1_27; Table S14) of the T_1 plant were cloned into the pGEM-T vector system (Promega, Mannheim, Germany) and transformed into *Escherichia coli*. Single colonies were picked for PCR and the amplicons were subjected to Sanger sequencing with pGEM-T primers M13_f and M13_r.

5.3 Results

5.3.1 Identification of *BnNST* homoeologs

Searching the NCBI Gene Database for *BnNST* gene copies in *B. napus* did not return any hits. Therefore, I performed *in silico* analyses. First, I retrieved *AtNST* and *BrNST* genes from the respective sequence databases and used them to identify *BoNST* homologs, which were also not yet annotated. Then, I performed a BLAST search with the *AtNST1* coding sequence against the rapeseed reference genome. I downloaded the coding sequences of the 50 best hits and constructed a phylogenetic tree including the *AtNST*, *BoNST*, and *BrNST* reference sequences. The clustering of the phylogenetic tree allowed for the differentiation of *NST1*,

NST2, and *NST3* paralogs (Figure 13). Furthermore, subclustering of *BnNST* genes with either *BrNST* or *BoNST* genes indicated their affiliation to the A and C subgenomes.
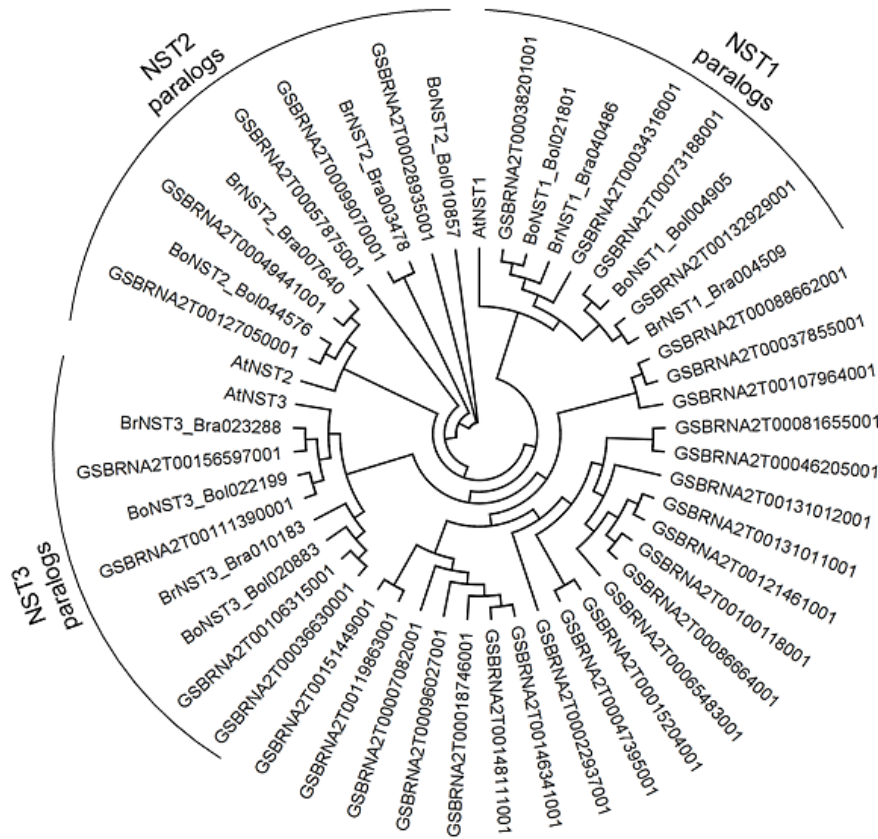
Figure 13. Phylogenetic tree of *AtNST, BoNST, BrNST,* and putative *BnNST* coding sequences. The tree was built with the Neighbor Joining algorithm (100 bootstrap replicates). Gene names starting with 'GSBRNA' refer to rapeseed gene models. For aliases and properties see Table 9. Rapeseed genes which do not cluster with homologs from Arabidopsis (bottom right corner) probably belong to a related out group.

The properties of the *NST* gene models are given in Table 9. I identified two *BoNST1,* two *BoNST2*, and two *BoNST3* paralogs. Furthermore, I annotated four *BnNST1*, five *BnNST2*, and four *BnNST3* homoeologs. As expected, the sum of *BnNST1* and *BnNST3* homoeologs equaled the sum of their putative *BrNST* and *BoNST* progenitors (2 *BrNST1* + 2 *BoNST1* = 4 *BnNST1*). Also, the chromosome affiliation was consistent. Only *BnaA.NST1.a* was not assigned to a specific chromosome in the annotated rapeseed reference genome. Interestingly however, I found an additional fifth *BnNST2* homoeolog (*BnaC.NST2.c*), which did not correspond to a *BoNST2* gene copy. *BnaC.NST2.c* is located on chromosome C06 and has a shorter coding sequence than the other *BnNST2* homoeologs, which at the same time is fragmented into more exons.

All further analyses focused only on the *BnNST1* genes, which, with the exception of *BnaA.NST1.a*, comprise coding sequences of almost 1,100 bp organized in three exons. Next, I conducted a prediction of functional protein domains. For this purpose, I performed an *in silico* translation of coding sequences into amino acid sequences and a comparison of these protein sequences with the Pfam database. Although *BnaA.NST1.a* lacks the third exon, it still contains a NAC DNA-binding domain in the N-terminal region, which is shared between all four *BnNST1* homoeologs (Figure 15A). The Pfam analysis did not identify any C-terminal transcriptional activation regions within *Bn*NST1 proteins, but this tool also did not assign any to *At*NST1, which I tested as a control. I assume that the conserved motifs described by Ooka et al. (2003) have not been added to the Pfam database. Therefore, I screened *At*NST1

and *Bn*NST1 protein sequences for such motifs by hand and indeed found motif iii, which Ooka et al. (2003) previously identified in *At*NAC3 (Figure S13).

Table 9. Properties of *NST1, NST2,* and *NST3* homologs from Arabidopsis, *B. napus, B. oleracea,* and *B. rapa.* While *AtNST* and *BrNST* gene models were already annotated, *BnNST* and *BoNST* homologs had to be identified by *in silico* analyses. For sources of aliases, locus names, and gene structures refer to Materials and methods (Chapter 5.2). n.a. = not assigned.

Gene model	Alias	Locus name	Chromosome	Gene (bp)	CDS (bp)	Exons
AtNST1	*ANAC043*	AT2G46770	2	2,192	1,098	3
BraA.NST1.a	n.a.	Bra040486	A04	2,345	1,095	3
BraA.NST1.b	n.a.	Bra004509	A05	1,914	1,080	3
BolC.NST1.a	n.a.	Bol021801	C04	2,257	1,095	3
BolC.NST1.b	n.a.	Bol004905	C04	2,207	1,074	3
BnaA.NST1.a	GSBRNA2T00034316001	n.a.	Ann	822	492	2
BnaA.NST1.b	GSBRNA2T00132929001	BnaA05g01110D	A05	1,914	1,080	3
BnaC.NST1.a	GSBRNA2T00038201001	BnaC04g51650D	C04	2,521	1,095	3
BnaC.NST1.b	GSBRNA2T00073188001	BnaC04g00680D	C04	2,205	1,074	3
AtNST2	*ANAC066*	AT3G61910	3	1,451	1,005	2
BraA.NST2.a	n.a.	Bra003478	A07	1,388	1,011	2
BraA.NST2.b	n.a.	Bra007640	A09	1,312	969	2
BolC.NST2.a	n.a.	Bol010857	C06	2,967	981	2
BolC.NST2.b	n.a.	Bol044576	C08	1,317	999	2
BnaA.NST2.a	GSBRNA2T00099070001	BnaA07g19100D	A07	1,381	1,011	2
BnaA.NST2.b	GSBRNA2T00049441001	BnaA09g39480D	A09	1,312	969	2
BnaC.NST2.a	GSBRNA2T00028935001	BnaC06g18290D	C06	2,967	981	2
BnaC.NST2.b	GSBRNA2T00127050001	BnaC08g31830D	C08	1,317	999	2
BnaC.NST2.c	GSBRNA2T00057875001	BnaC06g13570D	C06	2,760	627	5
AtNST3	*ANAC012, SND1*	AT1G32770	1	1,926	1,077	3
BraA.NST3.a	n.a.	Bra010183	A05	1,819	927	4
BraA.NST3.b	n.a.	Bra023288	A09	1,782	1,095	3
BolC.NST3.a	n.a.	Bol022199	C05	1,811	1,095	3
BolC.NST3.b	n.a.	Bol020883	C05	1,937	1,083	3
BnaA.NST3.a	GSBRNA2T00036630001	BnaA05g17950D	A05	1,819	927	4
BnaA.NST3.b	GSBRNA2T00156597001	BnaA09g24190D	A09	1,776	1,095	3
BnaC.NST3.a	GSBRNA2T00111390001	BnaC05g24890D	C05	1,832	1,116	3
BnaC.NST3.b	GSBRNA2T00106315001	BnaC05g28390D	C05	2,146	978	5

5.3.2   Cas9 target design for four *BnNST1* homoeologs

I wanted to knock-out the four *BnNST1* homoeologs simultaneously, using a single Cas9 target sequence. Therefore, I aligned the genomic sequences and searched for conserved regions within the exons. I selected a 20 bp target sequence next to a 'TGG' protospacer adjacent motif (PAM) in exon 1 (Figure 15A). The sequence is 100% identical between the *BnNST1* homoeologs and overlaps the beginning of the NAC domain.

Next, I was interested in similarities of the target sequence with regions outside of the *BnNST1* genes, to identify possible off-target sites. A BLAST search of the target sequence against the Darmor-*bzh* reference genome yielded eight hits apart from the expected *BnNST1* sequences (Figure 14). Among those hits were the five *BnNST2* homoeologs, two unspecified

gene models, and a non-coding region on scaffold Ann. However, the *BnNST2* homoeologs contain two SNPs and the remaining three sequences lack the PAM site, which is required for Cas9-mediated DNA restriction. I therefore anticipated the specificity of the construct.

```
Cas9 target + PAM                     GGACAATCTCAAGTGCCTCCNGG
BnaA.NST1.a                           GGACAATCTCAAGTGCCTCCTGG
BnaA.NST1.b                           GGACAATCTCAAGTGCCTCCTGG
BnaC.NST1.a                           GGACAATCTCAAGTGCCTCCTGG
BnaC.NST1.b                           GGACAATCTCAAGTGCCTCCTGG
BnaC.NST2.b                           GGACAGTCACAAGTGCCTCCCGG
BnaC.NST2.c                           GGACAGTCACAAGTGCCTCCTGG
BnaC.NST2.a                           GGACAGTCACAAGTGCCTCCTGG
BnaA.NST2.b                           GGACAGTCACAAGTGCCTCCTGG
BnaA.NST2.a                           GGACAGTCACAAGTGCCTCCTGG
BnaC07g23490D                         ----AATCTCAAGTGCCTC----
BnaA06g32990D                         ----AATCTCAAGTGCCTC----
Non-coding region on scaffold Ann     ----AATCTCAAGTGCCTC----
```

Figure 14. Alignment of the *BnNST1* Cas9 target sequence with BLAST hits obtained from the Darmor-*bzh* reference genome. The PAM site is underlined and polymorphisms are highlighted in red.

5.3.3 Rapeseed transformation and identification of mutations in T_1 plants

To combine the *BnNST1* Cas9 target with chimeric sgRNA, I first cloned it into the pChimera plasmid (Fauser et al. 2014). Then, the construct was restricted and ligated into the final pCas9-TPC vector (Figure S11; Fauser et al. 2014), which encodes a Cas9 nuclease and a resistance cassette for the herbicide phosphinothricin. This vector was used for the *Agrobacterium*-mediated transformation of 766 hypocotyl explants cut from 108 seedlings of the rapeseed line 'RS306'. I regenerated 323 independent shoots, out of which two survived the herbicide selection (named NP1 and NP2). Eight months after the hypocotyl transformation took place, NP1 and NP2 were transferred to the greenhouse as rooted T_1 plants. I vernalized the plants, bagged them at flowering to promote self-pollination, and began to harvest T_2 seeds (Figure S12). However, the T_1 plants are still setting new siliques so that the harvesting process is not yet finished. The T_1/T_2 nomenclature is in line with inbreeding generations where the first segregation occurs in the F_2.

I ran a PCR test to verify transgene insertions into the T_1 plants. For this purpose, I used the primers Cas1_f and Cas1_r to amplify a part of the T-DNA which contains the sgRNA and the target sequence (Figure S11). After agarose gel electrophoresis, I detected the expected amplification product only for NP1, indicating that NP2 was not transgenic although it survived herbicide selection. Consequently, the transformation efficiency of this experiment was 0.3% (1 plant out of 323 shoots).

Then, I wanted to identify targeted mutations in *BnNST1* homoeologs of NP1. Therefore, I amplified the four target regions by PCR with gene-specific primers (Table S14) and cloned the products into the pGEM-T vector. I sequenced two clones of *BnaA.NST1.a*, six clones of *BnaA.NST1.b*, seven clones of *BnaC.NST1.a*, and four clones of *BnaC.NST1.b* by Sanger sequencing. I found a total number of 13 mutant alleles which comprised small deletions (1-13 bp) and insertions (1 bp; Figure 15B; Table S15). Additionally, some wild type sequences were still present. I termed the wild type alleles A_{a1}, A_{b1}, C_{a1}, and C_{b1}, in accordance to the underlying gene names (*BnaA.NST1.a, BnaA.NST1.b,* and so on). Mutant alleles were designated with running numbers. Considering the identification of more than two alleles for all homoeologs apart from *BnaA.NST1.a*, I conclude that NP1 is chimeric and carrying different mutations within individual cells.
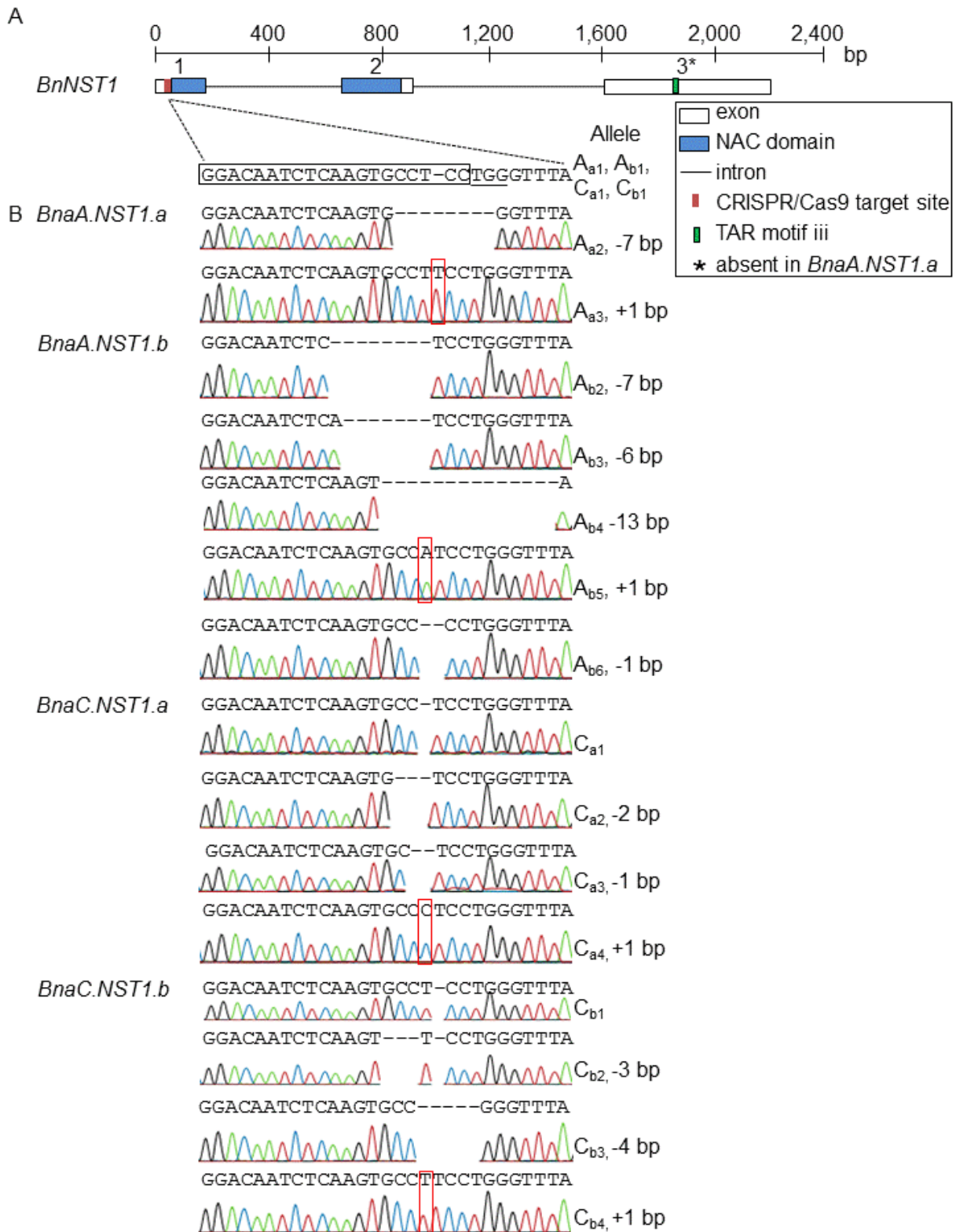
Figure 15. Cas9-mediated knock-out of four *BnNST1* homoeologs. A, Cas9 target upstream of the NAC domain of *BnNST1*. The protospacer-adjacent motif (PAM) is underlined. The boxed target sequence is conserved for all homoeologs. Exon 3 is missing in *BnaA.NST1.a.* Within the C-terminal region, I found a transcriptional activation region (TAR) motif of group iii (classification according to Ooka et al. 2003). B, Thirteen Cas9-induced mutant alleles detected by Sanger sequencing of a single chimeric T_1 rapeseed plant (NP1). The size of each deletion/ insertion and the name of the allele are indicated on the right. Inserted bases are highlighted by a red box.

5.4 Discussion

With this study, I aimed at the identification of *BnNST* homologs, the selection of a Cas9 target region conserved between all *BnNST1* genes, and the production of T_1 plants with altered *BnNST1* sequences. All objectives have been reached and laid the foundation for functional characterization of *BnNST1* homoeologs in rapeseed.

The *B. napus* genome has thirteen putative *BnNST* genes, out of these four *BnNST1*, five *BnNST2*, and four *BnNST3* homoeologs. Because *B. napus* arose from the hybridization of *B. rapa* (A subgenome) and *B. oleracea* (C subgenome), I verified the subgenome affiliation of the *BnNST* genes by sequence comparison with *BrNST* and *BoNST* coding sequences. With two exceptions, the number of *BnNST* genes and their chromosomal allocation are consistent with their assumed *BrNST* or *BoNST* progenitors: (1) *BnaA.NST1.a* was not assigned to any chromosome in the annotated rapeseed reference genome. On basis of the clustering pattern of the phylogenetic tree shown in Figure 13, I reason that this gene is an ortholog of *BraA.NST1.a* and therefore probably situated on chromosome A04. This hypothesis could be tested by linkage analysis. If the assumption was true, one would observe a significant deviation from the free recombination of the *BnaA.NST1.a* locus with other markers on A04 (recombination frequency < 50%). (2) Based on the number of *BrNST2* and *BoNST2* genes (2 paralogs each), I expected to find four *BnNST2* genes. However, the phylogenetic analysis revealed a fifth *BnNST2* gene (*BnaC.NST2.c*), which is located on chromosome C06 and comprises a shorter coding sequence fragmented into more exons compared with the other four homoeologs. Although gene models annotated on the reference genome were derived from both RNA sequencing data and gene prediction (Chalhoub et al. 2014), the 'Brassica napus Genome Browser' does not contain cDNA sequences which could verify the different gene structure of *BnaC.NST2.c* (http://www.genoscope.cns.fr/brassicanapus/, accessed 23.08.2017). Therefore, I suggest performing an alignment of genomic *BnNST2* sequences to find out whether the missing parts of the coding sequence are truly absent or just falsely annotated as non-coding. The final proof, however, would require cloning of cDNA sequences.

I found a PAM site neighboring a stretch of 100% sequence conservation by studying aligned genomic sequences of the four *BnNST1* homoeologs. As this site is located at the beginning of the NAC transcription factor domain in exon 1, I suggest that Cas9-induced frameshift mutations will cause the desired complete loss of function. In order to identify putative off-target sites, I performed a BLAST search of the selected Cas9 target sequence. The analysis revealed eight rapeseed loci with at least two SNPs, so that I do not expect unintended mutations to occur. However, to exclude unintentional mutations, the respective loci need to be sequenced within transformed plants or within their progeny.

Following a hypocotyl transformation of the Cas9 construct with rapeseed line 'RS306', I achieved a transformation efficiency of 0.3%. This number is comparable to the 0.9% efficiency that was reported for the transformation of 'Haydn' with a similar protocol (Braatz et al. 2017). To obtain more than one transgenic plant per experiment, I suggest increasing the number of hypocotyl explants while in parallel improving the transformation procedure. Elevated $AgNO_3$ concentrations of up to 10 mg/l in tissue culture media could for example improve the regeneration rate (De Block et al. 1989). Furthermore, co-cultivation of explants and *Agrobacteria* under low light conditions instead of bright light conditions could be more effective (Bhalla and Singh 2008).

I identified induced *Bnnst1* mutations by sequencing of cloned PCR fragments amplified from genomic DNA of the T_1 plant NP1. Following this approach, I found two to five different

mutant alleles per homoeolog. However, the analysis was not yet exhaustive, because I sequenced only a few clones per gene (two to seven). For the purpose of this experiment, studying the mutant alleles inherited to the T_2 generation was of higher interest than aiming at a full list of mutations present in the T_1.

As the T_1 plant is chimeric, I conclude that the Cas9 nuclease did not restrict all targeted alleles in the first transformed rapeseed cell. Instead, mutations accumulated over time and during plant regeneration. Furthermore, the occurrence of wild type alleles suggests that the process of mutagenesis is not yet accomplished. These findings contrast the previous work of my co-workers and me where we demonstrated the efficient mutagenesis of four rapeseed alleles that lead to a non-chimeric, double heterozygous plant (Braatz et al. 2017). While I increased the number of targeted alleles from four to eight, the control of Cas9 expression remained under the same constitutive *Petroselinum crispum* Ubiquitin 4-2 promotor. I reason that Cas9 abundance can be a limiting factor for mutation induction (Yan et al. 2016).

The inheritance of *Bnnst1* mutant alleles or at least of the T-DNA insertion is a prerequisite for future experiments. Analyses of T_2 offspring are on the way. Given the successful transmission of mutations, I suggest to first phenotype the segregating quadruple mutants from which I expect a loss of lignification in the dehiscence zone and an increased shatter resistance. To test these hypotheses, one can perform tensile force measurements and microscopic observations of lignin stained silique cross sections as described in Chapter 3. Furthermore, the contribution of single homoeologs to the phenotype will be important to evaluate their potential for rapeseed breeding. Ideally, not all genes need to be knocked out to obtain shatter resistance. Most likely, the wild type allele of *BnaA.NST1.a* is already non-functional, because it lacks exon 3 which encodes the C-terminal end of the transcription factor and thus houses the transcriptional activation region (Ooka et al. 2003).

In Europe, utilization of Cas9-induced mutations for breeding requires a proof of absence of transgenes. Following Mendelian inheritance, a single locus T-DNA insertion will segregate in a 3:1 manner in the T_2 generation. The selection of non-transgenic offspring can therefore be easily achieved by PCR-based genotyping with the described Cas1_f and Cas1_r primers. However, this does not rule out the presence of possible vector backbone integrations which frequently occur among different plant species (Li et al. 2016c; Wang et al. 2016; Schouten et al. 2017; Braatz et al. 2017).

To summarize, studying *Bnnst1* mutants will provide novel insight into rapeseed fruit development. However, before breeders can profit from the broadened variation within shatter resistance, additional investigations regarding putative transgene content are inevitable.

5.5 Supplemental data

The following supplemental materials are available.

Figure S11. Vector map of the recombinant pCas9-TPC plasmid containing the 'NST1_TARG1' target.

Figure S12. Phenotype of the chimeric T_1 plant NP1, which contains Cas9-induced *Bnnst1* mutations in the 'RS306' background.

Figure S13. Result of the Pfam domain search within *At*NST1.

Table S13. Components of 1 l of medium used for hypocotyl transformation.

Table S14. Primers used for the *BnNST* study.

Table S15. Cas9-induced mutations identified in the chimeric T_1 plant NP1.

5.6 References

Aida M, Ishida T, Fukaki H, Fujisawa H, Tasaka M (1997) Genes involved in organ separation in *Arabidopsis*: an analysis of the cup-shaped cotyledon mutant. Plant Cell 9 (6):841-857. doi:10.1105/tpc.9.6.841

Ballester P, Ferrándiz C (2017) Shattering fruits: variations on a dehiscent theme. Curr Opin Plant Biol 35:68-75. doi:10.1016/j.pbi.2016.11.008

Baux A, Colbach N, Pellet D (2011) Crop management for optimal low-linolenic rapeseed oil production—Field experiments and modelling. Eur J Agron 35 (3):144-153. doi:10.1016/j.eja.2011.05.006

Bhalla PL, Singh MB (2008) *Agrobacterium*-mediated transformation of *Brassica napus* and *Brassica oleracea*. Nat Protocols 3 (2):181-189. doi:10.1038/nprot.2007.527

Braatz J, Harloff H-J, Mascher M, Stein N, Himmelbach A, Jung C (2017) CRISPR-Cas9 targeted mutagenesis leads to simultaneous modification of different homoeologous gene copies in polyploid oilseed rape (*Brassica napus*). Plant Physiol 174 (2): 935-942 doi:10.1104/pp.17.00426

Chalhoub B, Denoeud F, Liu SY, Parkin IAP, Tang HB, Wang XY, Chiquet J, Belcram H, Tong CB, Samans B, Correa M, Da Silva C, Just J, Falentin C, Koh CS, Le Clainche I, Bernard M, Bento P, Noel B, Labadie K, Alberti A, Charles M, Arnaud D, Guo H, Daviaud C, Alamery S, Jabbari K, Zhao MX, Edger PP, Chelaifa H, Tack D, Lassalle G, Mestiri I, Schnel N, Le Paslier MC, Fan GY, Renault V, Bayer PE, Golicz AA, Manoli S, Lee TH, Thi VHD, Chalabi S, Hu Q, Fan CC, Tollenaere R, Lu YH, Battail C, Shen JX, Sidebottom CHD, Wang XF, Canaguier A, Chauveau A, Berard A, Deniot G, Guan M, Liu ZS, Sun FM, Lim YP, Lyons E, Town CD, Bancroft I, Wang XW, Meng JL, Ma JX, Pires JC, King GJ, Brunel D, Delourme R, Renard M, Aury JM, Adams KL, Batley J, Snowdon RJ, Tost J, Edwards D, Zhou YM, Hua W, Sharpe AG, Paterson AH, Guan CY, Wincker P (2014) Early allopolyploid evolution in the post-Neolithic Brassica napus oilseed genome. Science 345 (6199):950-953. doi:10.1126/science.1253435

De Block M, De Brouwer D, Tenning P (1989) Transformation of *Brassica napus* and *Brassica oleracea* using *Agrobacterium tumefaciens* and the expression of the *bar* and *neo* genes in the transgenic plants. Plant Physiol 91 (2):694-701. doi:10.1104/pp.91.2.694

Duval M, Hsieh T-F, Kim SY, Thomas TL (2002) Molecular characterization of *AtNAM*: a member of the *Arabidopsis* NAC domain superfamily. Plant Mol Biol 50 (2):237-248. doi:10.1023/a:1016028530943

Ernst HA, Olsen AN, Skriver K, Larsen S, Leggio LL (2004) Structure of the conserved domain of ANAC, a member of the NAC family of transcription factors. EMBO reports 5 (3):297-303. doi:10.1038/sj.embor.7400093

Fauser F, Schiml S, Puchta H (2014) Both CRISPR/Cas-based nucleases and nickases can be used efficiently for genome engineering in *Arabidopsis thaliana*. Plant J 79 (2):348-359. doi:10.1111/Tpj.12554

Finn RD, Bateman A, Clements J, Coggill P, Eberhardt RY, Eddy SR, Heger A, Hetherington K, Holm L, Mistry J, Sonnhammer ELL, Tate J, Punta M (2014) Pfam: the protein families database. Nucleic Acids Res 42 (D1):D222-D230. doi:10.1093/nar/gkt1223

Gulden RH, Shirtliffe SJ, Thomas AG (2003) Harvest losses of canola (*Brassica napus*) cause large seedbank inputs. Weed Sci 51 (1):83-86

Li W-x, Wu S-l, Liu Y-h, Jin G-l, Zhao H-j, Fan L-j, Shu Q-y (2016) Genome-wide profiling of genetic variation in *Agrobacterium*-transformed rice plants. J Zhejiang Univ-Sc B 17 (12):992-996. doi:10.1631/jzus.B1600301

Liu J, Huang SM, Sun MY, Liu SY, Liu YM, Wang WX, Zhang XR, Wang HZ, Hua W (2012) An improved allele-specific PCR primer design method for SNP marker analysis and its application. Plant Methods 8. doi:10.1186/1746-4811-8-34

Lühs W, Friedt W (1994) Stand und Perspektiven der Züchtung von Raps (*Brassica napus* L.) mit hohem Erucasäure-Gehalt im Öl für industrielle Nutzungszwecke. Eur J Lipid Sci Tech 96 (4):137-146. doi:10.1002/lipi.19940960405

Meakin PJ, Roberts JA (1990) Dehiscence of fruit in oilseed rape (*Brassica napus* L) .1. Anatomy of pod dehiscence. J Exp Bot 41 (229):995-1002. doi:10.1093/Jxb/41.8.995

Mitsuda N, Iwase A, Yamamoto H, Yoshida M, Seki M, Shinozaki K, Ohme-Takagi M (2007) NAC transcription factors, NST1 and NST3, are key regulators of the formation of secondary walls in woody tissues of *Arabidopsis*. Plant Cell 19 (1):270-280. doi:10.1105/tpc.106.047043

Mitsuda N, Ohme-Takagi M (2008) NAC transcription factors NST1 and NST3 regulate pod shattering in a partially redundant manner by promoting secondary wall formation after the establishment of tissue identity. Plant J 56 (5):768-778. doi:10.1111/j.1365-313X.2008.03633.x

Mitsuda N, Seki M, Shinozaki K, Ohme-Takagi M (2005) The NAC transcription factors NST1 and NST2 of *Arabidopsis* regulate secondary wall thickenings and are required for anther dehiscence. Plant Cell 17 (11):2993-3006. doi:10.1105/tpc.105.036004

Olsen AN, Ernst HA, Leggio LL, Skriver K (2005) DNA-binding specificity and molecular functions of NAC transcription factors. Plant Sci 169 (4):785-797. doi:10.1016/j.plantsci.2005.05.035

Ooka H, Satoh K, Doi K, Nagata T, Otomo Y, Murakami K, Matsubara K, Osato N, Kawai J, Carninci P, Hayashizaki Y, Suzuki K, Kojima K, Takahara Y, Yamamoto K, Kikuchi S (2003) Comprehensive analysis of NAC family genes in *Oryza sativa* and *Arabidopsis thaliana*. DNA Res 10 (6):239-247. doi:10.1093/dnares/10.6.239

Ostergaard L, King G (2008) Standardized gene nomenclature for the *Brassica* genus. Plant Methods 4 (1):10. doi:10.1186/1746-4811-4-10

Peltonen-Sainio P, Pahkala K, Mikkola H, Jauhiainen L (2014) Seed loss and volunteer seedling establishment of rapeseed in the northernmost European conditions. Agr Food Sci 23:327-339

Price JS, Hobson RN, Neale MA, Bruce DM (1996) Seed losses in commercial harvesting of oilseed rape. J Agr Eng Res 65 (3):183-191. doi:10.1006/jaer.1996.0091

Schouten HJ, vande Geest H, Papadimitriou S, Bemer M, Schaart JG, Smulders MJM, Perez GS, Schijlen E (2017) Re-sequencing transgenic plants revealed rearrangements at T-DNA inserts, and integration of a short T-DNA fragment, but no increase of small mutations elsewhere. Plant Cell Rep 36 (3):493-504. doi:10.1007/s00299-017-2098-z

Souer E, van Houwelingen A, Kloos D, Mol J, Koes R (1996) The *No Apical Meristem* gene of petunia is required for pattern formation in embryos and flowers and is expressed at meristem and primordia boundaries. Cell 85 (2):159-170. doi:10.1016/S0092-8674(00)81093-4

Wang G-P, Yu X-D, Sun Y-W, Jones HD, Xia L-Q (2016) Generation of marker- and/or backbone-free transgenic wheat plants via *Agrobacterium*-mediated transformation. Frontiers Plant Sci 7 (1324). doi:10.3389/fpls.2016.01324

Wang H, Zhao Q, Chen F, Wang M, Dixon RA (2011a) NAC domain function and transcriptional control of a secondary cell wall master switch. Plant J 68 (6):1104-1114. doi:10.1111/j.1365-313X.2011.04764.x

Yan W, Chen D, Kaufmann K (2016) Efficient multiplex mutagenesis by RNA-guided *Cas9* and its use in the characterization of regulatory elements in the *AGAMOUS* gene. Plant Methods 12 (23). doi:10.1186/s13007-016-0125-7

Zarhloul KM, Stoll C, Lühs W, Syring-Ehemann A, Hausmann L, Töpfer R, Friedt W (2006) Breeding high-stearic oilseed rape (*Brassica napus*) with high- and low-erucic background using optimised promoter-gene constructs. Mol Breeding 18 (3):241-251. doi:10.1007/s11032-006-9032-3

Zhong R, Lee C, McCarthy RL, Reeves CK, Jones EG, Ye Z-H (2011) Transcriptional activation of secondary wall biosynthesis by rice and maize NAC and MYB transcription factors. Plant Cell Physiol 52 (10):1856-1871. doi:10.1093/pcp/pcr123

Zhong R, Lee C, Ye Z-H (2010) Functional characterization of poplar wood-associated NAC domain transcription factors. Plant Physiol 152 (2):1044-1055. doi:10.1104/pp.109.148270

Zhong RQ, Richardson EA, Ye ZH (2007) Two NAC domain transcription factors, SND1 and NST1, function redundantly in regulation of secondary wall synthesis in fibers of *Arabidopsis*. Planta 225 (6):1603-1611. doi:10.1007/s00425-007-0498-y

6   Closing discussion

This study aimed at the production of shatter resistant rapeseed mutants, their characterization in greenhouse trials, and the validation of laboratory-based phenotyping strategies through comparisons with actual seed losses in field experiments. The selection of target genes included rapeseed homologs of transcription factors related to shatter resistance in Arabidopsis (*BnALC*, *BnIND*, *BnNST1*).

I successfully induced targeted mutations in *BnALC* and *BnNST1* homoeologs by the use of the CRISPR/Cas9 system (see Chapters 2 and 5). In both experiments, I targeted multiple genes simultaneously, namely two *BnALC* copies and four *BnNST1* copies. Sanger sequencing of T_1 and T_2 plants revealed a high mutation efficiency of the Cas9 nuclease: The *Bnalc* plant comprised four frameshift mutation alleles which were inherited in a Mendelian fashion. A more complex mutation pattern was found in the *Bnnst1* plant. I identified thirteen distinct mutations and some remaining wild type sequences, indicating a mosaic genotype. Subsequent analyses of the progeny will show whether quadruple knock-out mutants are present in the *Bnnst1* T_2. If not, Cas9 activity will have to be optimized for the purpose of target multiplexing.

While EMS-induced *Bnind* mutations had already been identified by Dr. N. Emrani from my institute, I performed TILLING screenings of the two *BnALC* homoeologs myself (see Chapter 4; polyacrylamide gels are included in Supplemental data on CD). Thereby, I found 23 novel mutant alleles, out of which I selected four for silique phenotyping.

In the following, I implemented three laboratory-based phenotyping strategies to assess shatter resistance of mature rapeseed siliques produced under greenhouse conditions. I identified the parameter 'silique length' as an influencing factor and considered the bias in the evaluation of each phenotyping trial. Through this approach, I was able to demonstrate statistically increased shatter resistance of *Bnind* and *Bnalc* double mutants, whereas single mutants did not differ significantly from the control variety (see Chapters 3 and 4). This finding verified my initial hypothesis that each functional homoeolog of a dehiscence zone identity gene needs to be impaired to observe shatter resistance.

The reliability of the phenotyping systems was mainly demonstrated by two observations: (1) All laboratory-based trials consistently detected high shatter resistance of the *Bnind* double mutant. (2) Furthermore, the control varieties for high shatter resistance ('Artoga'; advertised by Limagrain) and low shatter resistance ('Apex'; Bruce et al. 2002; Summers et al. 2003) were ranked as expected. For the final verification of the greenhouse results, I planned three field trials with *Bnind* mutants. Unfortunately, two of them could not be evaluated due to severe frost damage. Nonetheless, the third location yielded preliminary data which I describe in a detailed survey which is accessible through the Supplemental data on CD (see Appendix). In brief, the field trial comprised F_3 double mutant, single mutant, and wild type lines obtained from a cross of the best performing *Bnind* double mutant (*ind-2 ind-6*) with 'Express'. For reference, the cultivars 'Express' and 'Penn' were included as well. Each genotype was sown in three repetitions in a completely randomized block design. Prior to harvest, I placed catch trays between the rows to collect shed seeds. Then, the collected seeds were set in relation to the plot harvest. The harvest was deliberately postponed by eleven days compared to the recommended harvest date, with the aim to observe a clear segregation between mutants and controls. Until the first seed sampling date, nine days prior to the recommended harvest date, only marginal losses occurred with no statistical difference between genotypes (0.11% to 0.42%; Table S16). However, with the ongoing ripening

process, more seeds were shed until the second sampling date, nine days after the recommended harvest date. Until then, 'Express' and 'Penn' lost 5.24% and 6.87% of their final yield. In contrast, the double mutant only shattered 1.15%. However, the *BnIND* wild type with EMS mutation background also lost less seeds than the control cultivars (1.66%), which is why these preliminary results require further careful revision. I assume that this phenomenon is related to the EMS mutation load. A decreased fertility, for example, could lead to a smaller silique number per plant which would reduce impacts of siliques knocking into each other due to wind.

While the literature suggests that *Atind* and *Brind* mutations in Arabidopsis and *B. rapa*, respectively, confer shatter resistance through the loss of the lignified cell layer at the valve margin (Liljegren et al. 2004; Girin et al. 2010), I could not observe such a drastic phenotype in *Bnind* double mutants (see Chapter 3). However, the described *Atind* and *Brind* mutants comprised knock-out alleles, which I could not mimic with rapeseed double mutants because I lacked a premature stop codon mutation in *BnaC.IND.a*. Nonetheless, I showed in light microscopic studies that *Bnind* siliques had a larger valve-replum joint area, which made up the biggest part of the contact surface between valve and replum. Moreover, scanning electron microscopy revealed that the contact surfaces of *Bnind* siliques consist of smaller cells compared with the control variety. These observations formed the basis for a new model for the mechanism of *Bnind* shatter resistance: While an induced crack in the dehiscence zone of the wild type silique can easily spread through the long cells, it needs to be reinitiated more often in the mutant (at each small cell), which is a common principle called crack trapping (Hui et al. 2004). An interesting objective for future collaborations with biophysicists would be the assessment of other putative mechanisms for shatter resistance, for example with regard to reduced silique stiffness. Likewise, it will be worthwhile to investigate the mechanisms underlying shatter resistance in available cultivars like 'Artoga'. Such studies have the potential to reveal novel target genes for shatter resistance breeding.

Additional target genes can also be chosen up- or downstream of *BnALC, BnIND,* and *BnNST1.* Both the disruption of the upstream transcription factors SHP1/2 and the downstream polygalacturonase ADPG1 yielded indehiscent Arabidopsis siliques (Liljegren et al. 2000; Ogawa et al. 2009). However, five *BrSHP* (Bra003356, Bra004716, Bra007419, Bra014552, Bra016128) and four *BrADPG1* (Bra003286, Bra007332, Bra014620, Bra016912) homologs were annotated on the *B. rapa* genome (http://brassicadb.org, accessed 30.08.2017), and assuming similar numbers of *B. oleracea* gene copies, the number of expected rapeseed homoeologs would be too high to be efficiently handled by breeders. An interesting alternative to dehiscence zone modification was proposed by Swain et al. (2011): Pre-harvest seed losses could also be tackled by preventing the development of the seed abscission zone, which promotes the detachment of the seed from the funiculus. The seeds of Arabidopsis *seedstick* (*stk*) mutants stay on the funiculus, even after the silique walls have dropped (Pinyopich et al. 2003).

In order to give an overview of the current knowledge about the gene network which is underlying dehiscence zone formation, I updated the introductory figure. The model now includes information about the number of rapeseed homoeologs (Figure 16). While the functionality of both *BnALC* and both *BnIND* homoeologs was previously demonstrated (Hua et al. 2009; Laga 2013; Laga et al. 2015) and confirmed by my experiments, it is not yet known whether all *BnNST1* gene copies are transcriptionally active as their Arabidopsis orthologs. However, *in silico* analysis revealed that *BnaA.NST1.a* lacks a whole exon compared with *NST1* (see Chapter 5). Consequently, I suggest either functional divergence or complete loss of function. For other genes, even less is known. For example, the number of *SHP1* and *ADPG1* homologs in *B. napus* (*BnSHP1*, *RDPG1*) was only estimated from the

number of annotated *B. rapa* gene copies. Apart from identifying all rapeseed homoeologs, it will also be interesting to study the interactions of specific gene copies to elucidate putative neo-functionalization, sub-functionalization or complete redundancy.
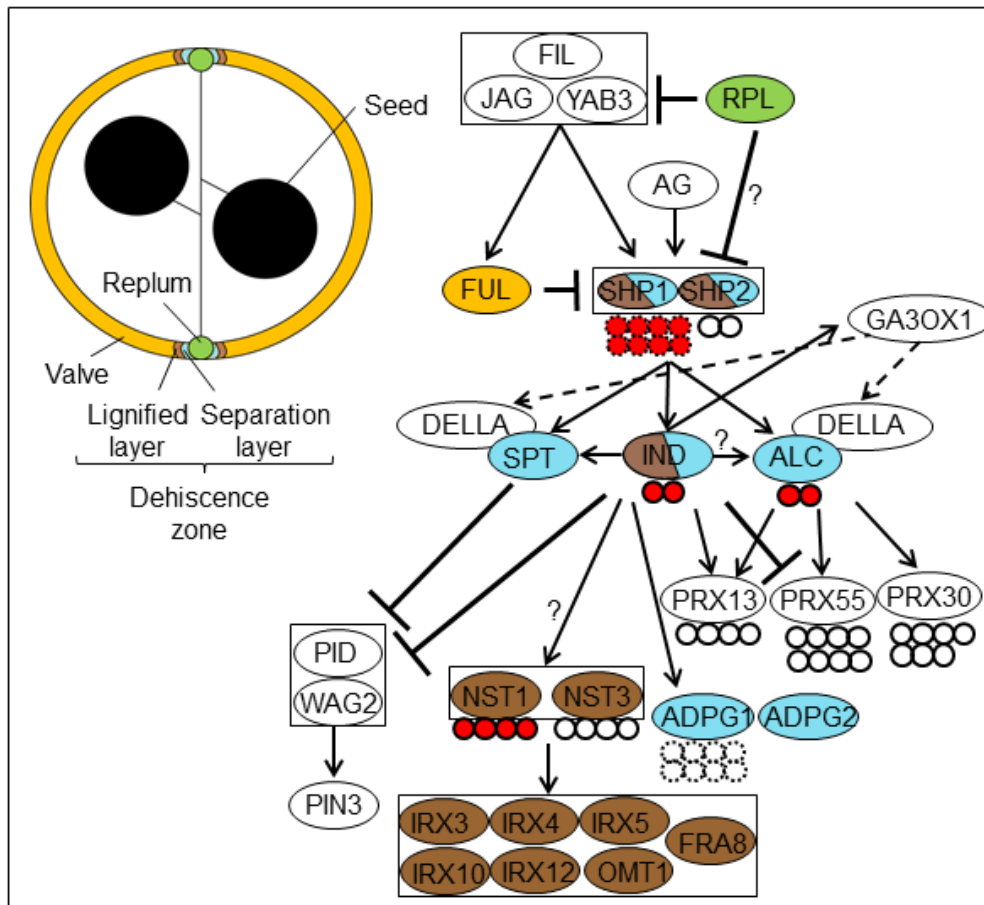
Figure 16. Current knowledge about the gene network which controls dehiscence zone formation. The number of rapeseed homoeologs is indicated by circles below the gene name. Dashed circle lines denote an estimated gene number based on annotated *B. rapa* homologs. Circles filled with red color represent availability of rapeseed mutants (*BnSHP1* Kord et al. 2015; *BnIND* Laga et al. 2015 and this study; *BnALC* Laga 2013 and this study; *BnNST1* this study). *BnSHP2* homoeologs were identified by Tan et al. (2009) and *PRX13/30/55* homoeologs by Elisha (2016).

To make the *Bnalc, Bnind,* and *Bnnst1* mutants available for rapeseed breeding, different issues have to be considered for Cas9- and EMS-induced mutations, respectively. The initial M_3 EMS mutants contain probably up to 94,000 uncharacterized background mutations (Harloff et al. 2012). Consequently, some plants show various unfavorable phenotypes including but not limited to dwarfism, (partial) sterility, and silique deformation (Figure S14). I therefore suggest several cycles of backcrossing with marker assisted background selection to reduce the mutation load (Jung 2010). Meanwhile, the Cas9-treated *Bnalc* mutants in the variety 'Haydn' can by eye not be differentiated from the wild type (see Chapter 2). I was able to select T-DNA free segregants in the T_2 generation. Unexpectedly, however, the whole genome sequence of the T_1 plant revealed multiple vector backbone integrations into the rapeseed genome. I developed a set of PCR primers for the detection of the bacterial sequences which can be utilized to screen the progeny (Supplemental data on CD). The primers are specific for pUC19 origin of replication sequences, but further efforts will be necessary to develop genotyping assays for the specific insertion sites. Eliminating all bacterial sequences by marker-assisted selection in segregating progenies will be a requirement for de-regulation of the genome edited plants.

The major advantage of Cas9-mediated mutagenesis, which is the induction of desired mutations without random mutation background, is partially negated by the uncontrolled insertion of vector backbones. The development of alternative, *A. tumefaciens*-free rapeseed transformation methods is necessary to efficiently use the Cas9 system in the future. DNA-free transformation protocols have already been successfully established through delivery of pre-assembled ribonucleoproteins to protoplasts of Arabidopsis, tobacco, lettuce, and rice and to immature wheat embryos (Woo et al. 2015; Liang et al. 2017). An application of this technique for rapeseed is expected soon.

7 Summary

Seeds of rapeseed (*Brassica napus*) are commonly processed into edible vegetable oil, animal feed, and biodiesel. However, the natural propagation of oilseed rape involves the development of a dry fruit (silique) which easily bursts at maturity. Consequently, large amounts of seeds can be lost prior to harvest. Breeders aim at an increased silique shatter resistance to assure yield stability. A network of transcription factors controlling the establishment of the predetermined breaking point of the silique, the dehiscence zone, has been identified in Arabidopsis (*Arabidopsis thaliana*). *SHATTERPROOF1/2* (*SHP1/2*) are upstream regulators of the tissue differentiation process and induce the expression of further transcription factors, *INDEHISCENT* (*IND*) and *ALCATRAZ* (*ALC*). *ALC* is required for the establishment of a partially degraded separation layer, whereas *IND* additionally initiates the lignification of neighboring cells. Proposed downstream players of *IND* are the *NAC SECONDARY WALL THICKENING PROMOTING FACTORs 1* and *3* (*NST1/3*).

The objective of my study comprised the production and analysis of *Bnalc*, *Bnind*, and *Bnnst1* rapeseed mutants, which I expected to be shatter resistant. The mutants were obtained by following two approaches: TILLING of an EMS-mutagenized rapeseed population and Cas9-mediated targeted mutagenesis. Subsequently, I wanted to demonstrate the mutants' shatter resistance through laboratory-based phenotyping strategies and under field conditions.

I transformed the rapeseed cultivar 'Haydn' with a CRISPR/Cas9 construct targeting the two *BnALC* homoeologs *BnaA.ALC*.a and *BnaC.ALC*.a. With a transformation efficiency of 0.9%, I obtained a single transgenic T_1 plant which carried four mutated alleles and no wild type *BnALC* sequences. I demonstrated that Cas9 can efficiently restrict four loci simultaneously. A tensile force test suggested the increased shatter resistance of the T_2 *Bnalc* double mutants. However, the effect was masked by the innate silique robustness of 'Haydn'. Consequently, I screened an EMS-mutagenized rapeseed population derived from the easily shattering cultivar 'Express' for *Bnalc* mutations by TILLING. The analysis of 2,688 and 3,840 M_2 plants, respectively, yielded 79 mutant candidates. Out of those, I verified 38 by Sanger sequencing (15 silent, 23 potentially disruptive). I crossed single mutations with high disruptive potential (premature stop codon, splice site, and missense mutations within functional domains) to obtain double mutants. As expected, tensile force measurements revealed a bigger effect of *Bnalc* mutations in 'Express' than in 'Haydn'.

To study the effect of EMS-induced *Bnind* mutations, I utilized TILLING mutants which were previously identified in my institute. Out of seven double mutants, three were shatter resistant. The highest shatter resistance was obtained by combining a premature stop codon mutation in *BnaA.IND.a* with a missense mutation within the transcription factor domain of *BnaC.IND.a*. The phenotype was confirmed by three independent shatter resistance tests: a random impact test, a tensile force test, and a cantilever test. Preliminary field data suggested that the greenhouse test results are correlated with actual yield losses. To elucidate the underlying mechanism of *Bnind* shatter resistance, I performed microscopic observations. While I did not find altered lignification patterns in the dehiscence zone, *Bnind* mutants did have a larger replum-valve joint area compared with 'Express'. Scanning electron microscopy of dehiscence zone surfaces revealed predominantly small, rounded cells in the mutant compared with larger, oblong cells in 'Express'. I concluded that the *Bnind* shatter resistance is based on a joint effect of a larger dehiscence zone together with smaller cells, which cause a phenomenon called 'crack trapping'. This mechanism differs from the described lignification defects in Arabidopsis *ind* mutants.

By phenotyping *Bnalc* and *Bnind* single and double mutants, I showed that the respective homoeologs have redundant functions. The mutant alleles can be introduced into rapeseed breeding programs for a sequence based improvement of shatter resistance.

For my last experiment, I identified putative *BnNST* genes by *in silico* analyses. I annotated four *BnNST1*, five *BnNST2*, and four *BnNST3* homoeologs. Then, I induced Cas9-targeted mutagenesis of the four *BnNST1* homoeologs in the resynthesized winter rapeseed line 'RS306'. After selection, I obtained a single transgenic plant which corresponds to a transformation efficiency of 0.3%. However, this T_1 plant was chimeric with up to five mutated alleles per gene and some remaining wild type sequences. As in the case of *BnALC*, I expect the completed mutagenesis and thus absence of wild type alleles in the next generation.

8 Zusammenfassung

Raps (*Brassica napus*) ist die wichtigste Ölpflanze Deutschlands, die zudem großflächig in Kanada, China und Indien angebaut wird. Typisch für die Gattung *Brassica* ist die Bildung von Schoten, welche zur Reife entlang einer Zellschicht zwischen Schotenwand und Replum (Dehiszenz-Zone) aufplatzen. Auf dem Feld wird das Platzen beispielsweise durch landwirtschaftliche Maschinen, Hagel oder Tiere ausgelöst. Zusätzlich zum Ernteverlust bereitet der Durchwuchsraps Probleme. Demnach ist die Selektion von Rapssorten mit platzfesten Schoten ein wichtiges Zuchtziel.

Ein Ansatz zur Entwicklung fester Schoten ist die Modifikation der Sollbruchstelle. In der Modellpflanze *Arabidopsis thaliana* sind die Transkriptionsfaktoren INDEHISCENT (IND) und ALCATRAZ (ALC) maßgeblich an der Differenzierung des Gewebes beteiligt. Während ALC und IND den enzymatischen Abbau der sogenannten Trennschicht einleiten, induziert IND auch die Lignifizierung der benachbarten Zellschicht, vermutlich über die Gene *NAC SECONDARY WALL THICKENING FACTOR 1* und *3* (*NST1/3*).

Ziel meiner Arbeit war es, durch die Mutagenese von Genen, welche die Differenzierung des Gewebes der Sollbruchstelle kontrollieren, Raps mit platzfesteren Schoten zu erzeugen. Nachfolgend sollte die Platzfestigkeit durch Labortests und Feldversuche untersucht werden. Zur Materialgewinnung wählte ich folgende Ansätze: Die gezielte Mutagenese von zwei *BnALC* und vier *BnNST1* Homöologen mit der CRISPR/Cas9 Methode sowie die chemische Mutagenese mit Ethylmethansulfonat (EMS) zur Induktion zufälliger Punktmutationen. *Bnind* EMS Mutanten standen zu Beginn der Arbeit bereits zur Verfügung.

Zur gezielten Mutagenese transformierte ich CRISPR/Cas9 Konstrukte mit *Agrobacterium tumefaciens* in Rapshypokotyle und regenerierte transgene T_1 Pflanzen. Ich bestätigte die effiziente Mutagenese aller *Bnalc* Sequenzen bei Abwesenheit von Wildtypallelen. Dagegen fand ich für jedes *BnNST1* Gen bis zu fünf mutierte Allele sowie verbliebene Wildtypsequenzen. Eine Analyse der *Bnnst1* Vererbung steht noch aus. *Bnalc* Mutationen spalteten in der T_2 nach Mendel und zeigten in einem Zugkrafttest die erwartete Schotenfestigkeit. Allerdings erwies sich die transformierte Sorte „Haydn" als *per se* platzfest, sodass der Effekt gering ausfiel. Um den Phänotyp zu bestätigen, untersuchte ich bis zu 3.840 EMS-mutagenisierte M_2 Pflanzen der platzenden Sorte „Express" nach *Bnalc* Mutationen. Aus 79 Kandidaten selektierte ich vier Mutationen, die ich durch Kreuzung zu drei Doppelmutanten kombinierte. Eine der im Gewächshaus angebauten Doppelmutanten erwies sich im Zugkrafttest als platzfest, was den *Bnalc* Phänotyp untermauerte.

Die *Bnind* Mutanten wurden ebenfalls im Gewächshaus untersucht und die Platzfestigkeit der geernteten Schoten mit drei Tests (Zugkrafttest, Aufpralltest, Biegebalkentest) bestätigt. Erste Felddaten legten eine Korrelation von Laborergebnissen und tatsächlichen Ernteverlusten nahe. Durch mikroskopische Analysen gefärbter Kryoschnitte schloss ich eine atypische Lignifizierung der *Bnind* Doppelmutante aus. Nähere Untersuchungen zeigten hingegen eine vergrößerte Auflagefläche zwischen Schotenwand und Replum sowie kleinere, abgerundete Zellen. Diese Beobachtungen suggerierten ein neues Modell der *Bnind* Wirkung: In „Express" kann sich ein Riss entlang der Sollbruchstelle leichter ausbreiten als in der Mutante, weil er dort häufiger (an jeder kleinen Zelle) neu initiiert werden muss. Dieser Effekt wird durch die große Kontaktfläche verstärkt.

9   Appendix

9.1   Supplemental tables

Table S1. Primers used in this study. Lower case letters indicate mismatches introduced at the primers' 3' ends to increase specificity as described by Liu et al. (2012).

Gene	Primer name	Sequence (5' → 3')	Purpose
BnaA.ALC.a	ALC33 ALC16	CTCACAATTTCCTAATCTCACCAGG ATCTGACTTCGAATCCTCTTCAtTC	Genotyping
BnaC.ALC.a	ALC13 ALC12	GACGAACTCTCGAGCATcCTC CTTCGAATCCTCTTCACTGTCTG	Genotyping
Multiple cloning site and *bar* cassette of pCas9-TPC	Cas1_f Cas1_r	CAGTCTTTCACCTCTCTTTGG CCATCTTTGGGACCACTGTC	Verification of transgene insertion
BnaC04g13390D	ALC27 ALC28	TGGGTAATTCCGACGCCAGAG TGATCTTGCTCCTCCTATCTGC	Evaluation of putative off-target site
Non-coding region on chromosome C02	OFF1 OFF2	CCATTAGCTTTAGGCATGTTTAGGC TGATGAGGTTCTAATCAGCGCC	Evaluation of putative off-target site

Table S2. Results of silique shatter trials. Displayed are mean peak tensile forces (N) and standard deviation of n siliques in three size classes.

Genotype	3 - 4 cm	n	4 - 5 cm	n	5 - 6 cm	n
alc T$_2$	3.360 ± 1.154	19	3.771 ± 1.240	41	4.217 ± 1.173	85
Haydn	3.400 ± 1.013	19	3.625 ± 1.210	41	3.822 ± 1.107	94

Table S3. Nucleotide positions and amino acid exchanges of EMS mutations detected in *BnaA.IND.a* and *BnaC.IND.a.* Silent mutations are not specified in this table.

Gene	Mutation	Amino acid substitution	Mutant code
BnaA.IND.a	G45A	Met15Ile	*ind-1*
	C118T	His40Tyr	
	C125T	Pro42Leu	
	C127T	His43Tyr	
	G161A	Ser54Asn	
	C172T	Pro58Ser	
	G217A	Glu73Lys	
	G282A	Met94Ile	
	C283T	Gln95STOP	*ind-2*
	C313T	Pro105Ser	
	C314T	Pro105Leu	
	C320T	Pro107Leu	
	G361A	Val121Met	
	G416A	Arg139Lys	
	C472T	Arg158Cys	*ind-3*
	C509T	Ala170Val	
	C512T	Ser171Phe	
	G544A	Val182Ile	
	G704A	3'UTR	
BnaC.IND.a	C224T	Pro75Leu	
	G247A	Gly83Arg	*ind-4*
	G274A	Glu92Lys	*ind-5*
	G278A	Gly93Glu	
	C323T	Ala108Val	
	G346A	Asp116Asn	
	C362T	Pro121Leu	
	C401T	Pro134Leu	*ind-6*
	G440A	Ser147Asn	
	C451T	Arg151Trp	
	G452A	Arg151Gln	
	G468A	Met156Ile	
	C623T	Ser208Leu	*ind-7*
	C694T	3'UTR	

Table S4. Rapeseed cultivars assessed for shatter resistance.

Cultivar	Breeder	Year of first release	Ecotype
Apex	Syngenta	1997[a]	Winter rapeseed
Artoga	Limagrain	2009[a]	Winter rapeseed
Avatar	Norddeutsche Pflanzenzucht Hans Georg Lembke KG	2011[a]	Winter rapeseed
Drakkar	Serasem	2002[a]	Spring rapeseed
Express	Norddeutsche Pflanzenzucht Hans Georg Lembke KG	1999[a]	Winter rapeseed
Haydn	Norddeutsche Pflanzenzucht Hans Georg Lembke KG	2000[a]	Spring rapeseed
Mozart	Norddeutsche Pflanzenzucht Hans Georg Lembke KG	2000[a]	Spring rapeseed
Westar	Agriculture Canada Research Station	1982[b]	Spring rapeseed

[a] year of first release in Europe, [b] year of first release in Canada

Table S5. RT-qPCR primers.

Gene	Accession numbers	Primer name	Sequence (5' → 3')	Amplicon size (bp)
BnACTIN2	XM_013786210.1, XM_013888645.1, XM_013893921.1, XM_013829442.1, XM_013830703.1	Act1	TCTGGTGATGGTGTGTCTCA	141
		Act2	GGTGAACATGTACCCTCTCTCG	
BnaA.IND.a	HB416515.1	IND17	GGAGCATCATCATCTCCTTATGCAT	220
		IND14	GTATTGCATCTTCTTCATCGGATCC	
BnaC.IND.a	HB416517.1	IND16	AGCCTCATCATCTCCTTATGCAC	220
		IND15	GTATTGCATCTCCTTCATCTCATCT	

Table S6. Homoeolog-specific primers used for TILLING and genotyping.

Gene	Primer name	Sequence (5' → 3')	Amplicon size (bp)	Purpose
BnaA.ALC.a	ALC68	GAGTGATTTGCCACGCGC	494	Genotyping
	ALC67	TTTCCTACCGAGTTATGGAATAGG		
BnaA.ALC.a	ALC33	CTCACAATTTCCTAATCTCACCAGG	986	Genotyping
	ALC16	ATCTGACTTCGAATCCTCTTCATTC		
BnaC.ALC.a	ALC13	GACGAACTCTCGAGCATCCTC	994	Genotyping
	ALC12	CTTCGAATCCTCTTCACTGTCTG		
BnaA.IND.a	IND7	GGCTCAAAAGCAGATGCAGCCATAG	789	TILLING + genotyping
	IND8	CCGGCAATGTTGCCTCCTTATAGAG		
BnaC.IND.a	IND5	GCAGATGCAGCAGCCATAGC	792	TILLING + genotyping
	IND4	CTAATCCGGCATGTTGCCTCCC		

Table S7. Original data of shatter resistance trials of M_4 *Bnind* single mutant families and Express. All force values expressed as regression values and standard error at a silique length of 4 cm. SM1/2 = single mutant 1/2. n = number of tested siliques.

Mutations		Genotype	Tensile force trial	
bnaA.ind.a	*bnaC.ind.a*		**n**	**(N_{max})**
ind-1	-	SM1	177	1.658 ± 0.153
ind-2	-	SM1	22	1.343 ± 0.285
-	*ind-4*	SM2	189	2.088 ± 0.171
-	*ind-5*	SM2	260	1.537 ± 0.156
-	*ind-7*	SM2	121	1.485 ± 0.163
-	-	Express	255	1.544 ± 0.110

Table S8. Original data of shatter resistance trials of *Brind* double mutant families and eight cultivars. All force values expressed as regression values and standard error at a silique length of 4 cm. RIT results expressed as means and standard deviation of 3- to 4-cm-long siliques. F_3 and F_4 were derived from crosses of M_3 mutants. F_2 was produced by crossing F_3 mutants with Express. WT = wild type, SM1/2 = single mutant 1/2, DM = double mutant. n = number of tested siliques.

Mutations	Genotype	Generation	Experiment	Tensile force trial n	Tensile force trial (N_{max})	Cantilever test n	Cantilever test (N_{max})	RIT n	RIT (s)
bnaA.ind.a bnaC.ind.a									
ind-1	WT	F_4	HH32	150	0.756 ± 0.285			80	84 ± 12
ind-5	DM	F_3	HH23	193	1.779 ± 0.113				
	DM	F_3	HH26	148	1.737 ± 0.144				
ind-2	WT	F_4	HH32	37	1.346 ± 0.393				
ind-4	SM1	F_3	HH26	18	1.224 ± 0.215				
	DM	F_3	HH23	161	1.919 ± 0.127				
	DM	F_3	HH26	43	1.897 ± 0.212				
ind-5	WT	F_3	HH26	16	1.522 ± 0.343				
	WT	F_3	HH26	84	1.794 ± 0.159				
	SM1	F_3	HH23	152	1.713 ± 0.114				
	SM2	F_3	HH23	148	1.400 ± 0.109				
	DM	F_3	HH26	83	2.470 ± 0.157				
ind-6	WT	F_2	HH32	150	1.608 ± 0.131				
	SM1	F_3	HH23	217	1.507 ± 0.112				
	SM1	F_3	HH23	52	1.690 ± 0.158				
	DM	F_3	HH23	51	2.648 ± 0.239				
	DM	F_3	HH26	249	2.794 ± 0.111	39	2.926 ± 0.201	80	208 ± 12
	DM	F_2	HH32	150	3.118 ± 0.130				

ind		gen.	marker	n	value	n	value	n	value
ind-2	WT	F$_3$	HH23	172	1.099 ± 0.120				
ind-7	WT	F$_3$	HH26	139	1.463 ± 0.139			80	51 ± 21
	DM	F$_3$	HH26	56	1.781 ± 0.218				
	DM	F$_3$	HH23	69	1.560 ± 0.179				
ind-3	DM	F$_3$	HH26	88	2.100 ± 0.189			80	71 ± 16
ind-4	WT	F$_3$	HH26	101	1.617 ± 0.159				
	DM	F$_3$	HH26	151	1.386 ± 0.133				
	WT	F$_4$	HH32	148	1.145 ± 0.289				
ind-5	DM	F$_4$	HH32	115	1.244 ± 0.298				
	Apex		HH26	219	1.184 ± 0.092			80	40 ± 14
	Artoga		HH26	9	2.632 ± 0.299	41	1.967 ± 0.339	80	223 ± 9
	Avatar		HH26	175	0.800 ± 0.115				
	Drakkar		HH32	150	0.976 ± 0.320				
	Express		HH26	348	1.296 ± 0.133	49	1.095 ± 0.128	80	66 ± 1
	Express		HH32	150	1.267 ± 0.363				
	Haydn		HH32	150	2.719 ± 0.363				
	Mozart		HH32	150	2.944 ± 0.314				
	Westar		HH32	150	1.919 ± 0.300				

Table S9. *BnALC* and *BnIND* amplicons of Artoga, Drakkar, Express, Haydn, and Mozart were sequenced. The analyzed region is displayed as a base pair range counted from the start codon.

Gene	Amplicon	Amplicon length (bp)	Analyzed region (bp)	Exon sequence coverage (%)
BnaA.ALC.a	ALC68_ALC67	494	1 – 403	83.7
	ALC33_ALC16	986	4,761 – 5,746	
BnaC.ALC.a	ALC13_ALC12	994	49 – 1,042	73.5
BnaA.IND.a	IND7_IND8	789	7 – 795	89.8
BnaC.IND.a	IND4_IND5	779	61 – 839	89.0

Table S10. Nucleotide positions and amino acid exchanges of EMS mutations detected in *BnaA.ALC.a* and *BnaC.ALC.a*. Mutant codes *alc-1* to *-5* were assigned to mutations which were used in this study.

M₂ plant	Seed code	Gene	Mutation	Amino acid substitution	Mutant code	Zygosity of M₂
1481_4	150037[a]	*BnaA.ALC.a*	G5053A	splice site mutation	*alc-1*	homozygous
1641_1		*BnaA.ALC.a*	G5071A	silent		heterozygous
1641_2		*BnaA.ALC.a*	G5071A	silent		heterozygous
1463_3		*BnaA.ALC.a*	C5079T	Ser93Leu		heterozygous
1487_1	150038	*BnaA.ALC.a*	G5229A	Glu116Lys	*alc-2*	homozygous
1148_2	150034	*BnaA.ALC.a*	G5274A[b]	splice site mutation	*alc-3*	heterozygous
1481_4	150037[a]	*BnaA.ALC.a*	G5387A[b]	Glu142Lys	*alc-4*	homozygous
1662_1		*BnaA.ALC.a*	C5393T	silent		heterozygous
1254_1		*BnaA.ALC.a*	C5417T	Gln152Stop		homozygous
1254_4		*BnaA.ALC.a*	C5417T	Gln152Stop		heterozygous
1706_1		*BnaA.ALC.a*	G5419A	silent		heterozygous
1536_2		*BnaC.ALC.a*	G152A	Arg51Gln		heterozygous
1536_3		*BnaC.ALC.a*	G152A	Arg51Gln		heterozygous
1402_3		*BnaC.ALC.a*	C162T	silent		heterozygous
1523_1		*BnaC.ALC.a*	C165T	silent		heterozygous
1523_4		*BnaC.ALC.a*	C165T	silent		heterozygous
1533_1		*BnaC.ALC.a*	G176A	Gly59Glu		heterozygous
1533_2		*BnaC.ALC.a*	G176A	Gly59Glu		heterozygous
1533_4		*BnaC.ALC.a*	G176A	Gly59Glu		heterozygous
1241_4		*BnaC.ALC.a*	C189T	silent		heterozygous
1551_1		*BnaC.ALC.a*	G199A	Ala67Thr		homozygous
1071_2		*BnaC.ALC.a*	G215A	Gly72Glu		homozygous
1548_1		*BnaC.ALC.a*	G227A	Cys76Tyr		homozygous
1242_3		*BnaC.ALC.a*	C240T	silent		heterozygous
1236_2	150035	*BnaC.ALC.a*	G352A	splice site mutation	*alc-5*	homozygous
1534_3		*BnaC.ALC.a*	C363T	Ala85Val		heterozygous
1549_1		*BnaC.ALC.a*	C363T	Ala85Val		heterozygous
1549_2		*BnaC.ALC.a*	C363T	Ala85Val		homozygous
1550_1		*BnaC.ALC.a*	G370A	silent		homozygous
1893_1		*BnaC.ALC.a*	G372A	Arg88Gln		heterozygous
1893_3		*BnaC.ALC.a*	G372A	Arg88Gln		homozygous
1395_1		*BnaC.ALC.a*	C378T	Ser90Leu		homozygous
1614_3		*BnaC.ALC.a*	G382A	silent		heterozygous
1539_1		*BnaC.ALC.a*	C412T	silent		homozygous
1326_4		*BnaC.ALC.a*	C542T	Ala117Val		heterozygous
1873_2		*BnaC.ALC.a*	C553T	silent		heterozygous
1873_3		*BnaC.ALC.a*	C553T	silent		heterozygous
1422_4		*BnaC.ALC.a*	G555A	silent		homozygous
1074_2		*BnaC.ALC.a*	C560T	Pro123Leu		heterozygous
1540_4		*BnaC.ALC.a*	G573A	silent		heterozygous

M$_2$ plant	Seed code	Gene	Mutation	Amino acid substitution	Mutant code	Zygosity of M$_2$
951_1		*BnaC.ALC.a*	G577A	intronic		heterozygous
951_2		*BnaC.ALC.a*	G577A	intronic		homozygous
951_3		*BnaC.ALC.a*	G577A	intronic		homozygous
1074_1		*BnaC.ALC.a*	C584T	intronic		heterozygous
996_3		*BnaC.ALC.a*	C697T	silent		heterozygous
1158_1		*BnaC.ALC.a*	C697T	silent		heterozygous
1688_1		*BnaC.ALC.a*	G881A	Gly175Arg		heterozygous
1095_2		*BnaC.ALC.a*	C897T	Ser180Leu		homozygous

[a] two mutations in one gene; [b] mutation described in patent application US20130291235A1 (Laga 2013)

Table S11. Primers used for *BnALC* TILLING. Lower case letters indicate mismatches introduced at the primers' 3' ends to increase specificity as described by Liu et al. (2012).

Gene	Primer name	Sequence (5' → 3')
BnaA.ALC.a	ALC43	TCTTACGCCGCTTGTGtAGC
	ALC16	ATCTGACTTCGAATCCTCTTCAtTC
BnaC.ALC.a	ALC13	GACGAACTCTCGAGCATcCTC
	ALC12	CTTCGAATCCTCTTCACTGTCTG

Table S12. Original data of shatter resistance trials of F_2 *Bnalc* double mutant families and 'Express'. n = number of tested siliques. All force values are expressed as regression values and standard error.

Genotype		Parental generation	n	Tensile force (N_{max})			Standard error (N)		
				4 cm	**5.5 cm**	**7 cm**	**4 cm**	**5.5 cm**	**7 cm**
'Express'	*AACC*		150	0.853	1.257	1.662	0.379	0.365	0.411
alc-1/alc-4 alc-5	*aacc*	F_1(M_3 x 'Express')	150	1.564	2.145	2.726	0.294	0.266	0.291
	aaCC	F_1(M_3 x 'Express')	132	1.602	1.900	2.198	0.298	0.273	0.300
	AAcc	F_1(M_3 x 'Express')	124	1.051	1.639	2.226	0.313	0.286	0.315
	AACC	F_1(M_3 x 'Express')	120	1.175	1.470	1.765	0.297	0.270	0.298
alc-2 alc-5	*aacc*	M_3	60	2.412	2.489	2.565	0.389	0.365	0.421
	aaCC	M_3	137	2.255	2.231	2.207	0.298	0.277	0.320
	AAcc	M_3	132	1.830	2.197	2.563	0.310	0.274	0.305
	AACC	M_3	126	1.813	1.976	2.139	0.294	0.273	0.315
alc-3 alc-5	*aacc*	F_1(M_3 x 'Express')	150	1.340	1.785	2.229	0.294	0.267	0.294
	AACC	F_1(M_3 x 'Express')	118	1.280	1.774	2.268	0.311	0.286	0.322

Table S13. Components of 1 l of medium used for hypocotyl transformation.

Medium	Ingredients
A1 (Germination Medium)	0.5x MS salts
	15 g sucrose
	4 g Gelrite
	pH 5.7 (KOH)
O2 (Co-Cultivation Medium, liquid)	1x MS
	0.5 g MES
	1 ml MS vitamins (x1000)
	0.3 g Myo-Inositol
	pH 5.5 (NaOH)
	after autoclaving:
	1 ml acetosyringone (0.39 mg / ml)
O3 (Co-Cultivation Medium, solid)	1x MS salts
	1 ml MS vitamins (1000x)
	0.5 g MES
	20 g sucrose
	3 g Gelrite
	0.3 g Myo-Inositol
	pH 5.7 (NaOH)
	after autoclaving
	1 ml acetosyringone (0.39 mg/ml)
O4 (Regeneration Medium)	1x MS salts
	0.5 g MES
	1 ml Gamborg vitamins (1000x)
	1 ml MS vitamins (1000x)
	20 g sucrose
	1 ml Fe-solution (3.73 g Na_2EDTA in 100 ml H_2O + 2.78 g $FeSO_4 7H_2O$ in 100 ml H_2O)
	3 g Gelrite
	0.3 g Myo-Inositol
	pH 5.7 (NaOH)
	after autoclaving:
	2 mg BAP
	100 µl silver nitrate (50 mg/ml)
	100 µl 2,4-D (0.001 mg/ml)
	1250 µl carbenicillin (400 mg/ml)
	1000 µl cefotaxime (50 mg/ml)
O5 (Selection Medium)	O4 medium + 5 mg phosphinothricin

Medium	Ingredients
O6 (Rooting Medium)	1x MS salts
	1 ml Gamborg vitamins (1000x)
	1 ml MS vitamins (1000x)
	0.5 g MES
	10 g sucrose
	0.3 g Myo-Inositol
	8 g Daishin Agar
	pH 5.8 (NaOH)
	after autoclaving:
	100 µl NAA (1 mg/ml)
	5 mg phosphinothricin
	1250 µl carbenicillin (400 mg/ml)
	1000 µl cefotaxime (50 mg/ml)
	12.5 µl BAP (0.0002 mg/ml)

Table S14. Primers used for the *BnNST* study. Lower case letters indicate mismatches introduced at the primers' 3' ends to increase specificity as described by Liu et al. (2012). All primer combinations ran with a PCR annealing temperature of 58 °C.

Gene	Primer name	Sequence (5' → 3')
BnaA.NST1.a	NST1_13	TCCTCTAGCTCTCTCATTCTCCAAT
	NST1_14	ATAAGGGTCAGTGGCTCATAATC
BnaA.NST1.b	NST1_15	GTACAAAGAGACACATGCGTTTA
	NST1_24	TCTCGTAAAAGGGTACATGACG
BnaC.NST1.a	NST1_11	CACATGTGTTTTCCTCATGCATCTTA
	NST1_25	GAACGTCATGTATCGAAAGAACTAC
BnaC.NST1.b	NST1_30	GCTAGCTTTCTCATTCCAACTTTTG
	NST1_27	GCCGaCGTAGCTCTGTTGG
Multiple cloning site and *bar* cassette of pCas9-TPC	Cas1_f	CAGTCTTTCACCTCTCTTTGG
	Cas1_f	CCATCTTTGGGACCACTGTC
pGEM-T multiple cloning site	M13_f	CACGACGTTGTAAAACGAC
	M13_r	GGATAACAATTTCACACAGG

Table S15. Cas9-induced mutations identified in the chimeric T_1 plant NP1. Positions of mutations were counted based on the start codon 'ATG'.

Gene	Mutation	Allele	Indel length (bp)
BnaA.NST1.a	49-55delCCTCCTG	A_{a2}	7
BnaA.NST1.a	52insT	A_{a3}	1
BnaA.NST1.b	44-50delAAGTGCC	A_{b2}	7
BnaA.NST1.b	45-50delAGTGCC	A_{b3}	6
BnaA.NST1.b	48-60delGCCTCCTGGGTTT	A_{b4}	13
BnaA.NST1.b	51delT	A_{b5}	1
BnaA.NST1.b	51insA	A_{b6}	1
BnaC.NST1.a	49-50delCC	C_{a2}	2
BnaC.NST1.a	50delC	C_{a3}	1
BnaC.NST1.a	51insC	C_{a4}	1
BnaC.NST1.b	48-50delGCC	C_{b2}	3
BnaC.NST1.b	51-54delTCCT	C_{b3}	4
BnaC.NST1.b	52insT	C_{b4}	1

Table S16. Average yield losses due to seed shattering assessed from the *Bnind* field trial at Rheinbach (2016/17). Shed seeds were collected at two dates, approximately nine days before and nine days after the recommended harvest date. Values are means of three plots in a completely randomized block design and standard deviation. Genotypes of *Bnind* mutant family *ind-2 ind-6* are indicated by small and capital letters (*a, A, c, C*), representing mutant and wild type alleles. Values within the same column that share the same letters (a, b, c) do not differ significantly ($p \geq 0.05$; two-sided *t*-test).

Genotype	Average yield loss until date 1 (%)	Average yield loss until date 2 (%)
aacc	0.27 ± 0.47 [a]	1.15 ± 0.59 [a]
aaCC	0.42 ± 0.33 [a]	4.33 ± 1.84 [b]
AAcc	0.14 ± 0.08 [a]	3.20 ± 2.11 [a,b]
AACC	0.11 ± 0.05 [a]	1.66 ± 0.59 [a]
'Express'	0.17 ± 0.10 [a]	5.24 ± 2.01 [b,c]
'Penn'	0.16 ± 0.12 [a]	6.87 ± 2.23 [c]

Table S17. Vectors constructed in the course of this study.

| Clone ID	Reference	Cas9 target name	Target gene	Target sequence	Resistance marker	Vector backbone	Construct size (bp)
CAU4171[a]	Chapter 2	TARGA1	BnaA.ALC.a	AGTTTCAGCGCGGCTGCACAAG	Spec, PPT	pCas9-TPC	14,542
CAU4175[a]		TARGA2	BnaC.ALC.a	AGTTTCAGCGACTGCACAAG	Spec, PPT	pCas9-TPC	14,542
CAU4179[a]		TARGA3	BnaA.ALC.a, BnaC.ALC.a	GGCGTAAGAAACCGGCTCCGC	Spec, PPT	pCas9-TPC	14,542
CAU4182		TARGA4	BnaA.ALC.a, BnaC.ALC.a	CAAAATGTGGTTTCGAAAAACA	Amp	pChimera	2,911
CAU4183		TARGA4	BnaA.ALC.a, BnaC.ALC.a	CAAAATGTGGTTTCGAAAAACA	Amp	pChimera	2,911
CAU4184		TARGA4	BnaA.ALC.a, BnaC.ALC.a	CAAAATGTGGTTTCGAAAAACA	Amp	pChimera	2,911
CAU4185		TARGA4	BnaA.ALC.a, BnaC.ALC.a	CAAAATGTGGTTTCGAAAAACA	Amp	pChimera	2,911
CAU4186		TARGA3, TARGA4	BnaA.ALC.a, BnaC.ALC.a	GGCGTAAGAAACCGGCTCCGC, CAAAATGTGGTTTCGAAAAACA	Spec, PPT	pCas9-TPC	15,079
CAU4187		TARGA3, TARGA4	BnaA.ALC.a, BnaC.ALC.a	GGCGTAAGAAACCGGCTCCGC, CAAAATGTGGTTTCGAAAAACA	Spec, PPT	pCas9-TPC	15,079
CAU4189		IND_TARG1	BnaA.IND.a, BnaC.IND.a	CATAGCCCCAATAGTCATGA	Amp	pChimera	2,911
CAU4190		IND_TARG1	BnaA.IND.a, BnaC.IND.a	CATAGCCCCAATAGTCATGA	Amp	pChimera	2,911
CAU4191	Chapter 5	NST1_TARG1	BnaA.NST1.a, BnaA.NST1.b, BnaC.NST1.a, BnaC.NST1.b	GGACAATCTCAAGTGCCTCC	Amp	pChimera	2,911
CAU4192		NST1_TARG1	BnaA.NST1.a, BnaA.NST1.b, BnaC.NST1.a, BnaC.NST1.b	GGACAATCTCAAGTGCCTCC	Amp	pChimera	2,911

Clone ID	Reference	Cas9 target name	Target gene	Target sequence	Resistance marker	Vector backbone	Construct size (bp)
CAU4193		CLV_TARG1	*BnaA.CLV3.a, BnaC.CLV3.a BnaC.CLV3.b*	TAATGAAGAAGGATAATGAA	Amp	pChimera	2,911
CAU4194		CLV_TARG1	*BnaA.CLV3.a, BnaC.CLV3.a BnaC.CLV3.b*	TAATGAAGAAGGATAATGAA	Amp	pChimera	2,911
CAU4195		IND_TARG1	*BnaA.IND.a, BnaC.IND.a*	CATAGCCCAATAGTCATGA	Spec, PPT	pCas9-TPC	14,542
CAU4196		IND_TARG1	*BnaA.IND.a, BnaC.IND.a*	CATAGCCCAATAGTCATGA	Spec, PPT	pCas9-TPC	14,542
CAU4197	Chapter 5	NST1_TARG1	*BnaA.NST1.a, BnaA.NST1.b, BnaC.NST1.a, BnaC.NST1.b*	GGACAATCTCAAGTGCCTCC	Spec, PPT	pCas9-TPC	14,542
CAU4198		NST1_TARG1	*BnaA.NST1.a, BnaA.NST1.b, BnaC.NST1.a, BnaC.NST1.b*	GGACAATCTCAAGTGCCTCC	Spec, PPT	pCas9-TPC	14,542
CAU4199		IND_TARG1	*BnaA.IND.a, BnaC.IND.a*	CATAGCCCAATAGTCATGA	Spec, PPT	pCas9-TPC	14,542
CAU4200		IND_TARG1	*BnaA.IND.a, BnaC.IND.a*	CATAGCCCAATAGTCATGA	Spec, PPT	pCas9-TPC	14,542

[a] vector constructed by M.Sc. student Shrikant Sharma

9.2   Supplemental figures
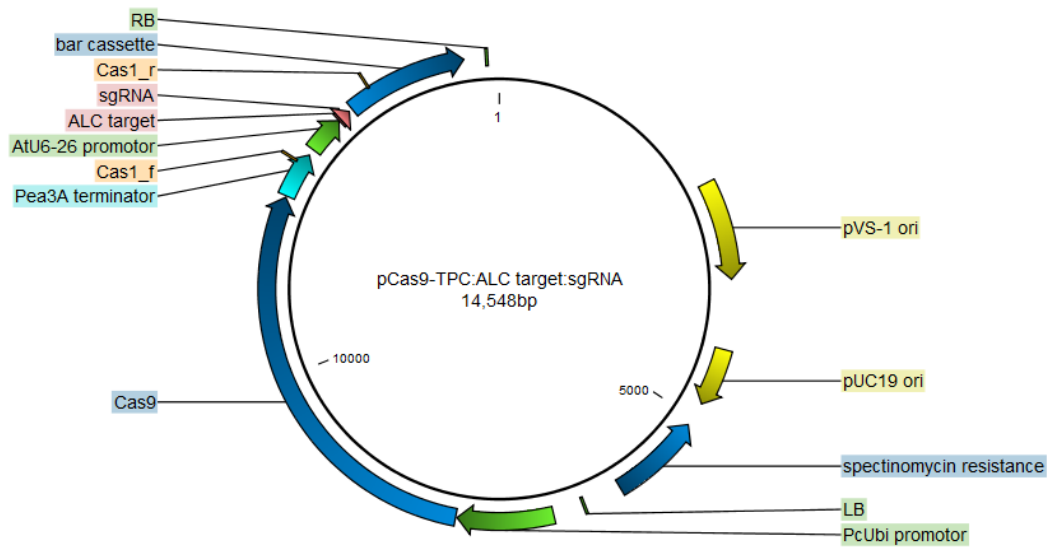
Figure S1. Vector map of the recombinant pCas9-TPC plasmid used for this study. pVS-1 ori and pUC19 ori = origins of bacterial replication, LB = left T-DNA border, RB = right T-DNA border, Cas1_f and Cas1_r = primers.
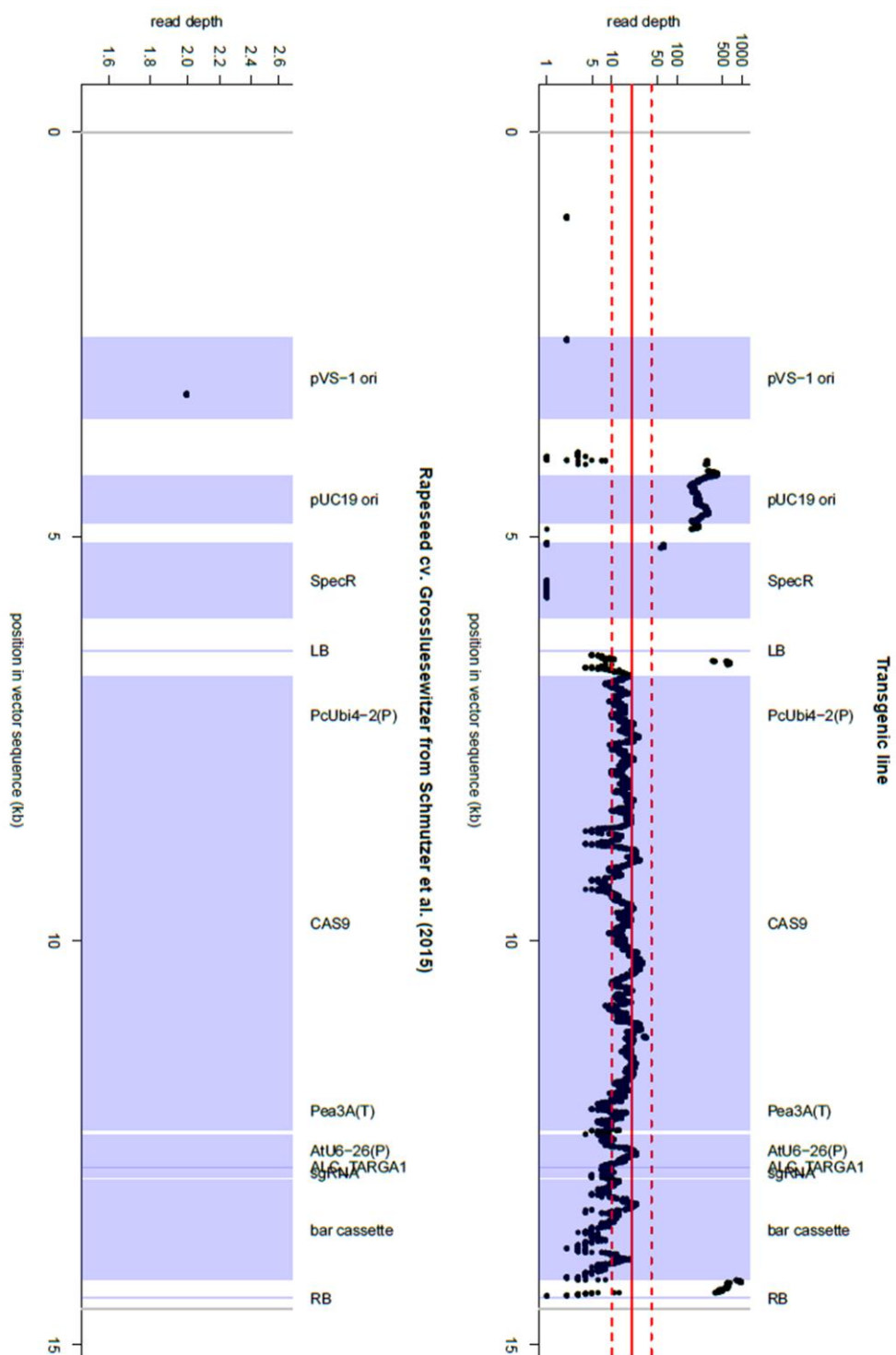
Figure S2. Mapping results of genome sequence of the transgenic T₁ plant CP1 (upper chart) and the negative control cv Grossluesewitzer (lower chart) against the transformation vector sequence. Blue boxes indicate the annotated vector regions. The solid red line marks the average genome coverage, the dashed lines the half and the double of the coverage. The T-DNA, which is enclosed by left and right border (LB/RB), shows a 20x coverage as expected for a single-copy locus.
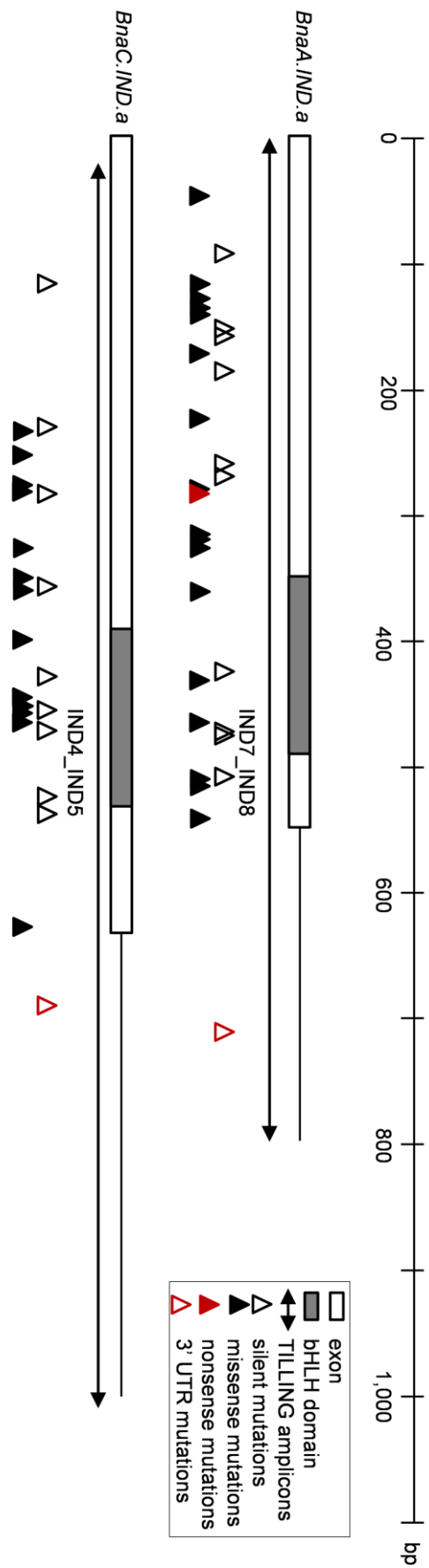
Figure S3. Positions of TILLING amplicons and detected mutations within *BnIND*.
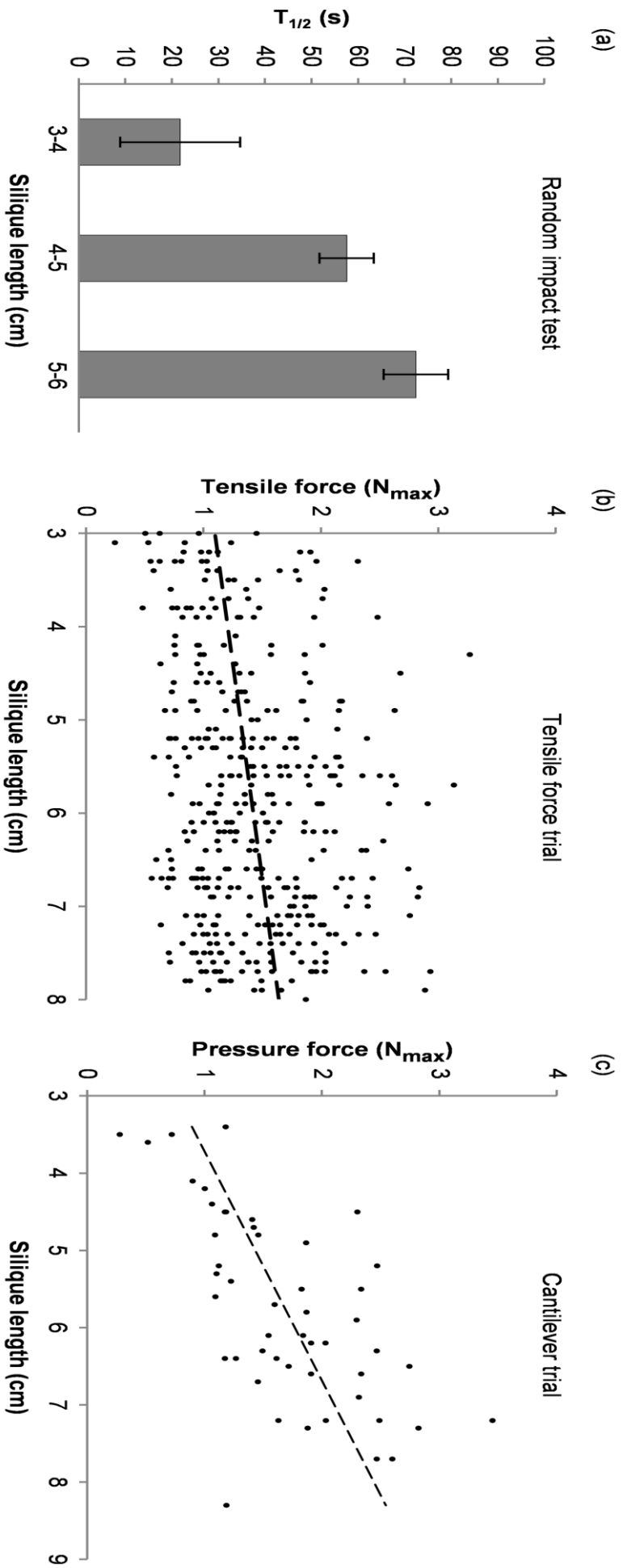
Figure S4. Positive correlation of silique length and shatter resistance of cultivar Express in three independent phenotyping methods. (a) Random impact test values are means of quadruple measurements and standard deviation. Values of all size classes differ significantly from each other as tested by a two-sided *t*-test. Raw data of tensile force trial (b) and cantilever trial (c) confirm positive correlation of silique length and applied force, indicated by linear regression.
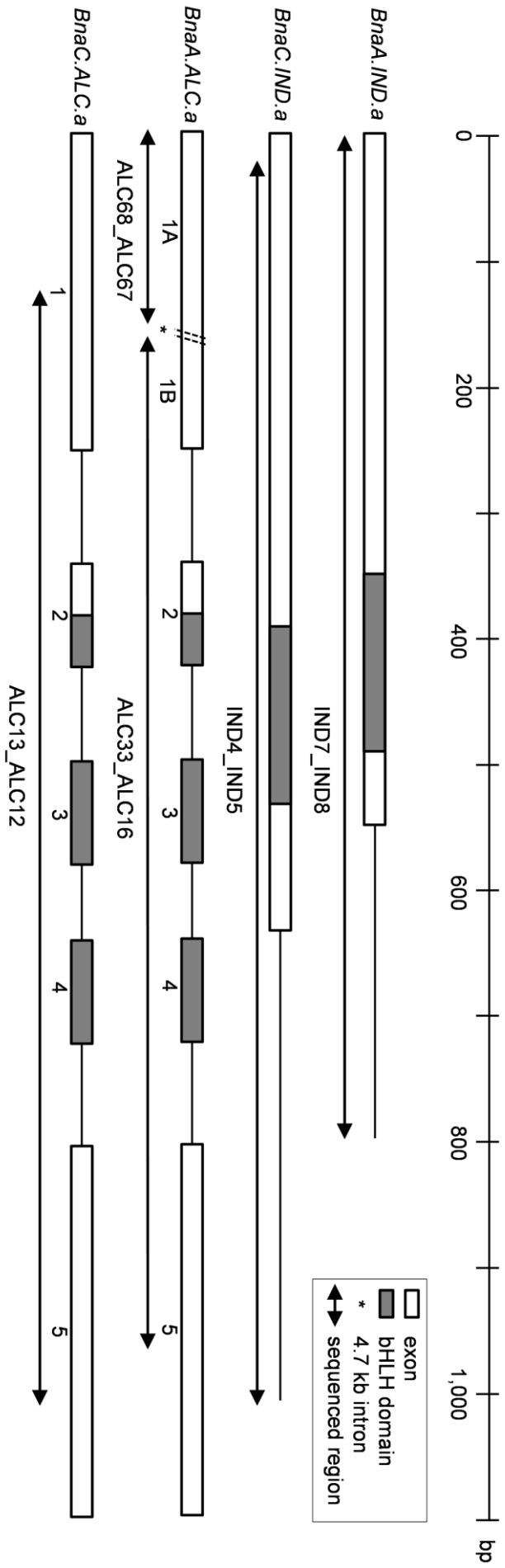
Figure S5. Localization of PCR amplicons for partial sequencing of *BnALC* and *BnIND*.
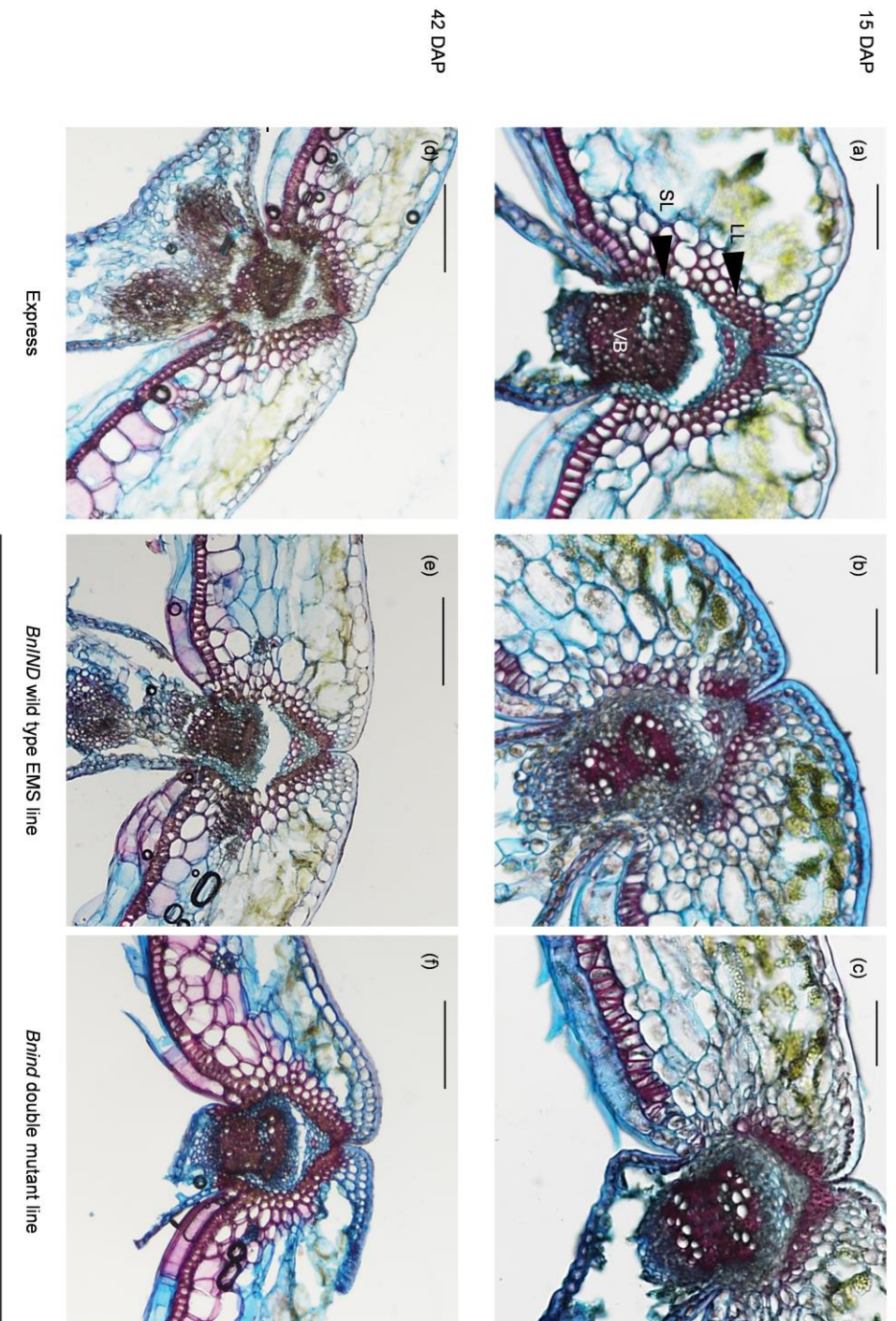
Figure S6. The observed *Bnind* mutations do not lead to a loss of the lignified layer of the dehiscence zone. Cryosections of siliques at 15 DAP (a-c) and 42 DAP (d-f) stained by FCA dye. Red stain = lignin (secondary cell walls), yellow-gold = suberin and cutin, blue = cellulose (primary cell walls). The scale bar for 15 DAP pictures represents 100 μm, for 42 DAP it is 500 μm. LL = lignified layer, SL = separation layer, VB = vascular bundle.
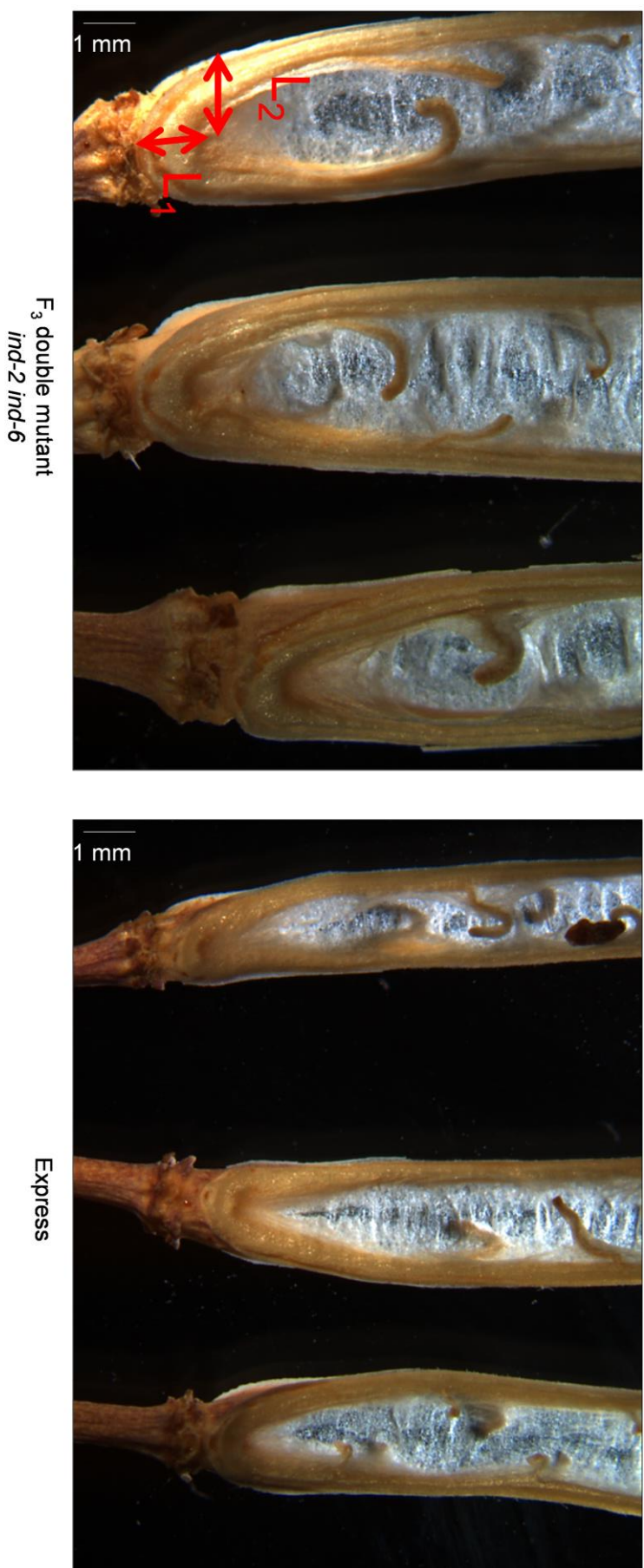
Figure S7. RJAI of Express and F_3 double mutant *ind-2 ind-6* at a silique length of 5 to 6 cm. L_1 and L_2 indicate measures used for the calculation of RJAI. Observation under light microscope Zeiss Stemi SV11.
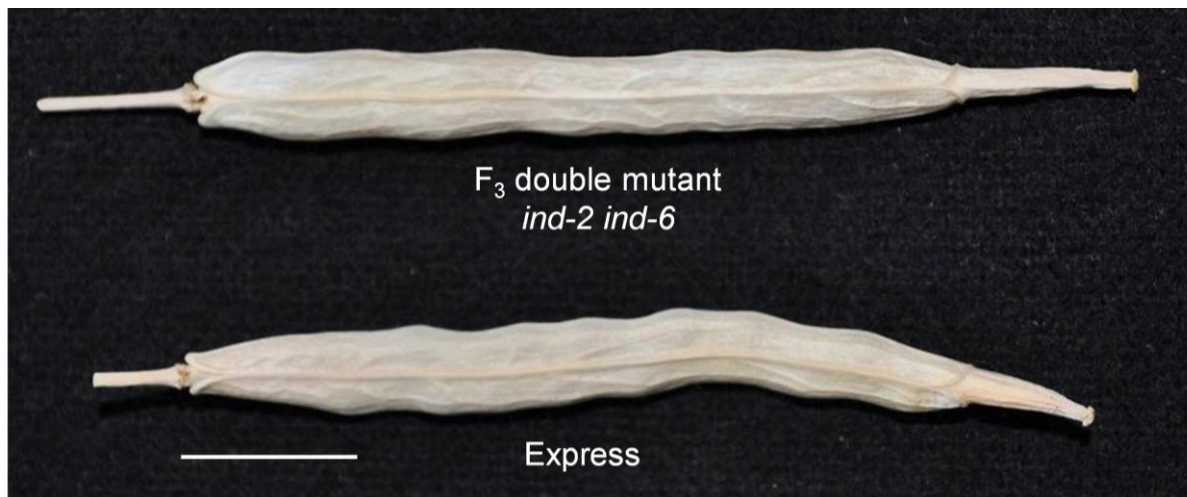
Figure S8. Siliques of Express and F₃ double mutant *ind-2 ind-6*. Bar represents 1 cm.

Figure S9. Experimental set-up of the tensile force measurement. (a) The Newton meter test-stand is loaded with a silique. (b) Close-up of a silique fixated with two alligator clamps. Tensile force will be applied in the direction of the black arrow.
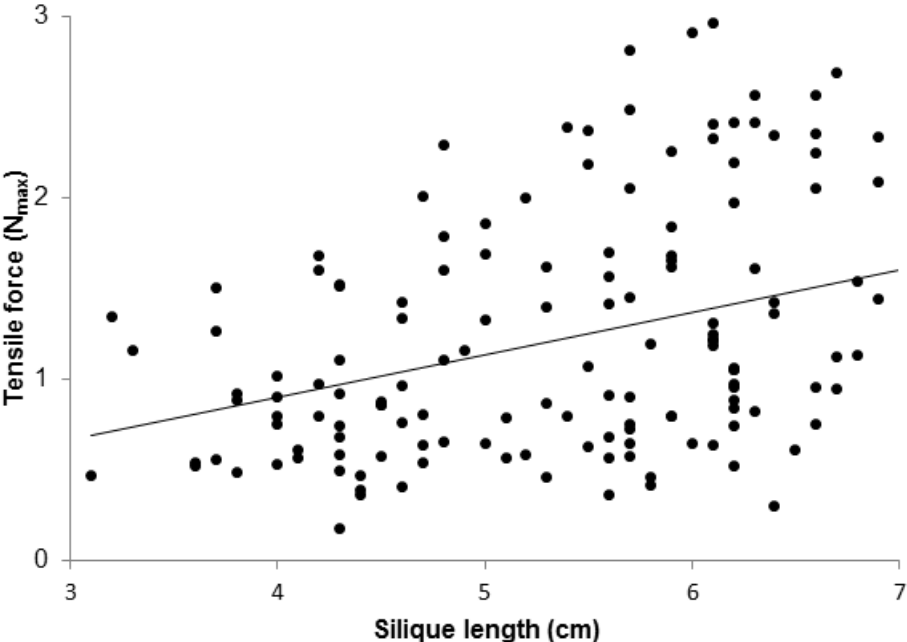
Figure S10. Raw data of tensile force measurement of variety 'Express'. n = 150 siliques. The regression indicates the correlation of silique length and force.
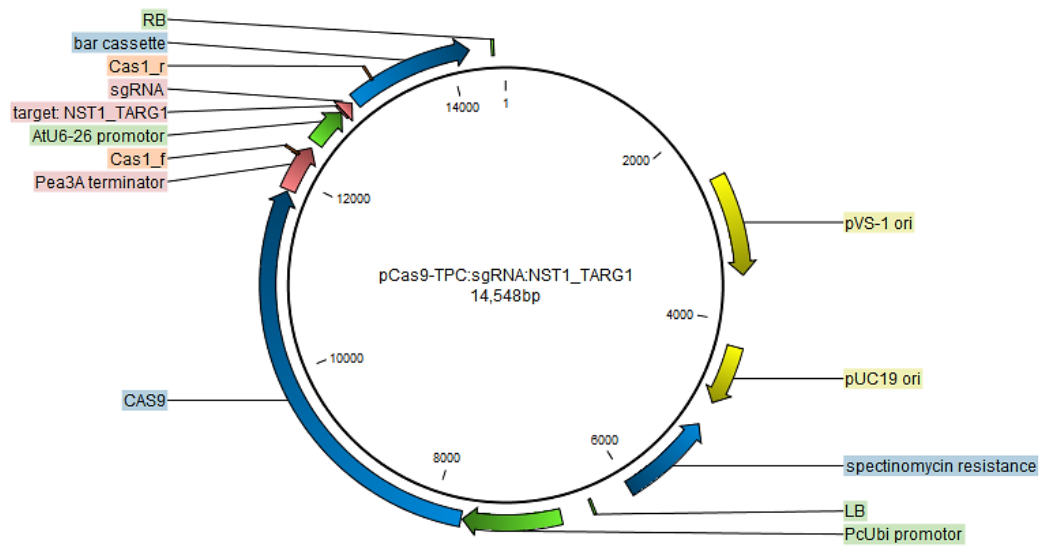
Figure S11. Vector map of the recombinant pCas9-TPC plasmid containing the 'NST1_TARG1' target. pVS-1 ori and pUC19 ori = origins of bacterial replication, LB = left T-DNA border, RB = right T-DNA border, Cas1_f and Cas1_r = primers.

Figure S12. Phenotype of the chimeric T$_1$ plant NP1, which contains Cas9-induced *Bnnst1* mutations in the 'RS306' background. A, Full plant in the silique elongation stage. B, Mature siliques contain only few seeds as can be concluded from the number of bulges (indicated by arrows). C, T$_2$ seeds vary in size and shape with a proportion of small, shriveled seeds. Bars represent 1 cm.

```
TAR motif iii                          LP[Q/x]L[E/x]S[P/A]

AtNST1                                 LPNLESP
BnaA.NST1.a                            -------
BnaA.NST1.b                            LPNLESP
BnaC.NST1.a                            LPNLESP
BnaC.NST1.b                            LPNLESS
```

Figure S13. Identification of transcriptional activation region (TAR) motif iii in *At*NST1 and *Bn*NST1 protein sequences. The motif was originally described by Ooka et al. (2003) and is located within exon 3, which is absent in *BnaA*.NST1.*a* (indicated by dashes). Square brackets indicate ambiguous amino acid positions where one out of the two shown options is present. x = any amino acid. The motif is conserved between Arabidopsis and rapeseed, with the exception of a single amino acid polymorphism in *BnaC*.NST1.*b* (highlighted in red).
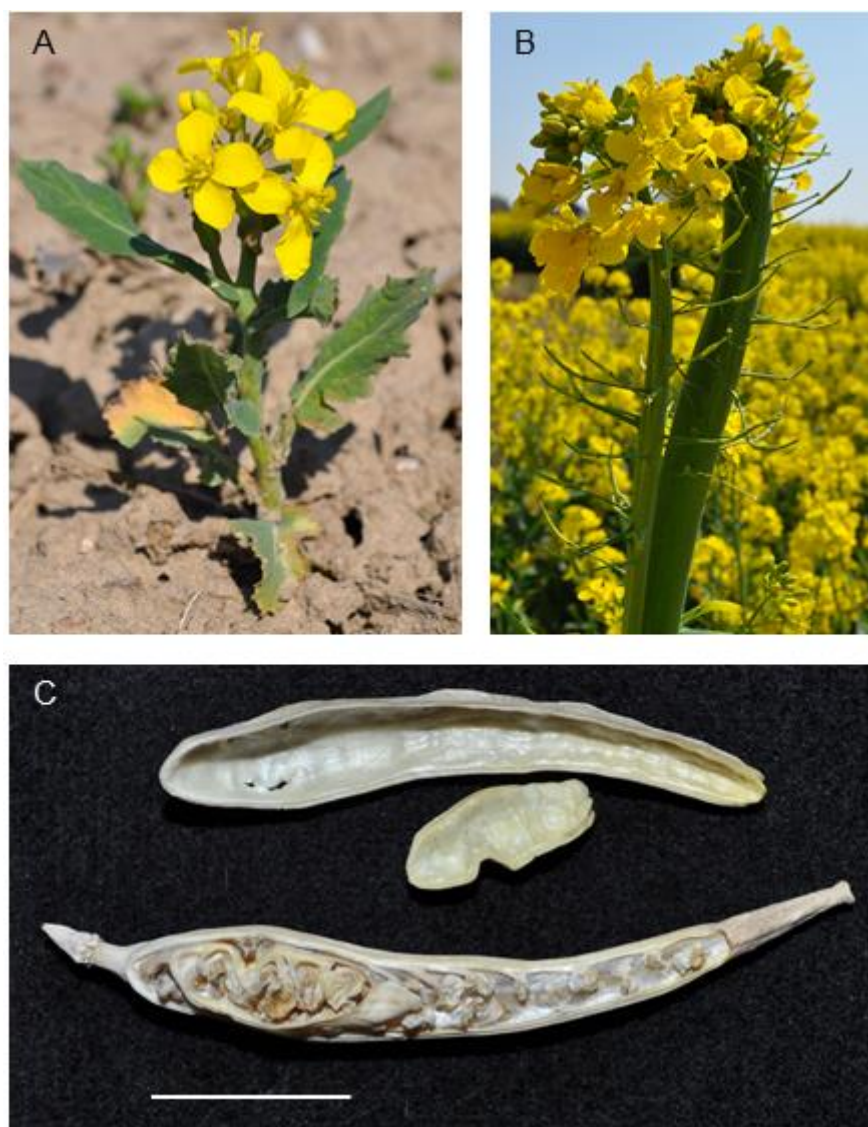
Figure S14. Abnormal phenotypes of plants from the EMS mutant population. A, Stunted growth. B, Atypically broadened stem growth. C, Deformed silique with woody structures instead of seeds. At the pedicel end, a smaller silique has formed within the silique. The bar represents 1 cm.

9.3 Supplemental data on CD

The following supplemental data are available on CD and can be distributed upon request (contact: Prof. Dr. Christian Jung, c.jung@plantbreeding.uni-kiel.de).

File name	Content	Format
Polyacrylamide-gels_TILLING_BnaA.ALC.a.zip	Polyacrylamide gels *BnaA.ALC.a* TILLING (700 nm and 800 nm images plus annotated .xml versions)	.xml and .tif, to be analyzed with GelBuddy TILLING Gel Analysis Tool (Zerr and Henikoff 2005)
Polyacrylamide-gels_TILLING_BnaC.ALC.a.zip	Polyacrylamide gels *BnaC.ALC.a* TILLING (700 nm and 800 nm images plus annotated .xml versions)	.xml and .tif, to be analyzed with GelBuddy TILLING Gel Analysis Tool (Zerr and Henikoff 2005)
Preliminary-data-Bnind-field-trial_2016-17.docx	Preliminary data of field trial with *Bnind* mutants in the growing season 2016/17	.docx, Microsoft Word file
pUC19-assay.docx	Protocol for PCR-based test for pUC19 vector backbone insertions	.docx, Microsoft Word file
Reference sequences	Reference sequences of *BnALC, BnIND, BnNST1*	.clc, annotated sequence files
Seed-codes.xlsx	Seed codes of produced plant material	.xlsx, Microsoft Excel file
TILLING-candidates-BnALC.xlsx	Information about all EMS mutation candidates identified by TILLING of *BnALC*	.xlsx, Microsoft Excel file

10 References

Agrotis A, Ketteler R (2015) A new age in functional genomics using CRISPR/Cas9 in arrayed library screening. Front Genet 6 (300). doi:10.3389/fgene.2015.00300

Aida M, Ishida T, Fukaki H, Fujisawa H, Tasaka M (1997) Genes involved in organ separation in *Arabidopsis*: an analysis of the cup-shaped cotyledon mutant. The Plant Cell 9 (6):841-857. doi:10.1105/tpc.9.6.841

Alonso JM, Stepanova AN, Leisse TJ, Kim CJ, Chen H, Shinn P, Stevenson DK, Zimmerman J, Barajas P, Cheuk R (2003) Genome-wide insertional mutagenesis of *Arabidopsis thaliana*. Science 301 (5633):653-657. doi:10.1126/science.1086391

Andersson M, Turesson H, Nicolia A, Falt AS, Samuelsson M, Hofvander P (2017) Efficient targeted multiallelic mutagenesis in tetraploid potato (*Solanum tuberosum*) by transient CRISPR-Cas9 expression in protoplasts. Plant Cell Rep 36 (1):117-128. doi:10.1007/s00299-016-2062-3

Arnaud N, Girin T, Sorefan K, Fuentes S, Wood TA, Lawrenson T, Sablowski R, Ostergaard L (2011) Gibberellins control fruit patterning in *Arabidopsis thaliana*. Gene Dev 24 (19):2127-2132. doi:10.1101/Gad.593410

Arzt E, Gorb S, Spolenak R (2003) From micro to nano contacts in biological attachment devices. Proc Natl Acad Sci 100 (19):10603-10606. doi:10.1073/pnas.1534701100

Avni R, Nave M, Barad O, Baruch K, Twardziok SO, Gundlach H, Hale I, Mascher M, Spannagl M, Wiebe K, Jordan KW, Golan G, Deek J, Ben-Zvi B, Ben-Zvi G, Himmelbach A, MacLachlan RP, Sharpe AG, Fritz A, Ben-David R, Budak H, Fahima T, Korol A, Faris JD, Hernandez A, Mikel MA, Levy AA, Steffenson B, Maccaferri M, Tuberosa R, Cattivelli L, Faccioli P, Ceriotti A, Kashkush K, Pourkheirandish M, Komatsuda T, Eilam T, Sela H, Sharon A, Ohad N, Chamovitz DA, Mayer KFX, Stein N, Ronen G, Peleg Z, Pozniak CJ, Akhunov ED, Distelfeld A (2017) Wild emmer genome architecture and diversity elucidate wheat evolution and domestication. Science 357 (6346):93-97. doi:10.1126/science.aan0032

Ballester P, Ferrándiz C (2017) Shattering fruits: variations on a dehiscent theme. Curr Opin Plant Biol 35:68-75. doi:10.1016/j.pbi.2016.11.008

Baux A, Colbach N, Pellet D (2011) Crop management for optimal low-linolenic rapeseed oil production - Field experiments and modelling. Europ J Agronomy 35 (3):144-153. doi:10.1016/j.eja.2011.05.006

Bhalla PL, Singh MB (2008) *Agrobacterium*-mediated transformation of *Brassica napus* and *Brassica oleracea*. Nat Protocols 3 (2):181-189. doi:10.1038/nprot.2007.527

Boch J, Scholze H, Schornack S, Landgraf A, Hahn S, Kay S, Lahaye T, Nickstadt A, Bonas U (2009) Breaking the code of DNA binding specificity of TAL-type III effectors. Science 326 (5959):1509-1512. doi:10.1126/science.1178811

Bolotin A, Quinquis B, Sorokin A, Ehrlich SD (2005) Clustered regularly interspaced short palindrome repeats (CRISPRs) have spacers of extrachromosomal origin. Microbiol 151 (8):2551-2561. doi:10.1099/mic.0.28048-0

Boszoradova E, Libantova J, Matusikova I, Poloniova Z, Jopcik M, Berenyi M, Moravcikova J (2011) *Agrobacterium*-mediated genetic transformation of economically important oilseed rape cultivars. Plant Cell Tiss Org 107 (2):317-323. doi:10.1007/s11240-011-9982-y

Braatz J, Harloff H-J, Mascher M, Stein N, Himmelbach A, Jung C (2017) CRISPR-Cas9 targeted mutagenesis leads to simultaneous modification of different homoeologous gene copies in polyploid oilseed rape (*Brassica napus*). Plant Physiol 174 (2): 935-942 doi:10.1104/pp.17.00426

Brooks C, Nekrasov V, Lippman ZB, Van Eck J (2014) Efficient gene editing in tomato in the first generation using the clustered regularly interspaced short palindromic repeats/CRISPR-associated9 system. Plant Physiol 166 (3):1292-1297. doi:10.1104/pp.114.247577

Bruce DM, Farrent JW, Morgan CL, Child RD (2002) Determining the oilseed rape pod strength needed to reduce seed loss due to pod shatter. Biosyst Eng 81 (2):179-184. doi:10.1006/bioe.2001.0002

Bruce DM, Hobson RN, Morgan CL, Child RD (2001) Threshability of shatter-resistant seed pods in oilseed rape. J Agr Eng Res 80 (4):343-350. doi:10.1006/jaer.2001.0748

Bus A, Körber N, Snowdon RJ, Stich B (2011) Patterns of molecular variation in a species-wide germplasm set of *Brassica napus*. Theor Appl Genet 123 (8):1413-1423. doi:10.1007/s00122-011-1676-7

Cavalieri A, Lewis DW, Gulden RH (2014) Pod drop and pod shatter are not closely related in canola. Crop Sci 54 (3):1184-1188. doi:10.2135/cropsci2013.09.0624

Chalhoub B, Denoeud F, Liu SY, Parkin IAP, Tang HB, Wang XY, Chiquet J, Belcram H, Tong CB, Samans B, Correa M, Da Silva C, Just J, Falentin C, Koh CS, Le Clainche I, Bernard M, Bento P, Noel B, Labadie K, Alberti A, Charles M, Arnaud D, Guo H, Daviaud C, Alamery S, Jabbari K, Zhao MX, Edger PP, Chelaifa H, Tack D, Lassalle G, Mestiri I, Schnel N, Le Paslier MC, Fan GY, Renault V, Bayer PE, Golicz AA, Manoli S, Lee TH, Thi VHD, Chalabi S, Hu Q, Fan CC, Tollenaere R, Lu YH, Battail C, Shen JX, Sidebottom CHD, Wang XF, Canaguier A, Chauveau A, Berard A, Deniot G, Guan M, Liu ZS, Sun FM, Lim YP, Lyons E, Town CD, Bancroft I, Wang XW, Meng JL, Ma JX, Pires JC, King GJ, Brunel D, Delourme R, Renard M, Aury JM, Adams KL, Batley J, Snowdon RJ, Tost J, Edwards D, Zhou YM, Hua W, Sharpe AG, Paterson AH, Guan CY, Wincker P (2014) Early allopolyploid evolution in the post-Neolithic *Brassica napus* oilseed genome. Science 345 (6199):950-953. doi:10.1126/science.1253435

Chandrasekaran J, Brumin M, Wolf D, Leibman D, Klap C, Pearlsman M, Sherman A, Arazi T, Gal-On A (2016) Development of broad virus resistance in non-transgenic cucumber using CRISPR/Cas9 technology. Mol Plant Pathol 17 (7):1140-1153. doi:10.1111/mpp.12375

Child RD, Summers JE, Babij J, Farrent JW, Bruce DM (2003) Increased resistance to pod shatter is associated with changes in the vascular structure in pods of a resynthesized *Brassica napus* line. J Exp Bot 54 (389):1919-1930. doi:10.1093/Jxb/Erg209

Cochran WG (1957) Analysis of covariance - its nature and uses. Biometrics 13 (3):261-281. doi:10.2307/2527916

Comai L, Facciotti D, Hiatt W, Thompson G, Rose R, Stalker D (1985) Expression in plants of a mutant *aroA* gene from *Salmonella typhimurium* confers tolerance to glyphosate. Nature 317 (6039):741-744. doi:10.1038/317741a0

Cradick TJ, Fine EJ, Antico CJ, Bao G (2013) CRISPR/Cas9 systems targeting β-globin and *CCR5* genes have substantial off-target activity. Nucleic Acids Res 41 (20):9584-9592. doi:10.1093/nar/gkt714

D'Halluin K, Vanderstraeten C, Hulle J, Rosolowska J, Den Brande I, Pennewaert A, D'Hont K, Bossut M, Jantz D, Ruiter R (2013) Targeted molecular trait stacking in cotton through targeted double-strand break induction. Plant Biotechnol J 11 (8):933-941. doi:10.1111/pbi.12085

Dally N, Xiao K, Holtgräwe D, Jung C (2014) The *B2* flowering time locus of beet encodes a zinc finger transcription factor. Proc Natl Acad Sci 111 (28):10365-10370. doi:10.1073/pnas.1404829111

Davies GC, Bruce DM (1997) Fracture mechanics of oilseed rape pods. J Mater Sci 32 (22):5895-5899. doi:10.1023/a:1018650608347

Davis RL, Cheng P-F, Lassar AB, Weintraub H (1990) The MyoD DNA binding domain contains a recognition code for muscle-specific gene activation. Cell 60 (5):733-746. doi:10.1016/0092-8674(90)90088-V

De Block M, De Brouwer D, Tenning P (1989) Transformation of *Brassica napus* and *Brassica oleracea* using *Agrobacterium tumefaciens* and the expression of the *bar* and *neo* genes in the transgenic plants. Plant Physiol 91 (2):694-701. doi:10.1104/pp.91.2.694

De Lucas M, Daviere J-M, Rodriguez-Falcon M, Pontin M, Iglesias-Pedraz JM, Lorrain S, Fankhauser C, Blázquez MA, Titarenko E, Prat S (2008) A molecular framework for light and gibberellin control of cell elongation. Nature 451 (7177):480-484. doi:10.1038/nature06520

Dening K, Heepe L, Afferrante L, Carbone G, Gorb SN (2014) Adhesion control by inflation: implications from biology to artificial attachment device. Applied Physics A 116 (2):567-573. doi:10.1007/s00339-014-8504-2

Dinneny JR, Yanofsky MF (2004) Drawing lines and borders: how the dehiscent fruit of *Arabidopsis* is patterned. Bioessays 27 (1):42-49. doi:10.1002/bies.20165

Doudna JA, Charpentier E (2014) The new frontier of genome engineering with CRISPR-Cas9. Science 346 (6213). doi:10.1126/science.1258096

Drake JW, Charlesworth B, Charlesworth D, Crow JF (1998) Rates of spontaneous mutation. Genetics 148 (4):1667-1686

Duval M, Hsieh T-F, Kim SY, Thomas TL (2002) Molecular characterization of *AtNAM*: a member of the *Arabidopsis* NAC domain superfamily. Plant Mol Biol 50 (2):237-248. doi:10.1023/a:1016028530943

Elisha, C (2016) Transcription profiling of seed shattering genes in rapeseed. Unpublished Master's Thesis, Christian-Albrechts-University of Kiel, Kiel, Germany

Emrani N, Harloff H-J, Gudi O, Kopisch-Obuch F, Jung C (2015) Reduction in sinapine content in rapeseed (*Brassica napus* L.) by induced mutations in sinapine biosynthesis genes. Mol Breeding 35 (1):37. doi:10.1007/s11032-015-0236-2

Endo M, Mikami M, Toki S (2015) Multigene knockout utilizing off-target mutations of the CRISPR/Cas9 system in rice. Plant Cell Physiol 56 (1):41-47. doi:10.1093/Pcp/Pcu154

Ernst HA, Olsen AN, Skriver K, Larsen S, Leggio LL (2004) Structure of the conserved domain of ANAC, a member of the NAC family of transcription factors. EMBO reports 5 (3):297-303. doi:10.1038/sj.embor.7400093

Etzold H (2002) Simultanfärbung von Pflanzenschnitten mit Fuchsin, Chrysoidin und Astrablau. Mikrokosmos 91 (5):316

Fauser F, Schiml S, Puchta H (2014) Both CRISPR/Cas-based nucleases and nickases can be used efficiently for genome engineering in *Arabidopsis thaliana*. Plant J 79 (2):348-359. doi:10.1111/Tpj.12554

Feng S, Martinez C, Gusmaroli G, Wang Y, Zhou J, Wang F, Chen L, Yu L, Iglesias-Pedraz JM, Kircher S, Schafer E, Fu X, Fan L-M, Deng XW (2008) Coordinated regulation of *Arabidopsis thaliana* development by light and gibberellins. Nature 451 (7177):475-479. doi:10.1038/nature06448

Feng ZY, Mao YF, Xu NF, Zhang BT, Wei PL, Yang DL, Wang Z, Zhang ZJ, Zheng R, Yang L, Zeng L, Liu XD, Zhu JK (2014) Multigeneration analysis reveals the inheritance, specificity, and patterns of CRISPR/Cas-induced gene modifications in *Arabidopsis*. P Natl Acad Sci USA 111 (12):4632-4637. doi:10.1073/pnas.1400822111

Ferrándiz C (2000) Negative regulation of the *SHATTERPROOF* genes by *FRUITFULL* during Arabidopsis fruit development. Science 289 (5478):436-438. doi:10.1126/science.289.5478.436

Finn RD, Bateman A, Clements J, Coggill P, Eberhardt RY, Eddy SR, Heger A, Hetherington K, Holm L, Mistry J, Sonnhammer ELL, Tate J, Punta M (2014) Pfam: the protein families database. Nucleic Acids Res 42 (D1):D222-D230. doi:10.1093/nar/gkt1223

Gao H, Ji B, Jäger IL, Arzt E, Fratzl P (2003) Materials become insensitive to flaws at nanoscale: lessons from nature. Proc Natl Acad Sci 100 (10):5597-5600. doi:10.1073/pnas.0631609100

Garcia M, Mather DE (2014) From genes to markers: exploiting gene sequence information to develop tools for plant breeding. In: Fleury D, Whitford R (eds) Crop Breeding: Methods and Protocols. Methods in Molecular Biology, vol 1145. Springer Science+Business Media, New York, pp 21-36. doi:10.1007/978-1-4939-0446-4_2

Gilchrist EJ, Sidebottom CHD, Koh CS, MacInnes T, Sharpe AG, Haughn GW (2013) A mutant *Brassica napus* (canola) population for the identification of new genetic diversity via TILLING and next generation sequencing. Plos One 8 (12):e84303. doi:10.1371/journal.pone.0084303

Girin T, Paicu T, Stephenson P, Fuentes S, Korner E, O'Brien M, Sorefan K, Wood TA, Balanza V, Ferrándiz C, Smyth DR, Ostergaard L (2011) INDEHISCENT and

SPATULA interact to specify carpel and valve margin tissue and thus promote seed dispersal in Arabidopsis. Plant Cell 23 (10):3641-3653. doi:10.1105/tpc.111.090944

Girin T, Stephenson P, Goldsack CMP, Kempin SA, Perez A, Pires N, Sparrow PA, Wood TA, Yanofsky MF, Østergaard L (2010) Brassicaceae *INDEHISCENT* genes specify valve margin cell fate and repress replum formation. Plant J 63 (2):329-338. doi:10.1111/j.1365-313X.2010.04244.x

Gobena D, Shimels M, Rich PJ, Ruyter-Spira C, Bouwmeester H, Kanuganti S, Mengiste T, Ejeta G (2017) Mutation in sorghum *LOW GERMINATION STIMULANT 1* alters strigolactones and causes *Striga* resistance. Proc Natl Acad Sci 114 (17):4471-4476. doi:10.1073/pnas.1618965114

Groszmann M, Paicu T, Alvarez JP, Swain SM, Smyth DR (2011) *SPATULA* and *ALCATRAZ*, are partially redundant, functionally diverging bHLH genes required for Arabidopsis gynoecium and fruit development. Plant J 68 (5):816-829. doi:10.1111/j.1365-313X.2011.04732.x

Gulden RH, Shirtliffe SJ, Thomas AG (2003) Harvest losses of canola (*Brassica napus*) cause large seedbank inputs. Weed Sci 51 (1):83-86

Guo Y, Harloff H-J, Jung C, Molina C (2014) Mutations in single *FT*- and *TFL1*-paralogs of rapeseed (*Brassica napus* L.) and their impact on flowering time and yield components. Front Plant Sci 5 (282). doi:10.3389/fpls.2014.00282

Harloff HJ, Lemcke S, Mittasch J, Frolov A, Wu JG, Dreyer F, Leckband G, Jung C (2012) A mutation screening platform for rapeseed (*Brassica napus* L.) and the detection of sinapine biosynthesis mutants. Theor Appl Genet 124 (5):957-969. doi:10.1007/s00122-011-1760-z

Hobson RN, Bruce DM (2002) Seed loss when cutting a standing crop of oilseed rape with two types of combine harvester header. Biosyst Eng 81 (3):281-286. doi:10.1006/bioe.2001.0011

Hsu PD, Scott DA, Weinstein JA, Ran FA, Konermann S, Agarwala V, Li Y, Fine EJ, Wu X, Shalem O, Cradick TJ, Marraffini LA, Bao G, Zhang F (2013) DNA targeting specificity of RNA-guided Cas9 nucleases. Nat Biotech 31 (9):827-832. doi:10.1038/nbt.2647

Hu Z, Yang H, Zhang L, Wang X, Liu G, Wang H, Hua W (2015) A large replum-valve joint area is associated with increased resistance to pod shattering in rapeseed. J Plant Res 128 (5):813-819. doi:10.1007/s10265-015-0732-9

Hua S, Shamsi IH, Guo Y, Pak H, Chen M, Shi C, Meng H, Jiang L (2009) Sequence, expression divergence, and complementation of homologous *ALCATRAZ* loci in *Brassica napus*. Planta 230 (3):493-503. doi:10.1007/s00425-009-0961-z

Hufford MB, Xu X, Van Heerwaarden J, Pyhäjärvi T, Chia J-M, Cartwright RA, Elshire RJ, Glaubitz JC, Guill KE, Kaeppler SM (2012) Comparative population genomics of maize domestication and improvement. Nat Genet 44 (7):808-811. doi:10.1038/ng.2309

Hui C-Y, Glassmaker N, Tang T, Jagota A (2004) Design of biomimetic fibrillar interfaces: 2. Mechanics of enhanced adhesion. J R Soc Interface 1 (1):35-48. doi:10.1098/rsif.2004.0005

Hwang SF, Ahmed HU, Zhou Q, Strelkov SE, Gossen BD, Peng G, Turnbull GD (2012) Assessment of the impact of resistant and susceptible canola on *Plasmodiophora brassicae* inoculum potential. Plant Pathology 61 (5):945-952. doi:10.1111/j.1365-3059.2011.02582.x

Hyten DL, Song Q, Zhu Y, Choi I-Y, Nelson RL, Costa JM, Specht JE, Shoemaker RC, Cregan PB (2006) Impacts of genetic bottlenecks on soybean genome diversity. Proc Natl Acad Sci 103 (45):16666-16671. doi:10.1073/pnas.0604379103

Isshiki M, Morino K, Nakajima M, Okagaki RJ, Wessler SR, Izawa T, Shimamoto K (1998) A naturally occurring functional allele of the rice *waxy* locus has a GT to TT mutation at the 5′ splice site of the first intron. Plant J 15 (1):133-138. doi:10.1046/j.1365-313X.1998.00189.x

Jinek M, Chylinski K, Fonfara I, Hauer M, Doudna JA, Charpentier E (2012) A programmable dual-RNA-guided DNA endonuclease in adaptive bacterial immunity. Science 337 (6096):816-821. doi:10.1126/science.1225829

Jore MM, Lundgren M, Van Duijn E, Bultema JB, Westra ER, Waghmare SP, Wiedenheft B, Pul Ü, Wurm R, Wagner R (2011) Structural basis for CRISPR RNA-guided DNA recognition by Cascade. Nat Struct Mol Biol 18 (5):529-536. doi:10.1038/nsmb.2019

Jørgensen T, Hauser TP, Jørgensen RB (2007) Adventitious presence of other varieties in oilseed rape (*Brassica napus*) from seed banks and certified seed. Seed Sci Res 17 (2):115-125. doi:10.1017/S0960258507708103

Jugulam M, Ziauddin A, So KK, Chen S, Hall JC (2015) Transfer of Dicamba tolerance from *Sinapis arvensis* to *Brassica napus* via embryo rescue and recurrent backcross breeding. Plos One 10 (11):e0141418. doi:10.1371/journal.pone.0141418

Jung C (2010) Breeding with genetically modified plants. In: Kempken F, Jung C (eds) Genetic modification of plants: Agriculture, horticulture and forestry. Biotechnology in agriculture and forestry, vol 64. Springer Berlin Heidelberg, Berlin, Heidelberg, pp 103-116. doi:10.1007/978-3-642-02391-0_6

Kadkol GP, Macmillan RH, Burrow RP, Halloran GM (1984) Evaluation of *Brassica* genotypes for resistance to shatter. I. Development of a laboratory test. Euphytica 33 (1):63-73. doi:10.1007/bf00022751

Kahrizi D, Salmanian AH, Afshari A, Moieni A, Mousavi A (2007) Simultaneous substitution of Gly96 to Ala and Ala183 to Thr in 5-enolpyruvylshikimate-3-phosphate synthase gene of *E. coli* (k12) and transformation of rapeseed (*Brassica napus* L.) in order to make tolerance to glyphosate. Plant Cell Rep 26 (1):95-104. doi:10.1007/s00299-006-0208-4

Kay P, Groszmann M, Ross JJ, Parish RW, Swain SM (2013) Modifications of a conserved regulatory network involving INDEHISCENT controls multiple aspects of reproductive tissue development in Arabidopsis. New Phytol 197 (1):73-87. doi:10.1111/j.1469-8137.2012.04373.x

Kelliher T, Starr D, Richbourg L, Chintamanani S, Delzer B, Nuccio ML, Green J, Chen Z, McCuiston J, Wang W (2017) MATRILINEAL, a sperm-specific phospholipase, triggers maize haploid induction. Nature 542 (7639):105-109. doi:10.1038/nature20827

Kim Y, Schumaker KS, Zhu J-K (2006) EMS mutagenesis of *Arabidopsis*. In: Salinas J, Sanchez-Serrano JJ (eds) *Arabidopsis* Protocols. Methods in Molecular Biology, vol 323, 2 edn. Humana Press, Totowa, New Jersey, pp 101-103

Kord H, Shakib A, Daneshvar M, Azadi P, Bayat V, Mashayekhi M, Zarea M, Seifi A, Ahmad-Raji M (2015) RNAi-mediated down-regulation of *SHATTERPROOF* gene in transgenic oilseed rape. 3 Biotech 5 (3):271-277. doi:10.1007/s13205-014-0226-9

Krautgartner R, Lefebvre L, Rehder LE, Boshnakova M, Dobrescu M, Flach B, Wilson J, Faniadis D, Guerrero M, Rossetti A (2017) EU-28 Oilseeds and Products Annual 2017. GAIN Report. USDA Foreign Agricultural Service

Kuai J, Yang Y, Sun Y, Zhou G, Zuo Q, Wu J, Ling X (2015) Paclobutrazol increases canola seed yield by enhancing lodging and pod shatter resistance in *Brassica napus* L. Field Crop Res 180:10-20. doi:10.1016/j.fcr.2015.05.004

Laga B (2013) Brassica plant comprising a mutant *ALCATRAZ* allele. US Patent US20130291235A1, 31.10.2013

Laga B, Lambert B, Boer Bd (2015) Brassica plant comprising a mutant *INDEHISCENT* allele. Europe Patent EP2220239B1, 20.05.2015

Laird NM, Ware JH (1982) Random-effects models for longitudinal data. Biometrics 38 (4):963-974. doi:10.2307/2529876

Lawrenson T, Shorinola O, Stacey N, Li C, Østergaard L, Patron N, Uauy C, Harwood W (2015) Induction of targeted, heritable mutations in barley and *Brassica oleracea* using RNA-guided Cas9 nuclease. Genome Biol 16:258. doi:10.1186/s13059-015-0826-7

Lenser T, Theißen G (2013) Conservation of fruit dehiscence pathways between *Lepidium campestre* and *Arabidopsis thaliana* sheds light on the regulation of *INDEHISCENT*. Plant J 76 (4):545-556. doi:10.1111/tpj.12321

Li H, Handsaker B, Wysoker A, Fennell T, Ruan J, Homer N, Marth G, Abecasis G, Durbin R, Proc GPD (2009) The Sequence Alignment/Map format and SAMtools. Bioinformatics 25 (16):2078-2079. doi:10.1093/bioinformatics/btp352

Li J, Meng XB, Zong Y, Chen KL, Zhang HW, Liu JX, Li JY, Gao CX (2016a) Gene replacements and insertions in rice by intron targeting using CRISPR-Cas9. Nat Plants 2 (10):16139. doi:10.1038/Nplants.2016.139

Li T, Liu B, Spalding MH, Weeks DP, Yang B (2012) High-efficiency TALEN-based gene editing produces disease-resistant rice. Nat Biotechnol 30 (5):390-392. doi:10.1038/nbt.2199

Li T, Yaokui L, Dan Z, Bigang M, Qiming L, Yuanyi H, Ye S, Yan P, Binran Z, Shitou X (2016b) Characteristic and inheritance analysis of targeted mutagenesis mediated by genome editing in rice. Yi Chuan 38 (8):746-755. doi:10.16288/j.yczz.16-052

Li W-x, Wu S-l, Liu Y-h, Jin G-l, Zhao H-j, Fan L-j, Shu Q-y (2016c) Genome-wide profiling of genetic variation in *Agrobacterium*-transformed rice plants. J Zhejiang Univ-Sc B 17 (12):992-996. doi:10.1631/jzus.B1600301

Li X, Song Y, Century K, Straight S, Ronald P, Dong X, Lassner M, Zhang Y (2001) A fast neutron deletion mutagenesis-based reverse genetics system for plants. Plant J 27 (3):235-242. doi:10.1046/j.1365-313x.2001.01084.x

Liang Z, Chen K, Li T, Zhang Y, Wang Y, Zhao Q, Liu J, Zhang H, Liu C, Ran Y, Gao C (2017) Efficient DNA-free genome editing of bread wheat using CRISPR/Cas9 ribonucleoprotein complexes. Nat Commun 8:14261. doi:10.1038/ncomms14261

Lieber MR (2008) The mechanism of human nonhomologous DNA end joining. J Biol Chem 283 (1):1-5. doi:10.1074/jbc.R700039200

Liljegren SJ, Ditta GS, Eshed HY, Savidge B, Bowman JL, Yanofsky MF (2000) *SHATTERPROOF* MADS-box genes control seed dispersal in *Arabidopsis*. Nature 404 (6779):766-770. doi:10.1038/35008089

Liljegren SJ, Roeder AHK, Kempin SA, Gremski K, Ostergaard L, Guimil S, Reyes DK, Yanofsky MF (2004) Control of fruit patterning in *Arabidopsis* by *INDEHISCENT*. Cell 116 (6):843-853. doi:10.1016/S0092-8674(04)00217-X

Liu J, Huang SM, Sun MY, Liu SY, Liu YM, Wang WX, Zhang XR, Wang HZ, Hua W (2012) An improved allele-specific PCR primer design method for SNP marker analysis and its application. Plant Methods 8:34. doi:10.1186/1746-4811-8-34

Liu J, Wang J, Wang H, Wang W, Mei D, Zhou R, Cheng H, Yang J, Raman H, Hu Q (2016) Multigenic control of pod shattering resistance in Chinese rapeseed germplasm revealed by genome-wide association and linkage analyses. Front Plant Sci 7:1058. doi:10.3389/fpls.2016.01058

Liu S, Liu Y, Yang X, Tong C, Edwards D, Parkin IAP, Zhao M, Ma J, Yu J, Huang S, Wang X, Wang J, Lu K, Fang Z, Bancroft I, Yang T-J, Hu Q, Wang X, Yue Z, Li H, Yang L, Wu J, Zhou Q, Wang W, King GJ, Pires JC, Lu C, Wu Z, Sampath P, Wang Z, Guo H, Pan S, Yang L, Min J, Zhang D, Jin D, Li W, Belcram H, Tu J, Guan M, Qi C, Du D, Li J, Jiang L, Batley J, Sharpe AG, Park B-S, Ruperao P, Cheng F, Waminal NE, Huang Y, Dong C, Wang L, Li J, Hu Z, Zhuang M, Huang Y, Huang J, Shi J, Mei D, Liu J, Lee T-H, Wang J, Jin H, Li Z, Li X, Zhang J, Xiao L, Zhou Y, Liu Z, Liu X, Qin R, Tang X, Liu W, Wang Y, Zhang Y, Lee J, Kim HH, Denoeud F, Xu X, Liang X, Hua W, Wang X, Wang J, Chalhoub B, Paterson AH (2014) The *Brassica oleracea* genome reveals the asymmetrical evolution of polyploid genomes. Nat Commun 5:3930. doi:10.1038/ncomms4930

Liu X, Macmillan R, Burrow R, Kadkol G, Halloran G (1994) Pendulum test for evaluation of the rupture strength of seed pods. J Texture Stud 25 (2):179-190. doi:10.1111/j.1745-4603.1994.tb01325.x

Lochlainn SO, Amoah S, Graham NS, Alamer K, Rios JJ, Kurup S, Stoute A, Hammond JP, Ostergaard L, King GJ, White PJ, Broadley MR (2011) High Resolution Melt (HRM)

analysis is an efficient tool to genotype EMS mutants in complex crop genomes. Plant Methods 7:43. doi:10.1186/1746-4811-7-43

Lu S, Zhao X, Hu Y, Liu S, Nan H, Li X, Fang C, Cao D, Shi X, Kong L (2017) Natural variation at the soybean *J* locus improves adaptation to the tropics and enhances yield. Nature 49:773–779. doi:10.1038/ng.3819

Lühs W, Friedt W (1994) Stand und Perspektiven der Züchtung von Raps (*Brassica napus* L.) mit hohem Erucasäure-Gehalt im Öl für industrielle Nutzungszwecke. Eur J Lipid Sci Tech 96 (4):137-146. doi:10.1002/lipi.19940960405

Lutman PJ, Berry K, Payne RW, Simpson E, Sweet JB, Champion GT, May MJ, Wightman P, Walker K, Lainsbury M (2005) Persistence of seeds from crops of conventional and herbicide tolerant oilseed rape (*Brassica napus*). Proc R Soc Lond B Biol Sci 272 (1575):1909-1915. doi:10.1098/rspb.2005.3166

Lysak MA, Koch MA, Pecinka A, Schubert I (2005) Chromosome triplication found across the tribe *Brassiceae*. Genome Res 15 (4):516-525. doi:10.1101/gr.3531105

Makarova KS, Haft DH, Barrangou R, Brouns SJJ, Charpentier E, Horvath P, Moineau S, Mojica FJM, Wolf YI, Yakunin AF, van der Oost J, Koonin EV (2011) Evolution and classification of the CRISPR–Cas systems. Nat Rev Micro 9 (6):467-477. doi:10.1038/nrmicro2577

Maki H (2002) Origins of spontaneous mutations: specificity and directionality of base-substitution, frameshift, and sequence-substitution mutageneses. Annu Rev Genet 36 (1):279-303. doi:10.1146/annurev.genet.36.042602.094806

Maluszynski M (2001) Officially released mutant varieties – The FAO/IAEA database. Plant Cell Tiss Org 65 (3):175-177. doi:10.1023/a:1010652523463

Marchant A, Bennett MJ (1998) The *Arabidopsis AUX1* gene: a model system to study mRNA processing in plants. Plant Mol Biol 36 (3):463-471

Mascher M, Richmond TA, Gerhardt DJ, Himmelbach A, Clissold L, Sampath D, Ayling S, Steuernagel B, Pfeifer M, D'Ascenzo M, Akhunov ED, Hedley PE, Gonzales AM, Morrell PL, Kilian B, Blattner FR, Scholz U, Mayer KFX, Flavell AJ, Muehlbauer GJ, Waugh R, Jeddeloh JA, Stein N (2013) Barley whole exome capture: a tool for genomic research in the genus *Hordeum* and beyond. Plant J 76 (3):494-505. doi:10.1111/tpj.12294

Mason AS, Higgins EE, Snowdon RJ, Batley J, Stein A, Werner C, Parkin IAP (2017) A user guide to the *Brassica* 60K Illumina Infinium™ SNP genotyping array. Theor Appl Genet 130 (4):621-633. doi:10.1007/s00122-016-2849-1

Meakin PJ, Roberts JA (1990a) Dehiscence of Fruit in Oilseed Rape (Brassica-Napus L) .2. The Role of Cell-Wall Degrading Enzymes and Ethylene. J Exp Bot 41 (229):1003-1011. doi:10.1093/jxb/41.8.1003

Meakin PJ, Roberts JA (1990b) Dehiscence of fruit in oilseed rape (*Brassica napus* L) .1. Anatomy of pod dehiscence. J Exp Bot 41 (229):995-1002. doi:10.1093/Jxb/41.8.995

Mei J, Liu Y, Wei D, Wittkop B, Ding Y, Li Q, Li J, Wan H, Li Z, Ge X (2015) Transfer of sclerotinia resistance from wild relative of *Brassica oleracea* into *Brassica napus* using a hexaploidy step. Theor Appl Genet 128 (4):639-644. doi:10.1007/s00122-015-2459-3

Messéan A, Sausse C, Gasquez J, Darmency H (2007) Occurrence of genetically modified oilseed rape seeds in the harvest of subsequent conventional oilseed rape over time. Europ J Agron 27 (1):115-122. doi:10.1016/j.eja.2007.02.009

Meyer RS, Purugganan MD (2013) Evolution of crop species: genetics of domestication and diversification. Nat Rev Genet 14 (12):840-852. doi:10.1038/nrg3605

Mikami M, Toki S, Endo M (2015) Parameters affecting frequency of CRISPR/Cas9 mediated targeted mutagenesis in rice. Plant Cell Rep 34 (10):1807-1815. doi:10.1007/s00299-015-1826-5

Mitsuda N, Iwase A, Yamamoto H, Yoshida M, Seki M, Shinozaki K, Ohme-Takagi M (2007) NAC transcription factors, NST1 and NST3, are key regulators of the formation of secondary walls in woody tissues of *Arabidopsis*. Plant Cell 19 (1):270-280. doi:10.1105/tpc.106.047043

Mitsuda N, Ohme-Takagi M (2008) NAC transcription factors NST1 and NST3 regulate pod shattering in a partially redundant manner by promoting secondary wall formation after the establishment of tissue identity. Plant J 56 (5):768-778. doi:10.1111/j.1365-313X.2008.03633.x

Mitsuda N, Seki M, Shinozaki K, Ohme-Takagi M (2005) The NAC transcription factors NST1 and NST2 of *Arabidopsis* regulate secondary wall thickenings and are required for anther dehiscence. Plant Cell 17 (11):2993-3006. doi:10.1105/tpc.105.036004

Mojica FJM, Díez-Villaseñor C, García-Martínez J, Almendros C (2009) Short motif sequences determine the targets of the prokaryotic CRISPR defence system. Microbiol 155 (3):733-740. doi:10.1099/mic.0.023960-0

Morgan CL, Bruce DM, Child R, Ladbrooke ZL, Arthur AE (1998) Genetic variation for pod shatter resistance among lines of oilseed rape developed from synthetic B. napus. Field Crop Res 58 (2):153-165. doi:10.1016/S0378-4290(98)00099-9

Morgan CL, Ladbrooke ZL, Bruce DM, Child R, Arthur AE (2000) Breeding oilseed rape for pod shattering resistance. J Agr Sci 135:347-359. doi:10.1017/S0021859699008424

Mulisch M, Welsch U (eds) (2015) Romeis - Mikroskopische Technik. 19 edn. Springer-Verlag Berlin Heidelberg. doi:10.1007/978-3-642-55190-1

Muller HJ (1927) Artificial transmutation of the gene. Science 66 (1699):84-87

Naito K, Kusaba M, Shikazono N, Takano T, Tanaka A, Tanisaka T, Nishimura M (2005) Transmissible and nontransmissible mutations induced by irradiating *Arabidopsis thaliana* pollen with γ-rays and carbon ions. Genetics 169 (2):881-889. doi:10.1534/genetics.104.033654

Nekrasov V, Staskawicz B, Weigel D, Jones JDG, Kamoun S (2013) Targeted mutagenesis in the model plant *Nicotiana benthamiana* using Cas9 RNA-guided endonuclease. Nat Biotech 31 (8):691-693. doi:10.1038/nbt.2655

Nunes AL, Ascari J, Pereira L, Sossmeier SG, Bervian N (2015) Pod sealant and canola harvest methods for pod shattering mitigation. Aust J Crop Sci 9 (9):865-869

Ogawa M, Kay P, Wilson S, Swain SM (2009) ARABIDOPSIS DEHISCENCE ZONE POLYGALACTURONASE1 (ADPG1), ADPG2, and QUARTET2 are polygalacturonases required for cell separation during reproductive development in Arabidopsis. Plant Cell 21 (1):216-233. doi:10.1105/tpc.108.063768

Olsen AN, Ernst HA, Leggio LL, Skriver K (2005) DNA-binding specificity and molecular functions of NAC transcription factors. Plant Sci 169 (4):785-797. doi:10.1016/j.plantsci.2005.05.035

Ooka H, Satoh K, Doi K, Nagata T, Otomo Y, Murakami K, Matsubara K, Osato N, Kawai J, Carninci P, Hayashizaki Y, Suzuki K, Kojima K, Takahara Y, Yamamoto K, Kikuchi S (2003) Comprehensive analysis of NAC family genes in *Oryza sativa* and *Arabidopsis thaliana*. DNA Res 10 (6):239-247. doi:10.1093/dnares/10.6.239

Ossowski S, Schneeberger K, Lucas-Lledó JI, Warthmann N, Clark RM, Shaw RG, Weigel D, Lynch M (2010) The rate and molecular spectrum of spontaneous mutations in *Arabidopsis thaliana*. Science 327 (5961):92-94. doi:10.1126/science.1180677

Ostergaard L, King G (2008) Standardized gene nomenclature for the *Brassica* genus. Plant Methods 4 (1):10. doi:10.1186/1746-4811-4-10

Pari L, Assirelli A, Suardi A, Civitarese V, Del Giudice A, Costa C, Santangelo E (2012) The harvest of oilseed rape (*Brassica napus* L.): The effective yield losses at on-farm scale in the Italian area. Biomass Bioenergy 46:453-458. doi:10.1016/j.biombioe.2012.07.014

Pavletich NP, Pabo CO (1991) Zinc finger-DNA recognition: crystal structure of a Zif268-DNA complex at 2.1 A. Science 252 (5007):809

Peltonen-Sainio P, Pahkala K, Mikkola H, Jauhiainen L (2014) Seed loss and volunteer seedling establishment of rapeseed in the northernmost European conditions. Agr Food Sci 23:327-339

Pfaffl MW (2001) A new mathematical model for relative quantification in real-time RT-PCR. Nucleic Acids Res 29 (9):e45. doi:10.1093/nar/29.9.e45

Pinyopich A, Ditta GS, Savidge B, Liljegren SJ, Baumann E, Wisman E, Yanofsky MF (2003) Assessing the redundancy of MADS-box genes during carpel and ovule development. Nature 424 (6944):85-88. doi:10.1038/nature01741

Pourcel C, Salvignol G, Vergnaud G (2005) CRISPR elements in *Yersinia pestis* acquire new repeats by preferential uptake of bacteriophage DNA, and provide additional tools for evolutionary studies. Microbiol 151 (3):653-663. doi:10.1099/mic.0.27437-0

Price JS, Hobson RN, Neale MA, Bruce DM (1996) Seed losses in commercial harvesting of oilseed rape. J Agr Eng Res 65 (3):183-191. doi:10.1006/jaer.1996.0091

Puchta H (2004) The repair of double-strand breaks in plants: mechanisms and consequences for genome evolution. J Exp Bot 56 (409):1-14. doi:10.1093/jxb/eri025

Puchta H, Dujon B, Hohn B (1996) Two different but related mechanisms are used in plants for the repair of genomic double-strand breaks by homologous recombination. Proc Natl Acad Sci 93 (10):5055-5060

Rajani S, Sundaresan V (2001) The *Arabidopsis* myc/bHLH gene *ALCATRAZ* enables cell separation in fruit dehiscence. Curr Biol 11 (24):1914-1922. doi:10.1016/S0960-9822(01)00593-0

Raman H, Raman R, Kilian A, Detering F, Carling J, Coombes N, Diffey S, Kadkol G, Edwards D, McCully M, Ruperao P, Parkin IAP, Batley J, Luckett DJ, Wratten N (2014) Genome-wide delineation of natural variation for pod shatter resistance in *Brassica napus*. Plos One 9 (7):e101673. doi:10.1371/journal.pone.0101673

R Core Team (2015) R: A language and environment for statistical computing., 3.2.0 edn. R Foundation for Statistical Computing, Vienna

Reisz JA, Bansal N, Qian J, Zhao W, Furdui CM (2014) Effects of ionizing radiation on biological molecules - mechanisms of damage and emerging methods of detection. Antioxid Redox Signal 21 (2):260-292. doi:10.1089/ars.2013.5489

Roeder AHK, Ferrándiz C, Yanofsky MF (2003) The role of the REPLUMLESS homeodomain protein in patterning the *Arabidopsis* fruit. Curr Biol 13 (18):1630-1635. doi:10.1016/j.cub.2003.08.027

Sander JD, Dahlborg EJ, Goodwin MJ, Cade L, Zhang F, Cifuentes D, Curtin SJ, Blackburn JS, Thibodeau-Beganny S, Qi Y (2011) Selection-free zinc-finger-nuclease engineering by context-dependent assembly (CoDA). Nat Methods 8 (1):67-69. doi:10.1038/nmeth.1542

Sander L, Child R, Ulvskov P, Albrechtsen M, Borkhardt B (2001) Analysis of a dehiscence zone endo-polygalacturonase in oilseed rape (*Brassica napus*) and *Arabidopsis thaliana*: evidence for roles in cell separation in dehiscence and abscission zones, and in stylar tissues during pollen tube growth. Plant Mol Biol 46 (4):469-479. doi:10.1023/A:1010619002833

Sauer NJ, Narváez-Vásquez J, Mozoruk J, Miller RB, Warburg ZJ, Woodward MJ, Mihiret YA, Lincoln TA, Segami RE, Sanders SL (2016) Oligonucleotide-mediated genome editing provides precision and function to engineered nucleases and antibiotics in plants. Plant Physiol 170 (4):1917-1928. doi:10.1104/pp.15.01696

Savidge B, Rounsley SD, Yanofsky MF (1995) Temporal relationship between the transcription of two *Arabidopsis* MADS box genes and the floral organ identity genes. The Plant Cell 7 (6):721-733. doi:10.1105/tpc.7.6.721

Scarth R, Tang J (2006) Modification of *Brassica* oil using conventional and transgenic approaches. Crop Sci 46 (3):1225-1236. doi:10.2135/cropsci2005.08-0245

Schmutzer T, Samans B, Dyrszka E, Ulpinnis C, Weise S, Stengel D, Colmsee C, Lespinasse D, Micic Z, Abel S, Duchscherer P, Breuer F, Abbadi A, Leckband G, Snowdon R, Scholz U (2015) Species-wide genome sequence and nucleotide polymorphisms from the model allopolyploid plant *Brassica napus*. Sci Data 2:150072. doi:10.1038/Sdata.2015.72

Schondelmaier J, Steinrücken G, Jung C (1996) Integration of AFLP markers into a linkage map of sugar beet (*Beta vulgaris* L.). Plant Breed 115 (4):231-237. doi:10.1111/j.1439-0523.1996.tb00909.x

Schouten HJ, vande Geest H, Papadimitriou S, Bemer M, Schaart JG, Smulders MJM, Perez GS, Schijlen E (2017) Re-sequencing transgenic plants revealed rearrangements at T-DNA inserts, and integration of a short T-DNA fragment, but no increase of small mutations elsewhere. Plant Cell Rep 36 (3):493-504. doi:10.1007/s00299-017-2098-z

Shan QW, Wang YP, Li J, Zhang Y, Chen KL, Liang Z, Zhang K, Liu JX, Xi JJ, Qiu JL, Gao CX (2013) Targeted genome modification of crop plants using a CRISPR-Cas system. Nat Biotechnol 31 (8):686-688. doi:10.1038/Nbt.2650

Shi J, Lai J (2015) Patterns of genomic changes with crop domestication and breeding. Curr Opin Plant Biol 24:47-53. doi:10.1016/j.pbi.2015.01.008

Simard M-J, Légère A, Pageau D, Lajeunesse J, Warwick S (2002) The frequency and persistence of volunteer canola (*Brassica napus*) in Quebec cropping systems. Weed Technol 16 (2):433-439

Simmonds J, Scott P, Brinton J, Mestre TC, Bush M, del Blanco A, Dubcovsky J, Uauy C (2016) A splice acceptor site mutation in *TaGW2-A1* increases thousand grain weight in tetraploid and hexaploid wheat through wider and longer grains. Theor Appl Genet 129 (6):1099-1112. doi:10.1007/s00122-016-2686-2

Smith J, Bibikova M, Whitby FG, Reddy A, Chandrasegaran S, Carroll D (2000) Requirements for double-strand cleavage by chimeric restriction enzymes with zinc finger DNA-recognition domains. Nucleic Acids Res 28 (17):3361-3369. doi:10.1093/nar/28.17.3361

Sorefan K, Girin T, Liljegren SJ, Ljung K, Robles P, Galván-Ampudia CS, Offringa R, Friml J, Yanofsky MF, Østergaard L (2009) A regulated auxin minimum is required for seed dispersal in Arabidopsis. Nature 459 (7246):583-586. doi:10.1038/nature07875

Souer E, van Houwelingen A, Kloos D, Mol J, Koes R (1996) The *No Apical Meristem* gene of petunia is required for pattern formation in embryos and flowers and is expressed at meristem and primordia boundaries. Cell 85 (2):159-170. doi:10.1016/S0092-8674(00)81093-4

Squires TM, Gruwel MLH, Zhou R, Sokhansanj S, Abrams SR, Cutler AJ (2003) Dehydration and dehiscence in siliques of *Brassica napus* and *Brassica rapa*. Can J Bot 81 (3):248-254. doi:10.1139/B03-019

Steinrücken HC, Amrhein N (1980) The herbicide glyphosate is a potent inhibitor of 5-enolpyruvylshikimic acid-3-phosphate synthase. Biochem Bioph Res Co 94 (4):1207-1212. doi:10.1016/0006-291X(80)90547-1

Stoddard BL (2011) Homing endonucleases: From microbial genetic invaders to reagents for targeted DNA modification. Struct 19 (1):7-15. doi:10.1016/j.str.2010.12.003

Summers JE, Bruce DM, Vancanneyt G, Redig P, Werner CP, Morgan C, Child RD (2003) Pod shatter resistance in the resynthesized *Brassica napus* line DK142. J Agr Sci 140 (1):43-52. doi:10.1017/s002185960200285x

Svitashev S, Schwartz C, Lenderts B, Young JK, Mark Cigan A (2016) Genome editing in maize directed by CRISPR–Cas9 ribonucleoprotein complexes. Nat Commun 7:13274. doi:10.1038/ncomms13274

Swain S, Kay P, Ogawa M (2011) Preventing unwanted breakups: using polygalacturonases to regulate cell separation. Plant Signal Behav 6 (1):93-97. doi:10.4161/psb.6.1.14147

Tan XL, Xia ZW, Zhang LL, Zhang ZY, Guo ZJ, Qi CK (2009) Cloning and sequence analysis of oilseed rape (*Brassica napus*) *SHP2* gene. Bot Stud 50 (4):403-412

Till BJ, Zerr T, Comai L, Henikoff S (2006) A protocol for TILLING and Ecotilling in plants and animals. Nat Protoc 1 (5):2465-2477. doi:10.1038/nprot.2006.329

Townsend JA, Wright DA, Winfrey RJ, Fu F, Maeder ML, Joung JK, Voytas DF (2009) High frequency modification of plant genes using engineered zinc finger nucleases. Nature 459 (7245):442-445. doi:10.1038/nature07845

Tripathi M, Mishra A (2007) Glucosinolates in animal nutrition: A review. Anim Feed Sci Technol 132 (1):1-27. doi:10.1016/j.anifeedsci.2006.03.003

Udall JA, Quijada PA, Lambert B, Osborn TC (2006) Quantitative trait analysis of seed yield and other complex traits in hybrid spring rapeseed (*Brassica napus* L.): 2. Identification of alleles from unadapted germplasm. Theor Appl Genet 113 (4):597-609. doi:10.1007/s00122-006-0324-0

van Gelderen K, van Rongen M, Liu Aa, Otten A, Offringa R (2016) An INDEHISCENT-controlled auxin response specifies the separation layer in early *Arabidopsis* fruit. Mol Plant 9 (6):857-869. doi:10.1016/j.molp.2016.03.005

Varenberg M, Pugno NM, Gorb SN (2010) Spatulate structures in biological fibrillar adhesion. Soft Matter 6 (14):3269-3272. doi:10.1039/C003207G

Verbeke G, Lesaffre E (1997) The effect of misspecifying the random-effects distribution in linear mixed models for longitudinal data. Comput Stat Data An 23 (4):541-556. doi:10.1016/S0167-9473(96)00047-3

Voronova A, Baltimore D (1990) Mutations that disrupt DNA binding and dimer formation in the E47 helix-loop-helix protein map to distinct domains. Proc Natl Acad Sci 87 (12):4722-4726. doi:10.1073/pnas.87.12.4722

Wang G-P, Yu X-D, Sun Y-W, Jones HD, Xia L-Q (2016) Generation of marker- and/or backbone-free transgenic wheat plants via *Agrobacterium*-mediated transformation. Frontiers Plant Sci 7:1324. doi:10.3389/fpls.2016.01324

Wang H, Zhao Q, Chen F, Wang M, Dixon RA (2011a) NAC domain function and transcriptional control of a secondary cell wall master switch. Plant J 68 (6):1104-1114. doi:10.1111/j.1365-313X.2011.04764.x

Wang R, Ripley VL, Rakow G (2007) Pod shatter resistance evaluation in cultivars and breeding lines of *Brassica napus*, *B. juncea* and *Sinapis alba*. Plant Breed 126 (6):588-595. doi:10.1111/j.1439-0523.2007.01382.x

Wang X, Wang H, Wang J, Sun R, Wu J, Liu S, Bai Y, Mun J-H, Bancroft I, Cheng F, Huang S, Li X, Hua W, Wang J, Wang X, Freeling M, Pires JC, Paterson AH, Chalhoub B, Wang B, Hayward A, Sharpe AG, Park B-S, Weisshaar B, Liu B, Li B, Liu B, Tong

C, Song C, Duran C, Peng C, Geng C, Koh C, Lin C, Edwards D, Mu D, Shen D, Soumpourou E, Li F, Fraser F, Conant G, Lassalle G, King GJ, Bonnema G, Tang H, Wang H, Belcram H, Zhou H, Hirakawa H, Abe H, Guo H, Wang H, Jin H, Parkin IAP, Batley J, Kim J-S, Just J, Li J, Xu J, Deng J, Kim JA, Li J, Yu J, Meng J, Wang J, Min J, Poulain J, Hatakeyama K, Wu K, Wang L, Fang L, Trick M, Links MG, Zhao M, Jin M, Ramchiary N, Drou N, Berkman PJ, Cai Q, Huang Q, Li R, Tabata S, Cheng S, Zhang S, Zhang S, Huang S, Sato S, Sun S, Kwon S-J, Choi S-R, Lee T-H, Fan W, Zhao X, Tan X, Xu X, Wang Y, Qiu Y, Yin Y, Li Y, Du Y, Liao Y, Lim Y, Narusaka Y, Wang Y, Wang Z, Li Z, Wang Z, Xiong Z, Zhang Z (2011b) The genome of the mesopolyploid crop species *Brassica rapa*. Nat Genet 43 (10):1035-1039. doi:10.1038/ng.919

Wang YP, Cheng X, Shan QW, Zhang Y, Liu JX, Gao CX, Qiu JL (2014) Simultaneous editing of three homoeoalleles in hexaploid bread wheat confers heritable resistance to powdery mildew. Nat Biotechnol 32 (9):947-951. doi:10.1038/Nbt.2969

Weber S, Ünker F, Friedt W (2005) Improved doubled haploid production protocol for *Brassica napus* using microspore colchicine treatment in vitro and ploidy determination by flow cytometry. Plant Breeding 124 (5):511-513. doi:10.1111/j.1439-0523.2005.01114.x

Wells R, Trick M, Soumpourou E, Clissold L, Morgan C, Werner P, Gibbard C, Clarke M, Jennaway R, Bancroft I (2014) The control of seed oil polyunsaturate content in the polyploid crop species *Brassica napus*. Mol Breeding 33 (2):349-362. doi:10.1007/s11032-013-9954-5

Wen J, Tu J-x, Li Z-y, Fu T-d, Ma C-z, Shen J-x (2008) Improving ovary and embryo culture techniques for efficient resynthesis of *Brassica napus* from reciprocal crosses between yellow-seeded diploids *B. rapa* and *B. oleracea*. Euphytica 162 (1):81-89. doi:10.1007/s10681-007-9566-4

Woo JW, Kim J, Kwon SI, Corvalan C, Cho SW, Kim H, Kim S-G, Kim S-T, Choe S, Kim J-S (2015) DNA-free genome editing in plants with preassembled CRISPR-Cas9 ribonucleoproteins. Nat Biotech 33 (11):1162-1164. doi:10.1038/nbt.3389

Yan W, Chen D, Kaufmann K (2016) Efficient multiplex mutagenesis by RNA-guided *Cas9* and its use in the characterization of regulatory elements in the *AGAMOUS* gene. Plant Methods 12:23. doi:10.1186/s13007-016-0125-7

Yuan Y-X, Wu J, Sun R-F, Zhang X-W, Xu D-H, Bonnema G, Wang X-W (2009) A naturally occurring splicing site mutation in the *Brassica rapa FLC1* gene is associated with variation in flowering time. J Exp Bot 60 (4):1299-1308. doi:10.1093/jxb/erp010

Zarhloul KM, Stoll C, Lühs W, Syring-Ehemann A, Hausmann L, Töpfer R, Friedt W (2006) Breeding high-stearic oilseed rape (*Brassica napus*) with high- and low-erucic background using optimised promoter-gene constructs. Mol Breeding 18 (3):241-251. doi:10.1007/s11032-006-9032-3

Zerr T, Henikoff S (2005) Automated band mapping in electrophoretic gel images using background information. Nucleic Acids Res 33 (9):2806-2812. doi:10.1093/nar/gki580

Zhang Y, Shen YY, Wu XM, Wang JB (2016) The basis of pod dehiscence: anatomical traits of the dehiscence zone and expression of eight pod shatter-related genes in four species of *Brassicaceae*. Biol Plantarum 60 (2):343-354. doi:10.1007/s10535-016-0599-1

Zhong R, Lee C, McCarthy RL, Reeves CK, Jones EG, Ye Z-H (2011) Transcriptional activation of secondary wall biosynthesis by rice and maize NAC and MYB transcription factors. Plant Cell Physiol 52 (10):1856-1871. doi:10.1093/pcp/pcr123

Zhong R, Lee C, Ye Z-H (2010) Functional characterization of poplar wood-associated NAC domain transcription factors. Plant Physiol 152 (2):1044-1055. doi:10.1104/pp.109.148270

Zhong RQ, Richardson EA, Ye ZH (2007) Two NAC domain transcription factors, SND1 and NST1, function redundantly in regulation of secondary wall synthesis in fibers of *Arabidopsis*. Planta 225 (6):1603-1611. doi:10.1007/s00425-007-0498-y

Zhou H, He M, Li J, Chen L, Huang Z, Zheng S, Zhu L, Ni E, Jiang D, Zhao B, Zhuang C (2016) Development of commercial thermo-sensitive genic male sterile rice accelerates hybrid rice breeding using the CRISPR/Cas9-mediated *TMS5* editing system. Sci Rep 6:37395. doi:10.1038/srep37395

11 Curriculum vitae and publications

11.1 Curriculum vitae

Personal data

Name   Janina Braatz

Date of birth   06.06.1990

Place of birth   Kamp-Lintfort

Nationality   German

Education

2014 - 2017	**Christian-Albrechts-University of Kiel, Germany** **Doctoral candidate in Plant Breeding and Genetics** Doctoral Thesis: Production of oilseed rape with increased seed shattering resistance
2012 - 2014	**Christian-Albrechts-University of Kiel, Germany** **M.Sc. in Agricultural Genomics** Master's Thesis: Silique shattering resistance of oilseed rape (*Brassica napus* L.) genotypes with single and double mutations in the *INDEHISCENT* gene
2009 - 2012	**Bielefeld University, Germany** **B.Sc. in Bioinformatics and Genome Research** Bachelor's Thesis: Research on a putative zinc finger transcription factor in *Beta vulgaris*
2000 - 2009	**'Städtisches Gymnasium Straelen' high school, Straelen, Germany** **High school diploma: 'Abitur'** Focus subjects: Biology, Mathematics

11.2 Publications

11.2.1 Articles

Braatz J, Harloff H-J, Emrani N, Elisha C, Heepe L, Gorb S, Jung C. The effect of *INDEHISCENT* point mutations on silique shatter resistance in oilseed rape (*Brassica napus*). Under review.

Braatz J, Harloff H-J, Jung C. EMS-induced point mutations in *ALCATRAZ* homoeologs increase silique shatter resistance of oilseed rape (*Brassica napus*). Under review.

Braatz J, Harloff H-J, Mascher M, Stein N, Himmelbach A, Jung C (2017). CRISPR-Cas9 targeted mutagenesis leads to simultaneous modification of different homoeologous gene copies in polyploid oilseed rape (*Brassica napus*). Plant Physiol 174(2): 935-942. doi:10.1104/pp.17.00426

Jung C, Capistrano-Gossmann G, Braatz J, Sashidhar N, Melzer S (2017). Recent developments in genome editing and applications in plant breeding. Plant Breed, 00:1-9. doi:10.1111/pbr.12526

11.2.2 Oral presentations and posters

Braatz J, Harloff H-J, Emrani N, Heepe L, Gorb S, Mascher M, Stein N, Himmelbach A, Jung C (2017). Improved shatter resistance of canola by CRISPR/Cas9 and EMS mutagenesis, Canola Week 2017, Saskatoon, 05.-07.12.2017. Presentation.

Braatz J (2017). Engineering shatter resistant rapeseed through TILLING and Cas9-mediated mutagenesis, Botanikertagung 2017, Kiel, 17.-21.09.2017. Presentation.

Braatz J (2017). CRISPR-Cas9 targeted mutagenesis leads to simultaneous modification of different homoeologous gene copies in polyploid oilseed rape (*Brassica napus*), PP1530 International Workshop: 'Genome Engineering', Gatersleben, 22.-23.06.2017. Presentation.

Braatz J, Emrani N, Harloff H-J, Jung C (2017). Towards the production of shatter resistant rapeseed by use of mutations in dehiscence zone identity genes, International Plant & Animal Genome XXV, San Diego, 14.-18.01.2017. Presentation + poster.

Braatz J, Emrani N, Harloff H-J, Jung C (2016). Increasing seed shatter resistance in oilseed rape (*B. napus* L.) by TILLING and CRISPR/Cas9 mutagenesis, 2nd Sino-German Rapeseed Symposium, Kiel, 23.-26.05.2016. Presentation.

Braatz J, Emrani N, Harloff H-J, Jung C (2015). Seed shattering resistance in mutants of oilseed rape (*B. napus* L.), 18th Genome Research GPZ-Conference, Düsseldorf, 22.-24.09.2015. Presentation.

Braatz J, Emrani N, Harloff H-J, Jung C (2016). Comparing seed shatter resistance in mutants of oilseed rape (*B. napus* L.), German Plant Breeding Conference, Bonn, 08.-10.03.2016. Poster.

Braatz J, Emrani N, Harloff H-J, Jung C (2016). Erzeugung von Ölraps mit erhöhter Schotenplatzfestigkeit, 66. Öffentliche Hochschultagung der Agrar- und Ernährungswissenschaftlichen Fakultät, Kiel, 04.02.2016. Poster.

12 Declarations of co-authorship

Chapters 2, 3, and 4 were prepared as manuscripts for publication. The respective declarations of co-authorship are presented on the following pages. Meanwhile, chapter 5 includes work of the doctoral candidate alone.

C A U Christian-Albrechts-Universität zu Kiel | Agrar- und Ernährungs-
wissenschaftliche Fakultät

Declaration of co-authorship

1. Doctoral candidate
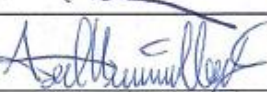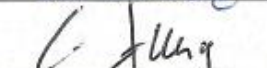
Name: Janina Braatz

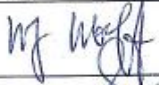### 2. This co-authorship declaration applies to the following article:
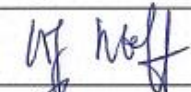
Braatz J, Harloff H-J, Mascher M, Stein N, Himmelbach A, Jung C (2017). CRISPR-Cas9 targeted mutagenesis leads to simultaneous modification of different homoeologous gene copies in polyploid oilseed rape (*Brassica napus*). Plant Physiol 174(2): 935-942. doi:10.1104/pp.17.00426

The extent of the doctoral candidate's contribution to the article is assessed on the following scale:
- A.   Has contributed to the work (0-33%)
- B.   Has made a substantial contribution (34-66%)
- C.   Did the majority of the work independently (67-100%)

3. Declaration on the individual phases of the scientific work (A,B,C)	Extent
Concept: Formulation of the basic scientific problem based on theoretical questions which require clarification, incl. a summary of the general questions which are assumed to be answerable via analyses or concrete experiments/investigations	B
Planning: Planning of experiments/analyses and formulation of investigative methodology, incl. choice of method and independent methodological development, in a way that the scientific questions asked can be expected to be answered	B
Execution: Involvement in the analysis or the concrete experiments/investigation	C
Manuscript preparation: Presentation, interpretation and discussion of the results obtained in article form	C

4. Signatures of all co-authors

Date	Name	Signature
15.6.17	Hans-Joachim Harloff	
27.6.17	Martin Mascher	
22.6.17	Nils Stein	
22.6.17	Axel Himmelbach	
28.6.17	Christian Jung	

5. Signature of doctoral candidate

Date	Name	Signature
15.06.17	Janina Braatz	Braatz

| C | A | U | Christian-Albrechts-Universität zu Kiel | Agrar- und Ernährungs-wissenschaftliche Fakultät |

Declaration of co-authorship

1. Doctoral candidate

Name: Janina Braatz

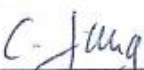### 2. This co-authorship declaration applies to the following article:

Braatz J, Harloff H-J, Emrani N, Heepe L, Gorb S, Elisha C, Jung C. The effect of *INDEHISCENT* point mutations on silique shatter resistance in oilseed rape (*Brassica napus*).

The extent of the doctoral candidate's contribution to the article is assessed on the following scale:

- A.   Has contributed to the work (0-33%)
- B.   Has made a substantial contribution (34-66%)
- C.   Did the majority of the work independently (67-100%)

3. Declaration on the individual phases of the scientific work (A,B,C)	Extent
Concept: Formulation of the basic scientific problem based on theoretical questions which require clarification, incl. a summary of the general questions which are assumed to be answerable via analyses or concrete experiments/investigations	B
Planning: Planning of experiments/analyses and formulation of investigative methodology, incl. choice of method and independent methodological development, in a way that the scientific questions asked can be expected to be answered	B
Execution: Involvement in the analysis or the concrete experiments/investigation	C
Manuscript preparation: Presentation, interpretation and discussion of the results obtained in article form	C

4. Signatures of all co-authors

Date	Name	Signature
28.8.17	Hans-Joachim Harloff	
24.8.17	Nazgol Emrani	
27.8.17	Lars Heepe	
29.08.17	Stanislav Gorb	
	Chirlon Elisha	
25.8.17	Christian Jung	

5. Signature of doctoral candidate

Date	Name	Signature
25.8.17	Janina Braatz	Braatz

| **C** | **A** | **U** | Christian-Albrechts-Universität zu Kiel | Agrar- und Ernährungs-wissenschaftliche Fakultät |

Declaration of co-authorship

1. Doctoral candidate
Name: Janina Braatz

2. This co-authorship declaration applies to the following article:
Braatz J, Harloff H-J, Emrani N, Heepe L, Gorb S, Elisha C, Jung C. The effect of *INDEHISCENT* point mutations on silique shatter resistance in oilseed rape (*Brassica napus*).

The extent of the doctoral candidate's contribution to the article is assessed on the following scale:
- A. Has contributed to the work (0-33%)
- B. Has made a substantial contribution (34-66%)
- C. Did the majority of the work independently (67-100%)

3. Declaration on the individual phases of the scientific work (A,B,C)	**Extent**
Concept: Formulation of the basic scientific problem based on theoretical questions which require clarification, incl. a summary of the general questions which are assumed to be answerable via analyses or concrete experiments/investigations	B
Planning: Planning of experiments/analyses and formulation of investigative methodology, incl. choice of method and independent methodological development, in a way that the scientific questions asked can be expected to be answered	B
Execution: Involvement in the analysis or the concrete experiments/investigation	C
Manuscript preparation: Presentation, interpretation and discussion of the results obtained in article form	C

4. Signatures of all co-authors		
Date	**Name**	**Signature**
	Hans-Joachim Harloff	
	Nazgol Emrani	
	Lars Heepe	
	Stanislav Gorb	
29.08.17	Chirlon Elisha	*[signature]*
	Christian Jung	

5. Signature of doctoral candidate		
Date	**Name**	**Signature**
	Janina Braatz	

| C | A | U | Christian-Albrechts-Universität zu Kiel | Agrar- und Ernährungs-wissenschaftliche Fakultät |

Declaration of co-authorship

1. Doctoral candidate

Name: Janina Braatz

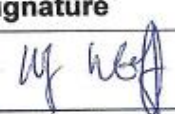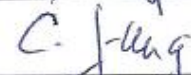### 2. This co-authorship declaration applies to the following article:

Braatz J, Harloff H-J, Jung C. EMS-induced point mutations in *ALCATRAZ* homoeologs increase silique shatter resistance of oilseed rape (*Brassica napus*).

The extent of the doctoral candidate's contribution to the article is assessed on the following scale:

- A. Has contributed to the work (0-33%)
- B. Has made a substantial contribution (34-66%)
- C. Did the majority of the work independently (67-100%)

3. Declaration on the individual phases of the scientific work (A,B,C)	Extent
Concept: Formulation of the basic scientific problem based on theoretical questions which require clarification, incl. a summary of the general questions which are assumed to be answerable via analyses or concrete experiments/investigations	B
Planning: Planning of experiments/analyses and formulation of investigative methodology, incl. choice of method and independent methodological development, in a way that the scientific questions asked can be expected to be answered	B
Execution: Involvement in the analysis or the concrete experiments/investigation	C
Manuscript preparation: Presentation, interpretation and discussion of the results obtained in article form	C

4. Signatures of all co-authors

Date	Name	Signature
28.8.17	Hans-Joachim Harloff	
25.8.17	Christian Jung	

5. Signature of doctoral candidate

Date	Name	Signature
25.8.17	Janina Braatz	Braatz

13 Acknowledgements

First and foremost, I would like to thank my thesis supervisors Prof. Dr. Christian Jung and Dr. Hans-Joachim Harloff for their continuous support and guidance. Your comments and advice shaped this thesis and inspired me to always give my best.

Nadine, Nirosha, and Sarah, you were the best office mates I could think of and I am not only saying this because of the loads of cookies and chocolate you provided. Just having to turn away from the computer screen to find someone to chat with, enlightened each working day. Niharika, thanks for all the late night coffees which were accompanied by delightful conversations about anything and everything. Hilke, the vegetables and fruits from your garden were the perfect balance to all the sugary stuff which fueled my thesis writing process. Moni, I will always keep our trip to Klein Altendorf in mind – thank you so much for working on the field until 8 P.M. and for taking the hotel room with the badly insulated windows. Dally, your hearty laugh was always catching and made me smile so often. Smit, with you every team is the winning team. Gina, thanks for stopping by my office on the way back from the coffee machine and keeping me informed about the latest institute news. Siegbert, your scientific advice was always appreciated. Antje, your organizational skills made so many things so much easier. Jonas, Dilan, Verena, Kerstin, Birgit, Brigitte, and Bettina, having you around was always a pleasure. Having such kind and helpful colleagues cannot be taken for granted. Ulrike, I already miss our joint lunch breaks. Roxana, if I will have to isolate *Cel*I ever again, I will give you a call so that we can revive memories while shredding bunches of celery. You are amazing to work with. Chirlon, Niloufar, and Lara, thanks a lot for your assistance in lab and greenhouse.

Last but certainly not least, I would like to express my gratitude to my parents, my sister, and my fiancée. Your moral support kept me going and was always the best source of motivation.